Characterisation of recombinant hyaluronidase-1 and -3, and of hyaluronan turnover in mineralising osteoblasts

By

Julian Robert James Adams BSc (Hons)

Thesis submitted for the degree of

Doctor of Philosophy

in

Department of Paediatrics

School of Medicine

Faculty of Health Science

University of Adelaide

December, 2006

Declaration

This work contains no material which has been accepted for the award of any other degree or diploma in any university or other tertiary institution and, to the best of my knowledge and belief, contains no material previously published or written by another person, except where due reference has been made in the text.

I give consent to this copy of my thesis, when deposited in the University Library, being available for loan and photocopying.

Julian Adams

25 July 2006

Acknowledgments

This has been a long and difficult journey; I would like to thank the people that have helped me along the way.

I would like to thank my supervisors, Dr Sharon Byers, Associate Professor Donald Anson and Dr Tom Litjens for their insight and guidance. Thank you to the members of the Matrix Biology laboratory: Belinda, Ashley, Ainslie, Kylie, Jackie, Miriam and Stanley. I would also like to thank past and present members of the Lysosomal Diseases Research Unit and the Department of Genetic Medicine (formerly the Department of Chemical Pathology) at the Women's and Children's Hospital: too many to names to mention but thank you all deeply.

I would like express my sincere gratitude to Guy Sanders for sharing his expertise with Real Time PCR analysis, and Barbara Triggs-Raine for supplying hyaluronidase-3 knock-out mouse tissues.

I would like to thank my parents for their love, support and faith in me throughout my life and in whatever I choose to do. Last but not least I would like to thank my fiancée Sarah who has endured the lows and celebrated the highs of this journey. I cannot thank her enough for being alongside me, and the next stage of our lives together can finally begin.

Abbreviations

% (v/v)	percent volume per volume
% (w/v)	percent weight per volume
°C	degrees Celsius
bp	base pairs
BSA	bovine serum albumin
BSP	bone-specific glycoprotein
C4S	chondroitin-4-sulphate
C6S	chondroitin-6-sulphate
Chon	de-sulphated chondroitin
CHO-K1	Chinese hamster ovary cell line
CS	chondroitin sulphate
cycA	cyclophilin-A (Real Time RT-PCR contol house-keeping gene)
Da	Dalton
dH_2O	deionised water
DMEM	Dulbecco's Modified Eagle's Media
DNA	deoxyribonucleic acid
dNTP	deoxynucleotides
DS	dermatan sulphate
ECM	extra-cellular matrix
EDTA	ethylene diamine tetra acetic acid
ER	endoplasmic reticulum
G418	geneticin (neomycin) Gentamycin-class aminoglycoside antibiotic

Gag(s)	glycosaminoglycan(s)
GAPDH	glyceraldehyde-3-phosphate dehydrogenase
GFP	green fluorescent protein
GPI	glycosylphosphatidylinositol
HA	hyaluronan
HAS(s)	hyaluronan synthase(s)
HYAL(s)	hyaluronidase(s)
HYAL-1	human hyaluronidase-1 gene
hyal-1	mouse hyaluronidase-1
HYAL-P1	human hyaluronidase pseudo gene-1
hyal-p1	mouse hyaluronidase pseudo gene-1
HYAL-1s	hyaluronidase-1 splice variant
HYAL-1U	human hyaluronidase-1 protein, isoform found in urine
HYAL-2	human hyaluronidase-2 (lysosomal HYAL)
hyal-2	mouse hyaluronidase-2 (lysosomal HYAL)
HYAL-3	human hyaluronidase-3
hyal-3	mouse hyaluronidase-3
HYAL-4	human hyaluronidase-4 (chondroitinase)
hyal-4	mouse hyaluronidase-4 (chondroitinase)
PH20	human testicular hyaluronidase
*ph*20	mouse testicular hyaluronidase
Hs	*Homo sapien,* used a a prefix to human
JSRV	Jaagsiekte sheep retrovirus
kb	kilobase
kDa	kilo-dalton

+ AS ?

L, mL, μL	litre, millilitre, microlitre
M, mM	moles per litre, millimoles per litre
MGEA-5	meningioma hyaluronidase
MGEA-5s	meningioma hyaluronidase splice variant
MGP	matrix γ-carboxyglutamic acid protein
Mm	*Mus musculus*, may act as prefix to gene name
mRNA	messenger RNA
NeoR	neomycin resistance
OD	optical density
O-GlcNAcase	O-linked N-acetylglucosamidase
PAGE	polyacrylamide gel electrophoresis
PBS	phosphate buffered saline
PCR	polymerase chain reaction
PG(s)	proteoglycan(s)
pGFP-N1	green fluorescent protein expression vector
pH	log of hydrogen ion concentration
PH20	human testicular hyaluronidase
pHYAL-1-His_6	expression vector of hyaluronidase-1-six histidines
pHYAL-3	expression vector of non-tagged hyaluronidase-3
pHYAL-3-GFP	expression vector of hyaluronidase-3-green fluorescent protein
pHYAL-3-His_6	expression vector of hyaluronidase-3-six histidines
PNGase F	N-glycosidase F
rHYAL-1-His_6	recombinant human hyaluronidase-1-six histidine protein
rHYAL-3	recombinant human hyaluronidase-3 protein (non-tagged)

rHYAL-3-GFP	recombinant human hyaluronidase-3-green fluorescent fusion protein
rHYAL-3-His_6	recombinant human hyaluronidase-3-six histidines protein
RNA	ribonucleic acid
rpm	revolutions per minute
RT	reverse transcriptase
SDS	sodium dodecyl sulphate
SLRP	small leucine-rich proteoglycans
SSC	saline sodium citrate
Tris	Tris hydroxymethylaminomethane
U	units
Xl	*Xenpous laevis,* used as prefix to Frog genes
Xl HYAL	frog hyaluronidase
Xl HYAL-2	frog hyaluronidase-2 (lysosomal)
Xl HYALK	frog kidney hyaluronidase

CONTENTS

Abstract

The mammalian hyaluronidases (HYALs) represent a family of enzymes that can degrade hyaluronan (HA). This thesis examines the properties of hyaluronidase-1 (HYAL-1) and hyaluronidase-3 (HYAL-3), as well as the production of hyaluronan and the expression of HYAL and hyaluronan synthases (HASs) in mineralising osteoblasts.

Recombinant hyaluronidase-1 (rHYAL-1) has a mass of 57 kDa, of which 10 kDa is due to glycoslyation and 47 kDa is primary protein translation product. rHYAL-1 was shown to not only degrade HA, but also to function as an endo-glucosaminidase in the degradation of the sulphated gags chondroitin sulphate and dermatan sulphate.

Recombinant hyaluronidase-3 (rHYAL-3) has a mass of 46 kDa, of which 9 kDa is due to glycoslyation and 37 kDa is primary protein translation product. Immunofluorescence analysis localised His-tagged rHYAL-3 to the endoplasmic reticulum and lysosomes. *In vitro* activity assays demonstrated that HYAL-3 showed no glycohydrolase activity against any glycosaminoglycan (gag) substrate tested. However, the HYAL-3 knock-out mouse (*hyal-3*$^{-/-}$) accumulates gag in testis, kidney and muscle, suggesting that HYAL-3 has a highly restrictive substrate specificity. A role for HYAL-3 in the testis is supported by previous data that has shown HYAL-3 is highly expressed in human testis.

HA, the primary substrate of HYAL, has previously been implicated to play an important role in the mineralisation of bone. In this study mRNA expression of the HASs that synthesise HA (HAS-1, HAS-2 and HAS-3), and the HYALs which degrade HA (HYAL-1, HYAL-2, HYAL-3, HYAL-4) were examined in an osteoblast cell line

that could be induced to mineralise *in vitro* and gene expression was compared to the amount of gag production. During mineralisation a 13-fold decrease in HAS-3 expression was observed, as well as a 62-fold increase in HYAL-2 expression, a 13-fold increase in HYAL-3 expression and a 3-fold increase in HYAL-4 expression. These changes in gene expression were coupled to a 5-fold decrease in the production of HA. Therefore, in mineralising osteoblasts, expression of the genes that control HA metabolism are co-ordinated such that a general decrease in the expression of HASs and an increase in HYAL expression corresponds to a decrease in HA. These data implicate a role for HA in the early stages of matrix synthesis and maturation, rather than the later process of mineralisation.

Chapter 1

Introduction

1.1 Glycosaminoglycans

1.1.1 Glycosaminoglycan structure and function

Glycosaminoglycans (gags) are unbranched carbohydrate structures that are generally characterised by a repeating disaccharide backbone composed of a hexosamine linked to hexuronic acid. An exception to the general structure of gags is found in keratan sulphate (KS), where the hexuronic acid is substituted by galactose. Five different types of gag have been defined, which vary in the types of monosaccharides present and their possible modifications, including sulphation, epimerisation and acetylation (Figure 1.1).

The sulphated gags, chondroitin sulphate (CS), dermatan sulphate (DS), heparan sulphate (HS) and KS exist as proteoglycans and are formed through elongation of the gag chain on a protein core backbone (section 1.1.2). A fifth unsulphated gag, hyaluronan (HA), is synthesised as a free gag chain, although it is found associated with proteins and glycoproteins in the extra-cellular matrix (ECM) (section 1.3).

The synthesis and turnover of gags is a fundamental part of tissue development (Toole, 1997) and organogenesis (Spooner *et al.*, 1993; Davies *et al.*, 2001; Hilfer 1996). The physical properties of gags allow a range of specialised functions, including the regulation of solute flow (Comper and Laurent, 1978), organisation of the ECM and structural definition of tissues (Scott, 1992).

1.1.2 Biosynthesis of glycosaminoglycans

The first event in the biosynthesis of CS, DS and HS is the formation of a linkage region through the transfer of a xylose to a serine residue on the core protein (Stoolmiller *et al.*, 1972).

Hyaluronan

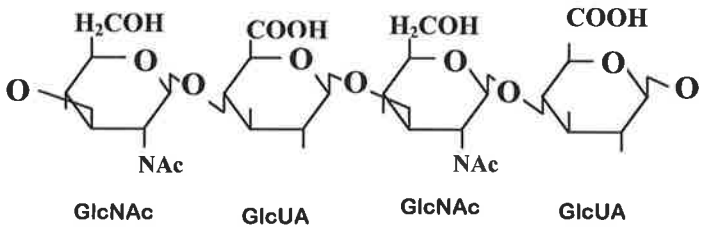

Chondroitin sulphate

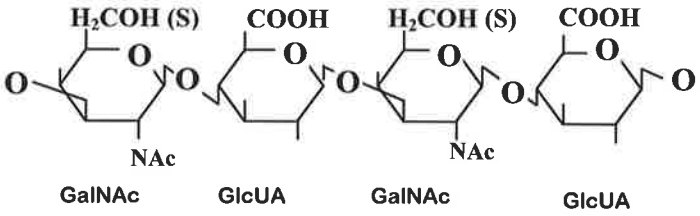

Dermatan sulphate

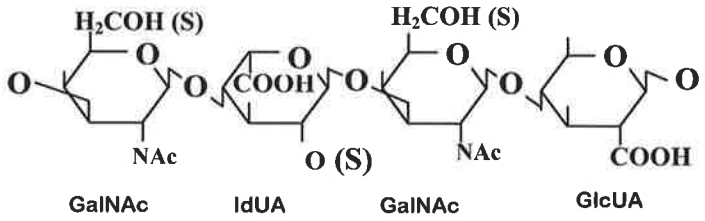

Keratan sulphate

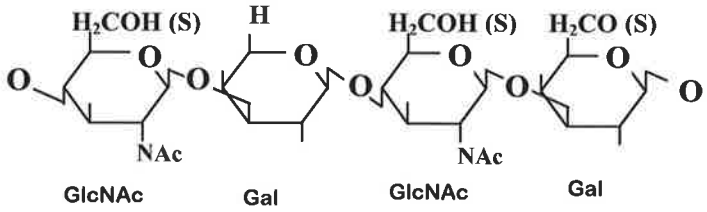

Heparan sulphate

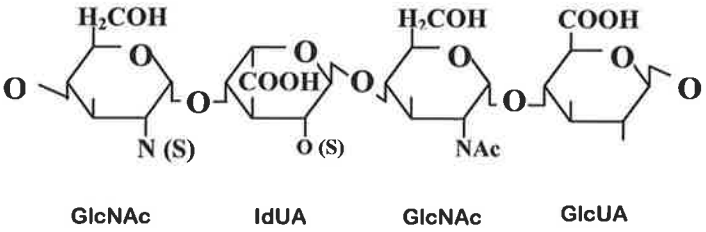

GlcNAc = N-acetylglucosamine IdUA = iduronate Gal=galactose
GalNAc= N-acetylgalactosamine Glc A=glucuronate

Figure 1.1 Repeating disaccharide structures of glycosaminoglycans

Gags share many similarities and differences within their repeating disaccharide structures: HA has the simplest structure and is the only unsulphated gag; DS is formed from CS by epimerisation of glucuronate to iduronate; KS has a galactosamine substituted for the uronic acid.

The linkage region is generated by the transfer of a xylose, followed by a first, then-second galactose and finally the addition of a glucuronate residue (Schwartz and Roden, 1975). The gag chain then elongates on this linkage region with the addition of alternative sugar residues of the particular gags to give their repeating disaccharide structure (Prydz and Dalen, 2000).

The precise mechanism that determines which serine residue is substituted and which particular type of gag is synthesised is not completely understood. However, possible regulatory mechanisms may include differences in the amino acid sequences flanking the serine residue (Dolan *et al.*, 1997; Zhang *et al.*, 1995; Zhang and Esko 1994), modification of the linkage region (Sugahara *et al.*, 1988; 1991; 1992; 1995a; 1995b), access to the monosaccharide precursors of each gag subtype (Lidholt *et al.*, 1988; Toma *et al.*, 1996) or the presence of specific gag-synthesising enzymes (Aikawa and Esko 1999; Fritz *et al.*, 1994; Rohrmann *et al.*, 1985)

KS biosynthesis occurs through a similar step-wise elongation process (Funderburgh, 2000), however the linkage region is different (Dickenson *et al.*, 1990; Hopwood and Robinson 1974). KS may be bound to its core protein through either an N-linkage to an asparagine (Baker *et al.*, 1975) or an O-linkage to a serine or threonine (Lohmander *et al.*, 1980). KS is then elongated through the action of specific KS-synthesising enzymes (Funderburgh, 2000).

HA is unique amongst the gags since it is synthesised as a free gag chain through the activity of HA synthases (HASs). HASs are a class of plasma membrane-spanning glycosyltransferases that add the alternating monosaccharides of HA to the growing gag chain (Yoshida *et al.*, 2000). The activity of HASs is further discussed in-section 1.3.

1.1.3 Glycosaminoglycan degradation

The degradation of HS proteoglycans (PGs) is well characterised, and can be used as a general model of gag turnover. Degradation begins with binding of PGs to cell surface receptors followed by endocytosis of PGs into endosomal compartments (Hausser and Kresse, 1991). The core protein may undergo proteolysis and, in the case of HS PG, some initial endolytic degradation occurs, cleaving the oligosaccharides to fragments of approximately 10 kDa (Bame, 1993; Iozzo, 1987; Yanagishita and Hascall, 1984; 1992). These HS gag chains are subsequently degraded by endoglycosidases to smaller oligosaccharides of approximately 5 kDa (Freeman and Hopwood, 1992). This endolytic degradation occurs in undefined acidic compartments, possibly lysosomes or pre-lysosomes (Iozzo, 1987; Yanagishita and Hascall, 1984).

These compartments become fully acidified and mature into lysosomes. HS is subsequently degraded exolytically in a step-wise manner from its non-reducing terminus into its constituent monomeric components. These monomeric components are then exported through the lysosomal membrane for reutilisation by the cell. The other gags (HA, CS and DS) may undergo a similar model of degradation to that observed for HS, a process that would involve initial internalisation of the gag chains, followed by endolytic digestion to intermediate fragments and then subsequent exolytic digestion. However, the endolytic component of degradation has only been demonstrated for HS (Freeman and Hopwood, 1992). Examining the activity of recombinant hyaluronidase (rHYAL) against a range of sulphated gags is an important aim of this thesis, as it has been proposed that the testicular HYAL can is an endo-glycosidases responsible for the internal cleavage of DS and CS (Knudson *et al.*, 1984), although each of the many mammalian hyaluronidase may have alternative roles.

1.2 Hyaluronidases

1.2.1 An introduction to hyaluronidases

HYALs are a class of endo-glycohydrolases that predominantly degrade HA, a non-sulphated gag, but they are also active against distinct unsulphated domains within CS (Byers *et al.*, 2005; Knudson *et al.*, 1984; Yamada *et al.*, 1977; Takagaki *et al.*, 2000). HYALs utilise either a glucosaminidase, glucuronidase or lyase mechanism of enzyme activity (Figure 1.2).

The mammalian plasma and testicular HYALs (sections 1.3.3 and 1.3) are glucosaminidases (EC 3.2.1.35). These enzymes use hydrolysis to cleave HA and CS, mainly to tetrasaccharides, and leave a glucuronic acid at the non-reducing terminus (Meyer, 1950; Hoffman *et al.*, 1956; Knudson *et al.*, 1984). Testicular HYAL also possesses a synthetic transglycosidase activity; although the hydrolytic activity predominates (Hoffman *et al.*, 1956; Takagaki *et al.*, 1994) (Figure 1.2).

HYALs that possess a glucosaminidase activity are present in a range of vertebrates, such as mice (Csoka *et al.*, 2001), humans (Csoka *et al.*, 1999), cows (Meyer *et al.*, 1997) and frogs (Hyde and Old, 1999; Mullegger and Lepperdinger, 2002; Reitinger *et al.*, 2001). HYALs with glucosaminidase activity are also found in the venom of invertebrates such as bees (Gmachl and Kreil, 1993) and hornets (Lu *et al.*, 1995). These glucosaminidases share amino acid similarities and belong to "family 56" of the glycosyl hydrolases (Henrissat and Bairoch, 1993).

Leech HYAL (EC 3.2.1.36) has a glucuronidase activity that digests only HA as a substrate. It cleaves HA to tetrasaccharides leaving a glucosamine at the non-reducing terminus (Fig 1.2; Hovingh and Linker, 1999; Linker *et al.*, 1957; 1960).

Indirect evidence for the presence of an endolytic enzyme on CS and DS is seen in the mucopolysaccharidoses (MPS) (Neufeld and Muenzer, 2001). MPS are a sub-class of Lysosomal storage disorder (LSD) that arise from the deficiency of enzymes involved in gag degradation (Neufeld and Muenzer, 2001), leading to the accumulation of an array of gags and their subsequent excretion into the blood and urine (Byers *et al.*, 1998); these fragments are thought to result from the activity of specific endo-glucosaminidases and endo-glucuronidases (Fuller *et al.*, 2006).

Bacterial HYALs are an example of the HYAL lyases (EC 4.2.2.1). These enzymes possess a β-eliminase activity and yield disaccharides consisting of a β–unsaturated uronic acid linked to N-acetylglucosamine (Greiling *et al.*, 1975). Bacterial HYALs can degrade CS as well as HA have been isolated (Hiyama and Okada, 1975; Tam and Chan, 1985), although HYAL lyases isolated from different types of bacteria do not all degrade CS (Ohya and Kaneko, 1970). The sulphation pattern on CS is an important factor in the ability of bacterial HYALs to degrade CS (Takagaki *et al.*, 2000). The role of the sulphation pattern on monosaccharides surrounding the cleavage site in the non-bacterial HYALs is yet to be characterised.

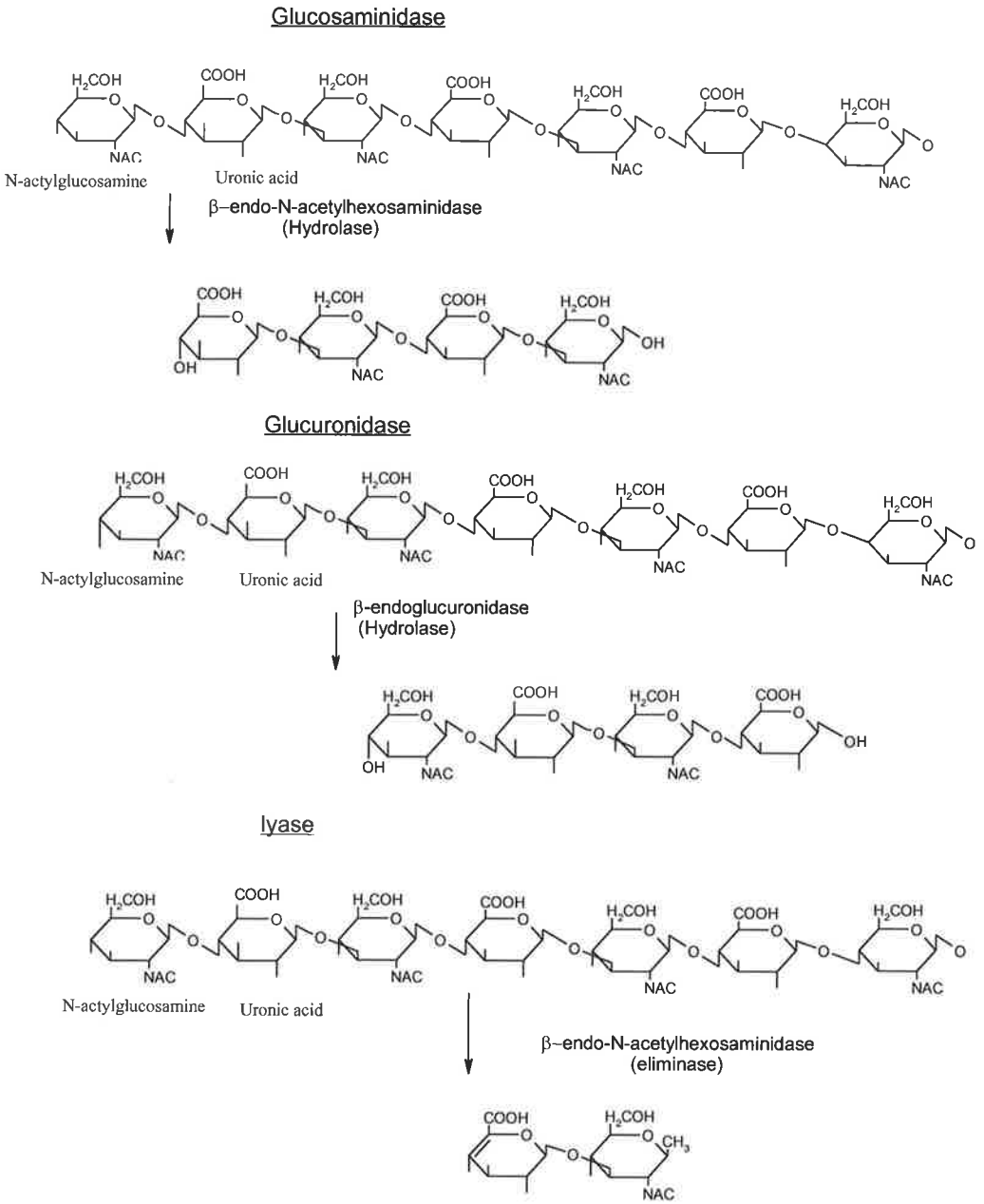

Figure 1.2 Hyaluronan-degrading enzymes

The theoretical end-product of exhaustive digestion of HA by each class of HYAL enzyme is shown above. Glucosaminidases (EC 3.2.1.35) can digest both CS and HA to mainly tetrasaccharides, leaving a glucuronic acid at the non-reducing terminus. Glucuronidases (EC 3.2.1.36) digest only HA, cleaving to tetrasaccharides and leaving a glucosamine at the non-reducing terminal. HYAL lyase (EC 4.2.2.1) acts through β-eliminase activity to form disaccharides consisting of a β-unsaturated uronic acid linked to an N-acetylglucosamine.

1.2.2 Human hyaluronidases

Six paralogous HYAL genes have been identified in humans (Csoka *et al.*, 1999). Of these only testicular HYAL (PH20; Jones *et al.*, 1995; Gmachl and Kreil, 1993; Gmachl *et al.*, 1993), plasma HYAL (HYAL-1, Frost *et al.*, 1997) and lysosomal HYAL (HYAL-2; Lepperdinger *et al.*, 1998) have been cloned, expressed and shown to have glucosaminidase HYAL activity. The activity of HYAL-3, HYAL-4 and HYAL-P1 has not been characterised.

1.2.2.1 PH20

Mammalian oocytes are surrounded by two very different extra-cellular matrices (Yanagimachi, 1994). To fertilise an oocyte a sperm must initially cross the viscoelastic cumulus ECM that consists of HA and protein. Subsequently, the sperm must penetrate the outer porous region of the glycoprotein ECM, the zona pellucida (Yanagimachi, 1994). PH20 (also known as SPAM1) was first identified as the sperm receptor for the zona pellucida (Myles *et al.*, 1987; Primakoff *et al.*, 1985). However, the sperm of PH20 knock-out mice can still pass through the cumulus cells and fertilise the egg (Baba *et al.*, 2002). This observation resulted in the identification of a non-PH20 55 kDa HYAL that is also important for fertilisation.

It was not until the PH20 gene was sequenced and found to be similar to Bee HYAL (Gmachl and Kreil, 1993) that it was suspected, and later confirmed, to have HYAL activity (Gmachl *et al.*, 1993). PH20 is now thought to play a role in the two distinct processes of cumulus penetration and zona recognition (Hunnicutt *et al.*, 1996; Lin *et al.*, 1994). PH20 is a highly glycoslated 53 kDa that utilises a glycosylphosphatidylinositol (GPI) anchored to locate the protein to the cell surface. PH20 has a broad bimodal pH range of activity

between 4.5 and 7.5 (Li *et al.*, 1997; Yudin *et al.*, 2001) and not only degrades HA, but also has specificity toward CS and distinct domains of DS (Knudson *et al.*, 1984).

Expression of PH20 was previously thought to be highly restricted to the testis (Jones *et al.*, 1995). However, PH20 expression has been detected in connective tissues (El Hajjaji *et al.*, 2005), the female reproductive tract (Zhang and Martin-DeLeon, 2003) and cancer cells (Liu *et al.*, 1996; Madan *et al.*, 1999) and is therefore suspected of playing a diverse role in a range of biological processes. PH20 is localised to the plasma membrane though a GPI anchor and is thought to mediate intra-cellular processes through a HA-binding domain that is independent of the HYAL domain (Cherr *et al.,* 2001). Thus, the role of PH20 in non-testicular tissue may utilise the alternative non-HYAL functions.

1.2.2.2 Hyaluronidase-1

HYAL-1 was first described as the human plasma HYAL (Bonner and Cantey, 1966). The production of monoclonal antibodies enabled the isolation of pure HYAL-1 and led to the cloning of the HYAL-1 gene (Frost *et al.*, 1997). Recombinant HYAL-1 (rHYAL-1) is a 57 kDa protein that degrades HA and has optimum activity at pH 3.5 (Frost *et al.*, 1997). HYAL-1 is expressed at a low level in many tissues: the highest expression is seen in the major parenchymal organs such as liver, kidney, spleen and heart (Csoka *et al.*, 2001). HYAL-1 can degrade sulphated and unsulphated gag, with a distinct preference for HA (Byers *et al.*, 2005).

HYAL activity is high in urine (Ginetzimsky, 1958). The predominant HYAL in urine (HYAL-1U) is a processed form of HYAL-1, in which 100 amino acids have been cleaved from a region near the carboxy terminus by two reactions (Figure 1.3). The resulting two polypeptide chains are bound by disulphide linkage, producing a 45 kDa pro-protein (Csoka *et al.*, 1997; 2001).

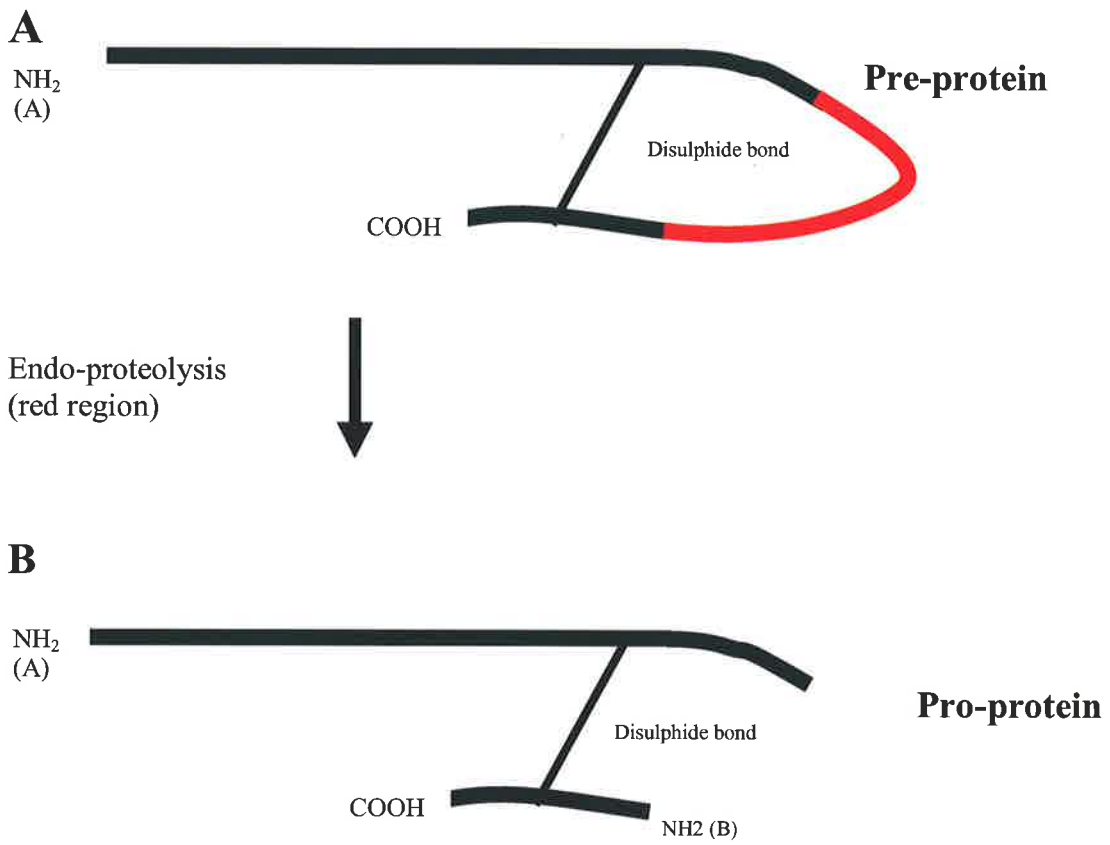

Figure 1.3 Urinary hyaluronidase-1

In urine, a 12 kDa fragment is cleaved from the unprocessed 57 kDa HYAL-1 (A) to form a processed 45 kDa HYAL-1U (B). The two peptides formed in the production of HYAL-1U remain bound through disulphide linkage. (Reproduced from Csoka *et al.*, 2001).

Splice variants of HYAL-1 (HYAL-1s) were identified by northern blot analysis (Triggs-Raine *et al.*, 1999) and subsequently cloned and expressed (Lokeshwar *et al.*, 2002). HYAL-1s has a range of splicing events within the first intron or a deletion of exon 2, resulting in a range of recombinant proteins that differ in size from 50 to 10 kDa. Only HYAL-1s variants that encode 50 and 47 kDa proteins have HYAL activity; however, the substrate specificity of each splice variant against gags other than HA and the tissue expression profile of HYAL-1s have not been fully examined: each HYAL-1s may have an entirely different function to the well-characterised HYAL-1.

A deficiency in HYAL-1 has been shown to result in the lysosomal storage disorder designated MPS IX (Triggs-Raine *et al.*, 1999). Clinical presentation of the only reported case of MPS IX is that of a child with short stature, multiple peri-articular soft tissue masses, mildly dystrophic craniofacial features and no observed neurological impairment (Natowicz *et al.*, 1996). Histological analysis of affected tissues revealed lysosomal storage of HA in macrophages and to a lesser extent in fibroblasts (Natowicz *et al.*, 1996). The disorder was biochemically characterised by the complete absence of HYAL activity in patient plasma and genetic analysis revealed a mutation in both HYAL-1 alleles (Natowicz *et al.*, 1996).

The single case of a MPS IX patient occurred in the complete absence of HYAL activity in plasma, yet it resulted in only a mild phenotypic presentation. Patients with aberrations in serum HYAL and HA levels displayed a similar phenotypes to those patients with MPS, although they do not have defining characterisitic of mucopolysaccharidurias that would be found in an MPS (Fiszer-Szafarz *et al.*, 2005). However, none of the patients presented in this study totally lack HYAL activity (Fiszer-Szafarz *et al.*, 2005).

These data indicate that disorders involving aberrations in serum HYAL-1 may be much more prevalent than the first reported case of MPS IX, and milder patients who have residual HYAL activity may be very difficult to detect because they present with a broad spectrum of clinical symptoms similar to that of MPS disorders.

Deficiency of an endo-glycohydrolase would not be expected to result in gag storage, since the exo-lytic enzymes β-N-acetylglucosaminidase and β-glucuronidase are still theoretically capable of turning over any stored gag from its non-reducing terminus. However, there may be some restriction on the size of gags that are recognised by these exo-hydrolases, and large gags such as HA may require an initial endolytic cleavage for efficient lysosomal degradation to occur.

This first case of MPS IX with a definite mutation in HYAL-1 stresses the importance of endo-lytic catabolism for the complete turnover of HA, demonstrating that in cases of MPS IX, HYAL-1 cleavage is the rate-limiting step in HA degradation due to its constituent monosaccharides. These data could be indicative of the crucial role that HYAL-1 plays in a more general mechanism of HA turnover.

1.2.2.3 Hyaluronidase-2

Hyaluronidase-2 (HYAL-2) was identified as an mRNA transcript with a theoretical translation product similar to other mammalian HYALs (Figure 3.2). The gene was then cloned and expressed (Lepperdinger *et al.*, 1998). Recombinant hyaluronidase-2 protein (rHYAL-2) localised to lysosomes and was found to have a pH optimum of 4 (Lepperdinger *et al.*, 1998). rHYAL-2 was shown to possess a novel specificity, degrading only high molecular weight HA into 20 kDa (approximately 80 saccharides) intermediate fragments (Lepperdinger *et al.*, 1998). A model of HA catabolism has been proposed where HYAL-2

degrades HA to 20 kDa intermediate fragments, which are then degraded to smaller fragments by HYAL-1 (Csoka *et al.*, 2001). However, the 20 kDa (Lepperdinger *et al.*, 1998) have also been produced by partial digestion with bovine testis HYAL (Rai *et al.*, 2001). These results demonstrate that the 20 kDa HA fragments may represent relatively stable intermediates formed during normal HA metabolism by all HYALs, and are not necessarily the product of a HYAL-2 specific activity.

An alternative function for rHYAL-2 also been shown to be a GPI-anchored cell surface protein that acts as a receptor for Jaagsiekte sheep retrovirus (JSRV) (Rai *et al.*, 2001). The GPI-anchored variant of HYAL-2 did not degrade HA (Rai *et al.*, 2001).

The variability in activity and localisation of rHYAL-2 that is produced by different groups can be explained through differences in expression systems, such as the choice of cell line (discussed further in section 4.1). Alternatively, these seemingly conflicting views about the action of HYAL-2 could both be correct, with HYAL-2 existing in two different forms (Lepperdinger *et al.*, 2001), i.e. as a GPI cell surface-anchored molecule involved in the internalisation or binding of HA and other related molecules, and also as a non-GPI-anchored lysosomal glycohydrolase HYAL-2 that degrades HA to 20 kDa intermediates.

1.2.2.4 Hyaluronidase-3 and hyaluronidase-4

Little is known about either hyaluronidase-3 (HYAL-3) or hyaluronidase-4 (HYAL-4) except that they encode proteins with sequences that are very similar to other mammalian HYALs (Csoka *et al.,* 1999). On the basis of this similarity they are postulated to belong to the HYAL family and are assumed to possess endo-glucosaminidase activity (Csoka *et al.*, 1999).

Based on unpublished data, Csoka *et al* (2001) have stated that HYAL-4 is a chondroitinase that lacks activity against HA. rHYAL-3 produced in an *in vitro* translation system has been shown to exhibit HYAL activity (Lokeshwar *et al.*, 2002), but no other reports have been made regarding the activity of recombinant or native HYAL-3 or HYAL-4.

This raises the question of whether HYAL-3 has any enzymatic properties associated with the lysosome or has a redundant activity. Characterisation of tissue gags in this mouse model is one of the aims of this thesis and may shed light on the function of this poorly characterised enzyme.

1.2.2.5 Hyaluronidase pseudogene-1

The sequence of hyaluronidase pseudogene-1 (HYAL-P1) is very similar to the other HYALs except for two deletions that encodes a premature stop codon and result in a truncated HYAL-P1 protein without many of the structural domains possessed by the other mammalian HYALs (Flannery *et al.*, 1998). HYAL-P1 is an expressed pseudo gene, with low levels of mRNA expression detected in all tissues examined (Csoka *et al.*, 1999). The mouse homologue, *hyal-p1* (similarity 68%) may encode a functional protein as the truncating stop codon has not been conserved (Csoka *et al.*, 2001). This suggests there may be a redundancy of the HYALs across the species, with the possibility of functional overlap between the HYALs such that HYAL-P1 is no longer required in humans.

1.2.2.6 Meningioma hyaluronidase

The meningioma hyaluronidase (MGEA-5) gene is located on chromosomal band 10q24.1-24.3. Phylogenetic analysis of HYALs demonstrated that MGEA-5 is homologous to a HYAL found in *C. elegans* and shares no significant sequence similarity to the paralogous

mammalian HYAL (Heckel *et al.*, 1998). MGEA-5 was first identified as a gene whose expression was elevated in a meningioma (Heckel *et al.*, 1998).

It was also shown that 20% of meningioma patients generated antibodies against recombinant MGEA-5 protein. Recombinant MGEA-5 protein produced in bacteria possessed a HYAL activity at a neutral pH (Heckel *et al.*, 1998). MGEA-5 exists as a 135 kDa cytoplasmic/cytosketetal protein; there is also a 75 kDa variant of MGEA-5 (MGEA-5s) that results from alternative splicing and localises to the nucleus (Comtesse *et al.*, 2001; Gao *et al.*, 2001).

MGEA-5 and MGEA-5s were not thought to represent simple HYALs, but were ascribed the alternative function of involvement in generating O-linked N-acetylglucosamine modifications (O-GlcNAcase) (Gao *et al.*, 2001; Comtesse *et al.*, 2001). O-GlcNAc modification of proteins occurs exclusively in the cytoplasm and nucleoplasm (Comtesse *et al.*, 2001; Kreppel *et al.*, 1997; Akimoto *et al.*, 1999); therefore the role of MGEA-5/MGEA-5s as an O-GlcNAcase is consistent with the localisation of recombinant MGEA-5 to the cytoplasm or nucleus, as is its neutral pH optimum (Gao *et al.*, 2001; Comtesse *et al.*, 2001).

The properties of the human hyaluronidase enzyme discussed in sections 1.2.2.1-1.2.2.6 are summarised in table 1.1.

Enzyme	Activity	Intra-cellular localisation	Additional information
HYAL-1	Endo-glycosaminidase end product: tetrasaccharide	Lysosomal	Studied further in this thesis Plasma HYAL Deficiency causes MPS IX
HYAL-2	Endo-glucosaminidase end product: 80 saccharide units (20 kDa)	Lysosomal	GPI-anchored form has no HYAL activity and is the JSCV receptor
HYAL-3	Unknown	Unknown	Studied further in this thesis
HYAL-4	Possible Chondroitinase	Unknown	None
PH20	Endo-glucosaminidase end product: tetrasacchide chondroitinase	Cell membrane Intra-cellular variant	Sperm HYAL GPI-anchored
MGEA	O-GlcNAcase	Cytoplasmic/ cytosketetal Nuclear variant	Elevated in meningioma
Bee HYAL	Endo-glucosaminidase end product: tetrasaccharide	Extra-cellular	Bee venom Crystal structure $(\alpha/\beta)_8$ TIM barrel
Leech HYAL	Endo – glucuronidase	Unknown	Leech HYAL

Table 1.1 Summary of hyaluronidase properities

1.3 Hyaluronan synthases

1.3.1 Introduction to hyaluronan synthases

The first HAS characterised was from the bacterium *Streptococcus pyrogenes*. Subsequently, three HAS enzymes have been identified in humans that share amino acid similarity (Itano and Kimata, 1996; Spicer *et al.*, 1997; Watanabe and Yamaguchi, 1996). Homologues have been identified for many other vertebrates, including mouse (Yoshida *et al.*, 2000; Spicer *et al.*, 1996; 1997), chicken (Spicer and McDonald, 1998) and frog (DeAngelis and Achyuthan, 1996; Meyer and Kreil, 1996). Each of the three HAS displays a distinct expression pattern, both in the developing embryo and adult (Spicer and McDonald, 1998). Expression patterns for each of the vertebrate HASs are highly conserved between species, demonstrating that these genes are not only similar in sequence, but represent functional homologues (Spicer and McDonald, 1998).

The precise function of the different HASs has not been fully characterised. Variation in protein sequence results in significant differences in function. The characteristics that define differences between the HAS enzymes include the length of the HA chain synthesised, the rate at which HA is synthesised, its ability to associate and interact with other proteins and its ultimate intra-cellular or extra-cellular location (Spicer *et al.*, 1997). This level of sophistication in the control of HA synthesis highlights the fundamental and diverse roles played by HA, a gag of the simplest repeating disaccharide structure.

Unlike the other gags, which are synthesised on a core protein, HA is synthesised as a free gag (Prehm, 1984). HA synthesis is proposed to occur through a novel swinging pendulum elongation model (Weigel, 2005) (Figure 1.4). This model proposes that the growing HA chain is elongated inside the plasma membrane through the addition of UDP-sugars to the

reducing terminus of the HA chain, the growing sugar chain is then extruded through the membrane pore into the ECM. However, the swinging pendulum elongation model has not been unequivocally proven as the only route to HA production. Intra-cellular cytoplasmic and nuclear HA has been postulated to result from the specific expression of HAS inside cells (Evanko and Wight, 1999). HA transporters have also been identified in bacteria and are required to actively transport HA from these cells (Ouskova *et al.*, 2004). A model of HA synthesis involving HA transporters could also occur in vertebrate cells, although this model still requires a HAS for HA synthesis. The HA transporter model would permit the active transport of HA, allowing access to stored intra-cellular pools of HA or the internalisation of extruded HA.

1.3.2 Hyaluronan synthase-1

HAS-1 was first identified in a mouse mammary carcinoma cell line that was deficient in the expression of an HA matrix. Transfection of cDNA that expressed the homologous HAS from *Xenopus laevesi* (DG42) or streptococcal HAS rescued the HA-deficient phenotype (Itano and Kimata, 1996). The use of degenerative PCR primers allowed the subsequent cloning of the isoenzymes HAS-2 and HAS-3 (Watanabe and Yamaguchi, 1996; Spicer *et al.*, 1996).

Subsequent studies of the HASs have shown that the rate and size of HA synthesis depends upon the cellular system in which the HAS is expressed (Itano *et al.*, 1999; Brink and Heldin, 1999); thus, HASs are probably not the only regulators of HA synthesis, and the process is likely to be influenced by other proteins (Weigel *et al.*, 1997). Site-directed mutagenesis of HAS-1 (Yoshida *et al.*, 2000) demonstrates that residues in the cytoplasmic central loop domain, conserved among various HAS proteins, are essential for HA oligosaccharide synthesis (Yoshida *et al.*, 2000).

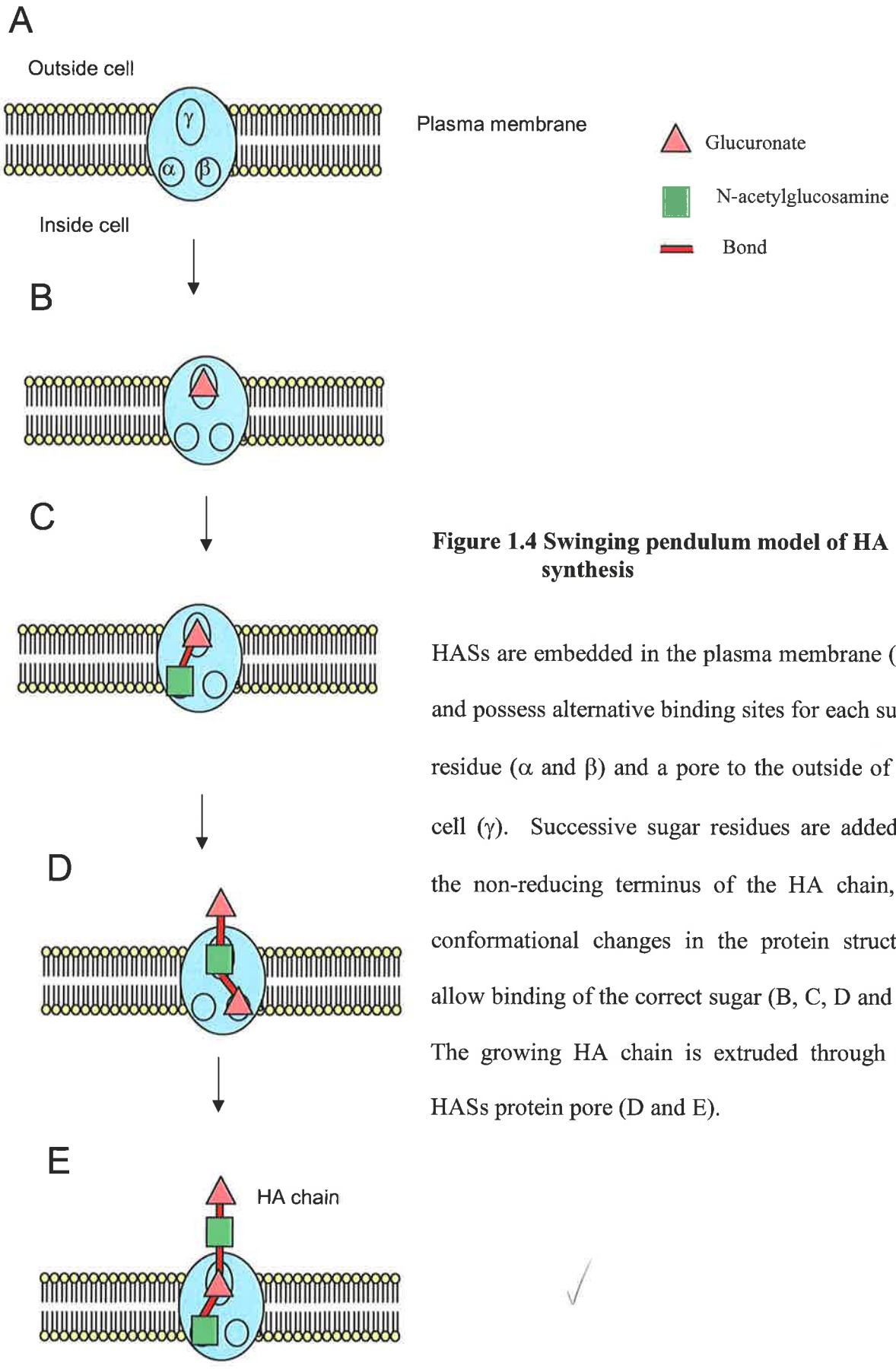

Figure 1.4 Swinging pendulum model of HA synthesis

HASs are embedded in the plasma membrane (A), and possess alternative binding sites for each sugar residue (α and β) and a pore to the outside of the cell (γ). Successive sugar residues are added to the non-reducing terminus of the HA chain, as conformational changes in the protein structure allow binding of the correct sugar (B, C, D and E). The growing HA chain is extruded through the HASs protein pore (D and E).

1.3.3 Hyaluronan synthase-2

HAS-2 was simultaneously cloned and expressed by two groups who both identified an enzyme that could synthesis and designated it HAS-2 (Watanabe and Yamaguchi, 1996, Spicer *et al.*,1996).

HAS-2 expression during development has been examined by *in situ* hybridisation in the normal mouse embryo and by the construction of a knock-out mouse model (McDonald and Camenisch 2003; Camenisch *et al.*, 2000). HAS-2 was found to be the most widely expressed HAS in the mid-gestation period of the mouse (Camenisch *et al.*, 2000). HAS-2 expression is essential for life and the HAS-2 null mice die in utero at E9.5 from cardiac malformation (Camenisch *et al.*, 2000). HA synthesis is a critical step in cumulus oophorus expansion in the pre-ovulatory follicle (Fulop *et al.*, 1997). HAS-2 is thought to be primarily responsible for the HA produced in this process since it was initially absent in ovarian cumulus cells but was expressed in higher amounts as HA synthesis occurs (Fulop *et al.*, 1997).

Expression of HAS-2 in COS-1 cells has been shown to result in the synthesis of a broad range of HA fragments that are generally of a much larger size than that synthesised by other HAS's (Itano *et al.*, 1999). The high molecular weight HA is important for the formation of ECM PGs complexes such as those present in cartilage (Morgelin *et al.*, 1994). HAS-2 is the most abundant HAS in cartilage-forming chondrocytes (Nishida *et al.*, 1999). Anti-sense inhibition of HAS-2 results in a decrease in the diameter of a cell-associated matrix and a decrease in the capacity to retain newly-synthesised PG, thus further promoting a role for HAS-2 in cartilage development (Nishida *et al.*, 1999). Epidermal growth factor-induced production of HA in keratinocytes has been shown to coincide with the sole up-

regulation of HAS-2 mRNA (Pienimaki *et al.*, 2001), suggesting that HAS-2 plays a role in the increase in peri-cellular and intra-cellular HA in keratinocytes.

1.3.4 Hyaluronan synthase-3

HAS-3 is generally ubiquitously expressed in adult tissue and shows a distinct increase in expression during gastrulation of the developing embryo (Spicer and McDonald, 1998) Recombinant HAS-3 produces lower molecular weight HA than HAS-1 or HAS-2 in transfected cells (Brink and Heldin, 1999; Itano *et al.*, 1999.) Varying the molecular weight of HA can alter its biological function, for example the lower molecular weight HA produced by HAS-3 is more effective at activating intra-cellular signaling pathways (Camenisch *et al.*, 2000, Slevin *et al.*, 1998, Oliferenko *et al.*, 2000), impling that the function of HAS-3 may be to produce the smaller HA fragments that have been shown to mediate intra-cellular signaling (McKee *et al.*, 1996).

1.3.5 Function of multiple hyaluronidase synthases

The existence of multiple HASs and HYALs generates a complex array of genes available to the cell to synthesise and degrade HA. The recombinant expression of HAS-1, HAS-2 and HAS-3 has revealed that each enzyme has distinct properties, with differences in their requirements for UDP precursor sugars, elongation rates and polymer size (Itano *et al.*, 1999). The lethal clinical outcome in the HAS-2 knock-out mouse suggests that the function of HAS-2 is unique and vital for life (McDonald and Camenisch, 2003). Knock-out models of the other HAS are not lethal and show no abnormal phenotype, suggesting that HAS-2 aside, HASs may to some extent be functionally redundant (Spicer and McDonald, 1998; Camenisch *et al.*, 2000). However, their unique enzymatic properties coupled with differences in cell and tissue expression patterns suggests, that, despite their overlap, HASs have evolved distinct functions.

1.4 Osteoblast biology

1.4.1 Introduction to bone

Bone is a composite material composed of cells embedded in a collagen-rich matrix that has become hardened due to the presence of calcium phosphate crystals. Bone is not brittle, but flexible, making it ideal for its role in supporting the body and protecting organs. Bone also serves as a reservoir for calcium, magnesium and phosphate, which are crucial for development, maintenance and function of many cells and tissues (Glimcher, 1992). Turnover of bone is constantly occurring through a balance of synthesis and degradation, a process that allows for bone growth, remodelling and repair.

Bone can be divided into organic matrix (70%), inorganic matrix (22%) and water (5-8%) (Triffit, 1980; Glimcher, 1992). The inorganic matrix is composed of an analogue of hydroxyapatite, $Ca_{10}(PO_4)_6(OH)_2$, which may contain a number of ionic substitutions such as carbonate, magnesium, potassium, fluoride, acid phosphate and citrate (Posner, 1985; Rey *et al.*, 1991; 1995; Glimcher, 1992). The organic matrix is composed of cells embedded in an extra-cellular matrix of predominantly type I collagen (90%) (Robey and Boskey, 1996). Other collagens (type II, V, IX and XI), glycoproteins, PGs, HA and regulatory factors constitute approximately 8% of the organic matrix (Triffit, 1980; Einhorna, 1996); the remaining 2% of the organic matrix is made up of bone cells; osteoblasts, osteoclasts, osteocytes and bone-lining cells (Buckwater *et al.*, 1996; Einhorna, 1996).

1.4.2 Bone formation

Bone formation is continuously occurring as the bone is remodeled during growth and maturity (Robey, 1992). Bone is formed through three distinct processes: endochondral ossification, intra-membranous ossification or appositional growth. Endochondral

ossification involves the production of bone on a cartilaginous template (Reddi, 1981); intra-membranous ossification arises from the aggregation of undifferentiated mesenchymal cells that differentiate into osteoblasts and secrete a matrix destined to become bone (Reddi *et al.*, 1987); and appositional bone formation occurs through the synthesis of osteoiod on an existing bone surface, which is subsequently mineralised (Buckwater *et al.*, 1996).

1.4.3 Matrix mineralisation

Bone and teeth are the only tissues that are mineralised under normal conditions. Mineralisation or calcification in other tissues is considered to be an abnormal state (Karsenty, 1998). Osteoblasts are the bone-forming cells, but the precise mechanism by which the matrix is transformed to hardened bone remains elusive. However, there are two factors that control bone formation: a stimulator is required to induce bone formation, and an inhibitor is required to stop mineralisation in non-calcified tissues.

Mineral nucleators are proteins that initiate bone formation and are expressed in the ECM at the beginning of mineralisation (Glimcher, 1989; Hunter *et al.*, 1996). Many of the genes expressed by bone-forming osteoblasts, such as bone sialoprotein, osteonectin and osteopotin, have been shown to have a role in the initiation of mineralisation. However, mice deficient in any one of these genes do not show any adverse mineralisation abnormalities, thus no single nucleator has absolute control over the initiation of mineralisation (Aubin *et al.*, 1996; Gilmour *et al.*, 1998; Liaw *et al.*, 1998).

Matrix vesicles (plasma membrane-derived organelles) are thought to play a role in mineralisation (Christoffersen and Landis, 1991). They contain several molecules that bind free calcium and can act as bone nucleators (Anderson, 1995; Boskey, 1996; Boskey *et al.*, 1997). Matrix vesicles are-secreted by osteoblasts *in vitro* (Montessuit *et al.*, 1995) and have

been identified at the mineralisation front in developing bone *in vivo* (Christoffersen and Landis, 1991). Thus, matrix vesicles have both spatial and temporal expression that coincides with bone formation, implying a role in bone mineralisation.

When combined in solution with calcium and phosphate ions, collagen is an *in vitro* initiator of mineralisation (Glimcher *et al.*, 1957). The *in situ* deposition of apatite–like material also occurs at specific sites along collagen bundles (Glimcher, 1984; Miller, 1984). This ability to induce mineralisation is not exclusive to collagen, and has also been shown for elastin and fibronectin (Seligman *et al.*, 1975; Daculsi *et al.*, 1999). These mineral-inducing molecules are present in other tissues, suggesting that inhibitors of mineralisation are present to stop the calcification of these tissues.

Matrix γ-carboxyglutamic acid protein (MGP) is a mineral-binding protein found in arteries and cartilage but not bone (Luo *et al.*, 1997). MGP knock-out mice display inappropriate mineralisation in various tissues, which suggests its function is to inhibit mineralisation in these tissues. The osteocalcin knock-out mouse also displays a phenotype of excessive mineralisation, suggesting that it also plays a role in the inhibition of inappropriate mineralisation (Ducy *et al.*, 1996).

1.4.4 Role of proteoglycans and glycosaminoglycan in mineralisation

The inhibition of hydroxyapatite formation and growth has been demonstrated *in vitro* by PGs derived from bovine nasal cartilage. The hydrodynamic size and high charge density of these PGs is associated with their ability to inhibit hydroxyapatite formation by interfering with the diffusion rate of the calcium and phosphate ions required for mineralisation (Chen *et al.*, 1984; Chen and Boskey, 1985). PGs may interact with the active growth sites on

hydroxyapatite nucleators; however, *in vivo,* PGs most likely regulate hydroxyapatite growth through many different complex mechanisms (Chen and Boskey, 1985).

1.4.5 Role of small leucine-rich proteoglycans in mineralisation

Small leucine-rich PGs (SLRPs) are important a sub class of secreted PGs define by their small size (varies between 36 and 40 kDa), conserved amino acid sequence, C-terminal leucine-rich motifs and N-terminal terminal varible region (Hocking *et al.*, 1998; Fisher *et al.,* 1989; Iozzo *et al.,* 1999). Biglycan and decorin are SLRPs that are highly expressed in the ECM of bone: biglycan is expressed at phases relating to cell proliferation and initiation of mineralisation, whereas decorin is expressed during early matrix synthesis and throughout mineralisation (Waddington *et al.*, 2003).

The type of gag chains attached to these core proteins varies, and a switches from DS chains to CS chains as mineralisation progresses (Waddington *et al.*, 2003). Gag chains can affect the ability of SLRPs to interact with growth factors (such as TGF-β), thereby regulating the ability of growth factors to affect bone cells by sequestering them to the ECM (Hildebrand *et al.*, 1994). Decorin SLRP, which display a high proportion of CS, have been shown to interact with hydroxyapatite and calcium ions, regulating crystal nucleation, growth size and morphology (Sugars *et al.*, 2003; Boskey *et al.*, 1997). Therefore, SLRPs could affect the proliferation state of osteoid tissues by affecting the formation of a collagenous framework that is supportive of mineralisation. The biglycan knock-out mouse shows an osteoporotic phenotype, with decreased bone formation and shortened bones (Xu *et al.*, 1998). A double knock-out mouse of both biglycan and decorin showed a more severe decrease in bone mass (Corsi *et al.*, 2002), further supporting the important positive role that SLRPs play in mineralisation.

1.4.6 Role of hyaluronan in mineralisation

The precise functional role of HA in bone is not known, although HA has been established as being present and important in many aspects of bone formation. HA accumulates in the early stage of fracture repair and during early limb development (Maurer and Hudack, 1952; Toole and Gross, 1971). The amount of HA in the ECM surrounding growth plate chondrocytes varies greatly as they progress towards hypertrophy (Noonan *et al.*, 1996; Pavasant *et al.*, 1994)

The effect of endogenous HA on a number of cell types has been studied. The size of HA defines its effect on cultured osteoblast cells: higher molecular weight HA plays a structural role in the ECM (Knudson and Knudson, 1993), whereas low molecular weight HA mediates cell signaling via a receptor-mediated process (Evanko and Wight, 1999; Collis *et al.*, 1998). The addition of high molecular weight HA (900 – 2300 kDa) to osteoblast culture enhances osteogenic and osteoinductive properties of the cells, increasing mineralisation in a dose-dependent manner (Huang *et al.*, 2003). Intermediate molecular weight HA (60 kDa) stimulates proliferation of osteoblasts (Huang *et al.*, 2003), whereas low molecular weight HA (30 kDa) has been shown to increase the number of bone-forming colonies in an *in vitro* model of intra-membranous osteogenesis (Pilloni and Bernard, 1998).

Cambrium periosteal pre-osteoblasts stain intensely for HA along their lacunae walls, whereas the mature periosteal lining osteoblasts do not (Midura *et al.*, 2003). Thus HA may have a role in coating the matrix for fluid exchange into the lacunare-canalicular system or serve to protect the osteocytes from direct contact with the mineralised phase of the bone.

HA is an important component of ECM in many tissues. Thus, HA in bone could be performing its established roles such as cell-matrix and cell-cell adhesion (Thomas *et al.*,

1993, 1992), expansion and hydration of the ECM to capture space destined to become bone (Fisher, 1985), affecting the in-growth of blood vessels (West *et al.*, 1985) or modulating growth factors (Bertolami and Messadi, 1994). HA binds PGs and other proteins to provide a dynamic scaffold that gives structure and form to the tissue. Thus, depending on the size, localisation and association of other proteins, HA can play diverse roles in the mineralising matrix, acting as an inhibitor, nucleator or to capture space.

Any HA present in the pre-mineralised matrix surrounding osteoblasts must be both synthesised and then removed as the matrix is mineralised. Understanding which genes are directly involved in HA turnover during mineralisation is an important aim of this thesis.

1.5 Aims

The aims of this study are to define the roles that HYALs play in the normal turnover of HA. The immediate goals of this project are to:-

1) Perform bioinformatics to predict the characteristic of human hyaluronidases.
2) Clone, express and characterise recombinant human HYAL-1 and HYAL-3 as candidate genes for the endolytic degradation of HA.
3) Determine the tissue distribution of gag in HYAL-3 knock-out mice.
4) Determine which HYALs and HASs are expressed in osteoblasts.
5) Determine the amount of gags, specifically HA, that are synthesised in mineralising osteoblasts.

Chapter 2

Methods

2.1 Molecular Biology

2.1.1 Synthesis of DNA oligonucleotides

All synthetic oligonucleotides were purchased as desalted 40 nM preparations (GIBCO BRL, Rockville, MD, USA). Each lyophilised oligonucleotide was resuspended in 1 mL sterile H_2O and stored at -20°C.

2.1.2 Standard cloning PCR protocol

Each PCR mix consisted of 1 unit of Platinum Taq DNA polymerase Pfx High Fidelity (Invitrogen, Carlsbad, CA, USA), 1 x Pfx buffer, 200 μM each dNTP, 10 pM sense primer and 10 pM antisense primer (section 2.1.11.2). Typical PCR conditions consisted of denaturation at 94°C for 30-sec, annealing at 50-65°C for 30-sec and elongation at 72°C for 2-min; these steps were cycled between 25 and 35 times. An additional elongation of 2-min at 72°C was then performed at the end of the cycling.

2.1.3 Restriction digest

Restriction digests were performed using the conditions provided by the appropriate manufacturer (Roche, Basel, Switzerland, or New England Biolabs, Ipswich, MA, USA). Generally, 1 μg of DNA was digested with 2 to 10 U of enzyme in the recommended buffer for 3-h at 37°C. Digestion was confirmed though agarose gel electrophoresis (section 2.1.4).

2.1.4 Agarose electrophoresis

DNA electrophoresis was performed by combining 10 ng – 1 μg of DNA sample, 10 x 0.1 volumes of 10 X loading dye (0.1% (w/v) bromophenol blue, 50% (v/v) glycerol, 1% SDS, 100 mM EDTA, pH 8.0) and resolving these samples on agarose gels in Tris

EDTA buffer (TE buffer: 40 mM Tris, 2 mM EDTA, pH 8.5). Depending on the size of the DNA fragment to be analysed the agarose concentration gel ranged from 0.8 – 3% (w/v) and gels were run at 80-100 V for 30 – 9-min. Gels were then stained for 10-min in 10 μg/mL ethidium bromide and destained in dH_2O for 10-min. DNA was then visualised under UV light and the image recorded on a UniPro gel documentation system (Unitech, Cambridge, UK).

2.1.5 Purification of DNA from agarose gel

DNA was purified from 1 x TE agarose using the gel purification kit (Qiagen, Hilden, Germany) according to the manufacturer's instructions.

2.1.6 Preparation of electro-competent cells

DH5α *E. coli* cells were inoculated into 1 mL of *Luria-Bertani* broth (LB; 10 g/L trypton, 5 g/L yeast extract, 10 g/L NaCl), autoclaved and grown at 37°C overnight. This 1 mL culture was transferred 200 mL LB and grown at 37°C with aeration until OD_{Ab} 600 nM was 0.2. The cells were centrifuged at 2500 x g for 10-min at 4°C. The pellet was resuspended in 200 mL filter-sterilised ice-cold 80% (v/v) glycerol. Cells were centrifuged as previously described and washed with 80% glycerol. Cells were centrifuged at 2500 x g for 10-min at 4°C and the pellet was resuspended in 800 μL 80% glycerol (v/v). The resuspended cells were placed in 100 μL aliquots and stored frozen at –80°C until use.

2.1.7 Bacterial transformation

Twenty-five μL of electro-competent cells (section 2.1.6) were thawed on ice and added to 1 μg vector; 1.5 kV of electricity was applied across the electro-competent/vector mix in an Electrocell Manipulator BTX ECM395 (Genetronics Inc, San Diego, CA,

USA). Transformed cells were immediately taken up into 1 mL of broth and grown for 1-h at 37°C; 500, 50 and 5 μL of the culture was then plated on LB-agar containing the appropriate antibiotic (either 100 μg/mL ampicillin or 50 μg/mL kanamycin). Plates were allowed to dry, then inverted and incubated at 37°C overnight.

2.1.8 Plasmid preparation

2.1.8.1 Mini plasmid preparations

A single colony of transfected bacteria (section 2.2.8) was inoculated into 2 mL of LB containing the appropriate antibiotic (either 50 μg/mL kanamycin or 100 μg/mL ampicillin) and grown overnight at 37°C, with aeration. One mL of each cell suspension was pelleted by centrifugation for 2-min at 13000 g. The pellet was resuspended in 10 μL of LiCl lysis buffer (2.5 mM LiCl, 50 mM Tris-HCl, pH 8.0, 62.5 mM EDTA, 4% (v/v) Triton X-100) and extracted with an equal volume of phenol/chloroform (1:1). The lysate was vortexed for 30-sec and centrifuged at 13000 rpm for 5 min. The top aqueous layer (90 μL) was transferred to a new tube and 60 μL isopropanol added, mixed by inversion and then centrifuged at 13000 rpm for 10-min. The DNA pellet was washed with 70% ethanol and then air-dried. The pellet was resuspended in 20 μL H_2O and stored at –20°C until analysis.

2.1.8.2 Midi plasmid preparations

Large-scale, highly pure DNA preparation was carried out using the Midi Prep Kit following the manufacturer's instructions (Gibco BRL Life Technologies, Rockville, MD, USA).

2.1.9 TOPO cloning

PCR was performed using gene-specific primers (section 2.1.11.2; HYAL-3-15 and HYAL-3-17) and the Platinum Taq Pfx DNA polymerase (Invitrogen, Carlsbad, CA, USA) with an annealing temperature of 55°C (all other conditions were as per-section 2.1.2). The PCR product was then incubated with 0.5 U standard Taq polymerase (Roche, Basel, Switzerland) and 2 M adenosine triphosphate at 72°C for 15-min and then gel-purified (sections 2.1.4 and 2.1.5). Twenty ng purified PCR product was mixed with 0.5 μL of pcDNA1 TOPO vector (Invitrogen, Carlsbad, CA, USA) and incubated at room temperature for 5-min and then transformed into DH5α *E. coli* (section 2.1.7).

2.1.10 DNA ligation

Plasmid vector and insert DNA had complementary blunt or sticky ends generated by restriction digest (section 2.1.3). The restricted vector DNA was incubated in 1 x calf intestinal phosphatase (CIP) buffer and 1 U of CIP (Roche, Basel, Switzerland) at 37°C for 30 min, followed by incubation at 75°C for 15-min to inactivate the CIP. Twenty-five ng of vector was used for all ligations, with an insert: vector molar ratio of 3:1. Vector-only controls were performed to determine background levels of re-ligated vector. DNA mixtures were ligated with 1 U of T4 DNA ligase (Roche, Basel, Switzerland) in 1 x T4 DNA ligase buffer (Roche, Basel, Switzerland) at room temperature for 4-h and then incubated at 75°C for 15-min to inactivate the ligase. One mL ligation or control mix was transformed into bacteria by electroporation (section 2.1.7)

2.1.11 Automated DNA sequencing

One μg of template DNA was mixed with 3.2 pM primer (section 2.1.11.2), 4 μL Big Dye terminator V2 reagent (PerkinElmer Life and Analytical Sciences, Boston, MA,

USA) and made up to 20 µL with H_2O. The sequencing reaction was carried out for one cycle of 95˚C for 5-min, 25 cycles of 95˚C for 15-sec, 50˚C for 10-sec and 60˚C for 3-min. The sequencing reaction was then purified by precipitation with 180 µL of 80% isopropanol. The mix was incubated at room temperature for 15-min and centrifuged at 13000 g for 10-min. The pellet was washed in 100 µL of 70% ethanol and centrifuged at 13000 g for 10-min. The pellet was air-dried and analysed on a PE 9700 sequencer (PerkinElmer Life and Analytical Sciences, Boston, MA, USA) at the Institute of Medical and Veterinary Science (IMVS, Adelaide, SA, Australia).

2.1.11.1 Sequencing primers

Primer	Sequence (5' – 3')	Sense (+) or Anti sense (-)
HYAL-3 – 1	GGACCTCGAGAGGCCAGCATCAACATGTTC	+
HYAL-3 – 2	CTGCCACTCAATGCTCTGGG	+
HYAL-3 – 3	CCTGAGACCTGGCTTTGCTG	+
HYAL-3 - 4	ACGCTGCGGGTGGCCAG	+
HYAL-3 – 5	CCCAGGCTGCCACCTGCC	+
HYAL-3 – 6	TGGTGCTCTGGGGGGACCT	+
HYAL-3 - 7	TGGCCAGACGGCAGCCTTG	+
HYAL-3 - 8	GGTGACGGAGAAGAAAAGGAGATCTGC	-
HYAL-3 - 9	TGGTCGCCACGGTACCGCT	-
HYAL-3 - 10	TAGACCCTCCAAGGACAGCG	-
HYAL-3 - 11	GTGGGAACGGGCGTTGTGA	-
HYAL-3 - 12	TAAGGGACTGGACCTGGGAG	-
HYAL-3 - 13	CCCCCGTAGGGGGTCCGA	-
HYAL-3 - 14	ATGGTGTCCAGGCACTTGGG	-
HYAL-3 -15	CTTGATGAGACAGGGTGAGATCGCG	+
HYAL-3 -17	AGTACACTCAGGAGGTACCGTAGATCTCG	-
HYAL-3-GFP -1	GGGAATTCTTGCCACCATGACCACGCA	+
HYAL-3-GFP-2	CGGGATCCCGTACTGCTTCTTTAGGCCCAGG	-

2.1.12 Site-directed mutagenesis

Site-directed mutagenesis was performed using a site-directed mutagenesis kit and following the manufacturer's instructions (Stratagene, La Jolla, CA, USA). The primers used are listed in the table below.

2.1.12.1 Human hyaluronidase-3 His_6 tagged vector mutagenesis primers

Primer	Sequence (5' – 3')	Sense (+) or Anti-sense (-)
HYAL-3 His - 1	CCTAAAGAAGCAGTACATCATCACCATCAC	+
HYAL-3 His - 2	GTGATGGTGATGATGTACTGCTTCTTTAGG	-

2.2 Tissue culture

2.2.1 Standard cell culture technique

Cells were grown in the appropriate media supplemented with 10% (v/v) fetal bovine serum (FBS), 50 U/mL penicillin and 5 µg/mL streptomycin, and maintained at 37°C in 5% CO_2 and 95% humidity. MG63, HT1080, COS-7 and 293T cells were grown in DMEM media supplemented with 10% (v/v) FBS, 50 U/mL penicillin and 5 µg/mL streptomycin. CHO-K1 cells were grown in Ham's F12 media supplemented with 10% (v/v) FBS, 50 U/mL penicillin and 5 µg/mL streptomycin. Media was changed every 3-days. At confluence cells were harvested by washing with phosphate-buffered saline (PBS) and then incubated in 5 mL of 0.1% (w/v) trypsin/0.02% (w/v) Na_2EDTA at 37°C. Once cells had detached from the flask the trypsin/Na_2EDTA was diluted by the addition of 45 mL PBS. Cells were centrifuged at 1500 g for 5 min. The supernatant was discarded and the pellet resuspended in the appropriate media. Pelleted cells were frozen in media supplemented with 10% (v/v) FBS and 10% (v/v) DMSO using an isopropanol temperature gradient generated in a Mr Frosty (Nalgene Nunc, Rochester,

NY, USA) at -80°C for 48-h. Frozen cells were then transferred into liquid nitrogen for long-term storage.

2.2.2 Cell number determination

An aliquot of harvested cell suspension (section 2.2.1) was diluted 1:5 with PBS and 0.08% (w/v) trypan blue solution added. The number of viable cells (i.e. that excluded the trypan blue) was counted using a haemocytometer.

2.2.3 Transient mammalian transfection

293T cells were split (section 2.2.1) and grown to 80% confluence in a 90 mm Petri dish. Media was removed and replaced with fresh 10 mL DMEM and 10% (v/v) FBS. Fifty μg of plasmid DNA was resuspended in 450 μL of sterile water, and 50 μL of 2.5 M $CaCl_2$ added. Five hundred μL of 2x HEPES (0.28 M NaCl, 0.05 M N-2-hydroxyethylpiperazine-N'-2-ethanesulphonic acid, 1.5 mM Na_2HPO_4, pH 7.05) was placed in a sterile 10 mL Falcon tube. The liquid was bubbled with a mechanical pipette and the DNA/$CaCl_2$ mix was added drop-wise to the bubbling solution. The HEPES/DNA/$CaCl_2$ mixture was vortexed for 5-sec and incubated at room temperature for 20-min. The precipitate mix was added to the cells for 16-h. Cells were washed twice in PBS and grown for 24-h in 10 mL of DMEM supplemented with 10% (v/v) FBS, after which the media was replaced with neat DMEM (no FBS) and cells were either fixed for immuno-staining (section 2.2.5) or the media harvested for protein purification (section 2.2.7).

2.2.4 Fugene transfection

Both COS-7 and CHO-K1 cells were transfected using the same protocol, with the only difference being the type of media required: CHO-K1 required Ham's F12 supplemented with 10% (v/v) FBS, whilst COS-7 cells were grown in DMEM supplemented with 10% (v/v) FBS. Cells were split (section 2.2.1) and grown to 80% confluence in a 90 mm Petri dish. Thirty μL of Fugene6 (Roche, Basel, Switzerland) was added to 10 μg of sterile plasmid DNA (or a no DNA negative control); 520 μL of fresh media (no FBS) was added drop-wise to the Fugene6/DNA mix and incubated at room temperature for 10-min. Media was removed from the cells and the Fugene6/DNA/media was mixed by flicking and then added to the cells. The liquid was swirled to cover all cells and then incubated at 37°C for 30 min. Ten mL of media and 10% (v/v) FBS were added to the cells and incubated for 24-h. At this stage cells were either used for intra-cellular localisation (section 2.2.5), protein production (section 2.2.7) or placed into geneticin aminoglycoside antibiotic (G418) selection to isolate a stable expression cell line (2.4.2.1).

2.2.4.1 Stable fugene transfection

Cells were transfected using Fugene (section 2.2.4) and stable transfectants were isolated by selection with 750 μg/mL G418. The media was changed every 3-days for 2-weeks, at which point all cells in the no DNA negative control had died. Plasmid-transfected cells were trypsinised (section 2.2.1) and serial dilutions made across a 96-well plate. Separate single clone cells were chosen and expanded to confluence in a T_{75} flask. A second round of cloning was performed, as above. Clonal cells were then expanded and aliquots of cells were used to either localise intra-cellular recombinant protein (section 2.2.6) or to produce recombinant protein (section 2.2.7).

2.2.5 Immunohistochemical localisation of recombinant protein

CHO-K1 cell lines transiently-transfected with the vector pHYAL-3-His_6 were grown on chamber slides to 80% confluence and then fixed in 4% formaldehyde (v/v)/PBS for 45-min at room temperature. Cells were washed twice in methanol for 5-min and then air dried. The cells' non-specific binding sites were blocked by three successive 15-min incubations in 10% heat-inactivated FBS (v/v) (HiFBS)/PBS at room temperature. Cells were then incubated with the primary antibody (1μg/mL mouse monoclonal anti-His_6 antibody, 10% HiFBS (v/v)/PBS) for 3-h at room temperature, washed 3-times in 10% HiFBS (v/v)/PBS for 5-min at room temperature. Cells were incubated in the-secondary antibody (1 in 15 dilution sheep anti-mouse FITC-conjugated antibody (Silenus, Hawthorn, Vic, Australia), 10% HiFBS (v/v)/PBS) and then washed three times in PBS for 5-min at room temperature. Cells were covered in anti-fade (2% (w/v) 1,4-diazabicyclo (2,2,2) octane (DABCO), 20 mM Tris/HCl, pH 7.5) with the addition of 0.15% nuclear stain 4',6-diamidine-2'-phenylindole dihydrochloride (DAPI) (w/v); slides were cover-slipped and visualised on a fluorescence microscope with a WU (DM540) filter for DAPI nuclear stain and an NB (DM500) filter for green fluorescent protein (GFP).

2.2.6 Intra-cellular localisation of recombinant protein in live cells

CHO-K1 cells were stably transfected with pHYAL-3-GFP (section 2.2.2.5) and grown to 60% to 80% confluence in 2-well chamber slides (Nalgene Nuc, Rochester, NY, USA).

2.2.6.1 Endoplamsic reticulum staining

Stably transfected HYAL-3-GFP-expressing cells were washed in Ham's F12 media and incubated at 37°C with the 250 pM endoplasmic reticulum (ER) Tracker Blue-White DPX (Molecular Probes, Eugene, OR, USA) for 30-min. Cells were washed in 3-times 1 mL of Ham's F12 media and incubated at 37°C for 30-min. Cells were washed a further 3 times in 1 mL Ham's F12 media, cover-slipped with anti-fade (section 2.2.5) and visualised under a microscope with a WU (DM540) filter for ER-tracker and an NB (DM500) filter for GFP fusion protein.

2.2.6.2 Golgi staining

BODIPy-C5 sphingolipid (Molecular Probes, Eugene, OR, USA) was prepared as a 5 mM sphingolipid:5 mM bovine serum albumin (BSA) (1:1, molar ratio) solution in water. Cells expressing HYAL-3-GFP were washed in Ham's F12 media and incubated at 4°C with 1.25 μM BODIPy-C_5:BSA solution in Ham's F12 media for 30-min. Cells were washed 3-times with 1 mL of cold Ham's F12 media and incubated in fresh F12 media at 37°C for 30-min. Cells were then washed with Ham's F12 and cover-slipped with anti-fade (section 2.2.5) and visualised under a microscope with a WU (DM540) filter for BODIPy-C_5 and a NB (DM500) filter for GFP.

2.2.6.3 Mitochondrial staining

A 50 μg vial of Mitotracker Red (Molecular Probes, Eugene, OR, USA) was resuspended in 100 μL of DMSO to give a 1 mM stock solution. HYAL-3-GFP expressing cells were washed in fresh Ham's F12 media and incubated at 37°C for 30-min with 40 nM Mitrotracker Red (Molecular Probes, Eugene, OR, USA) diluted in media. Cells were washed with 3 times in 1 mL of fresh media, cover-slipped with anti-

fade (section 2.2.5) and visualised under a microscope with a WG (DM570) filter for Mitotracker Red (Molecular Probes, Eugene, OR, USA) and NB (DM500) filter for GFP.

2.2.6.4 Lysosomal staining

HYAL-3-GFP expressing cells were washed in fresh neat media and incubated in 50 nM of Lysotracker (Mocleular Probes, Eugene, OR, USA) for 30-min at 37°C. Cells were washed 3-times in 1 mL of fresh media, cover-slipped with anti-fade (section 2.2.5) and then visualised under a microscope with a WG (DM570) filter for Lysotracker and an NB (DM500) filter for GFP.

2.2.7 Recombinant protein production

Clonal stably-transformed cell lines (section 2.2.4) or transiently-transfected cell lines (section 2.2.3) at approximately 80% confluence were washed once with PBS and placed into neat media (no FBS) for 48-h; the media was collected and stored at 4°C. For the stable cell lines only, repeat collections were performed by placing the cells into media + 10% (v/v) FBS for 48-h, after which the procedure was repeated three times. Conditioned media collected from mammalian tissue culture was centrifuged at 2500 g to remove any cell debris and the supernatant was concentrated to approximately 100-fold using the Amicon mini filtration system, with a YM10 membrane (Millipore, Billerica, MA, USA) under N_2 pressure.

2.3 Protein biochemistry methods

2.3.1 TNT reaction

A cell-free transcription and translation reaction was performed using the TNT T7 Quick Couple *in vitro* transcription and translation kit (TNT) (Promega, Madison, WI,

USA) according to the manufacturer's instructions. Five hundred ng of vector was mixed with 5 μCi of ^{35}S-methionine (Amersham Pharmacia, Piscataway, NJ, USA) and 10 μL of TNT master mix (Promega). The TNT reaction was made to 12.5 μL with H_2O and incubated at 30°C for 90-min, then mixed and centrifuged at 13000 x g for 1-min. One μL of TNT reaction was run on a 4-20% gradient SDS gel (section 2.3.4) with ^{14}C molecular weight markers (Amersham Pharmacia, Piscataway, NJ, USA). The gel was then dried and exposed to x-ray film. TNT reaction mix was also used in an activity assay (sections 2.4.1, 2.4.2 and 2.4.3).

2.3.2 Talon chelation ion affinity protein purification

One mL Talon resin (Clontech, Mountain View, CA, USA) was washed twice with Talon wash buffer (100 mM Na acetate, 50 mM NaCl, 0.5 % (v/v) Triton-X-100, pH 7). Concentrated media (section 2.2.7) was added to the washed resin at room temperature for 1-h on a rocker. Bound resin was placed in 5 mL columns and washed 5 times in 1 mL Talon wash buffer, pH 7. Protein was eluted with 10 x 500 μL of Talon elution buffer (100 mM Na acetate, 50 mM NaCl, 0.5 % (v/v) Triton X-100, pH 5). Samples were subsequently analysed by Western blot (section 2.3.4) and fractions that contained His_6 recombinant protein were pooled and stored at 4°C.

2.3.3 Bradford protein assay

The Bradford protein assay was performed as previously described (Bradford, 1976). Briefly, samples were diluted to 0.8 mL with H_20. A BSA protein standard curve containing 1 μg to 20 μg was prepared to a final volume of 0.8 mL. Sample and standard were incubated with 0.2 mL of Bradford reagent (BioRad, Hercules, CA, USA), vortexed and incubated at room temperature for 30-min. The samples were then

vortexed and the absorbance measured at OD 595 nM on an Ultraspec II spectrophotometer (LKB, Uppsala, Sweden).

2.3.4 SDS polyacryamide electrophoresis

Protein samples were separated on 10% SDS-PAGE incorporating a 4% stacking gel using standard conditions (Laemmli *et al.*, 1970). Alternatively, a 4%-20% gradient PAGE was used (Gradipore, French's Forest, NSW, Australia) following the manufacturer's instructions.

2.3.4.1 Running gel

In brief, samples were prepared by the addition of 2 x loading buffer (1% SDS, 4 M urea, 80 mM Tris-HCl, 0.1% (w/v) bromophenol blue, pH 8.2) and denatured by boiling at 100°C for 10-min in the presence of 10 mM DTT. The gel was run at 50 mA, 200 V for 3-4-h in SDS-PAGE running buffer (25 mM Tris-HCL, 0.192 M glycine, 0.1% (w/v) SDS, pH 8.3).

2.3.4.2 Transfer gel

PVDF membrane was soaked in methanol for 2-min. Protein samples were then transferred from the gel to the PVDF membrane in a Hoefer transfer system (Hoefer, San Francisco, CA, USA) at 0.5 A for 2-h. The protein bound to the membrane was visualised by either general staining for all proteins (section 2.3.5) or protein-specific staining with antibodies (section 2.3.4.3).

2.3.4.3 Western blot antibody detection of protein

After transfer the membrane was washed 3-times in wash buffer (20 mM Tris, 150 mM NaCl) for 5-min at room temperature, then blocked for 1-h in 20 mM Tris, 150 mM

NaCl and 5% BSA (w/v) at room temperature. The membrane was incubated with monoclonal mouse anti-His_6 primary antibody (Roche, Basel, Switzerland) for 16-h at 4°C (1 in 250 dilution of antibody in 5% BSA, 20 mM Tris, 150 mM NaCl) and then washed 3-times for 5-min in wash buffer (20 mM Tris, 150 mM NaCl) before being incubated with the appropriate secondary HRP-conjugated antibody (Silenus, Hawthorn, Vic, Australia) (1 in 200 in 5% (w/v) BSA, 20 mM Tris, 150 mM NaCl). The membrane was washed 3-times for 5-min in wash buffer, and developed in 4-chloro-1-naphthol substrate (C-1-N) (0.01539% (w/v) C-1-N, 17% (v/v) methanol, 0.00033% (v/v) hydrogen peroxide). Substrate was prepared by dissolving 18 mg C-1-N in 20 mL of methanol; 5.1 mL of this solution was combined with 24.9 mL wash buffer and 9.9 µL hydrogen peroxide. Development was stopped by rinsing the membrane with several changes of dH_2O.

2.3.5 Coomassie-stained SDS-PAGE

After electrophoresis (section 2.3.4.1), the gel was fixed in 10% (v/v) acetic acid, 50% (v/v) methanol for 1-h and stained for 16-h in 0.25% (w/v) Coomassie brilliant blue (R250; Sigma, St. Louis, MO, USA), in 50 % (v/v) methanol and 10% (v/v) acetic acid. The gel was then destained 3-times for 10-min in 10% (v/v) acetic acid and 25% (v/v) ethanol.

2.3.6 N-Glycosidase F digestion

N-Glycosidase F (PNGase F) digestion of recombinant proteins was performed following the manufacturer's instructions (New England Biolabs, Ipswich, MA, USA). Briefly, recombinant protein was denatured with glycoprotein denaturing buffer at 100°C for 10-min. The reaction was supplemented with the addition of G7 buffer, 1%

(v/v) NP-40 and 500 U PNGase F, and incubated for 1-h at 37°C. Reaction products of PNGase digestion were separated on 4-12% SDS-PAGE (run as-per section 2.3.4) and visualised by Western blot (section 2.3.4).

2.4 Carbohydrate biochemistry methods

2.4.1 Hyaluronidase zymography

HYAL zymography was performed as previously described (Miura *et al.*, 1995). Recombinant HYALs (section 2.2.7) were run on a 7.5% PAGE gel incorporating 170 µg/mL HA (ICN, Irvine, CA, USA) using standard non-denaturing buffers and conditions (Miura *et al.*, 1995). After electrophoresis, the gels were incubated in 0.1 M Na formate, 150 mM NaCl at pH 3.5 or pH 6, at 37°C for 16-h. The gels were washed twice in Milli-Q H_2O and incubated at 37°C for 2-h in 0.02% (w/v) pronase and 0.01% (w/v) trypsin. The gels were washed twice in Milli-Q H_2O and then stained with 0.5% (w/v) Alcian blue in 3% acetic acid for 1-h. Gels were destained in 20% (v/v) EtOH and 10% (v/v) acetic acid 3-times for 10-min.

2.4.2 ELISA-based hyaluronidase assay

A microtitre-based assay for HYAL activity (Frost and Stern, 1997) was used to analyse HA activity.

2.4.2.1 Preparation of biotinylated hyaluronan

One mg/mL human umbilical cord HA (ICN, Irvine, CA, USA) was dissolved in 0.1 M 2-(N-morpholino) ethane sulphonic acid (MES), pH 5.0, and agitated for 24-h at 4°C; 0.18 mg/mL sulpho-NHS, 100 mM biotin hydrazide, 30 µM ethyl-3(3-dimethylaminopropyl) carbodiimide (EDAC) were added to the solution and which was then incubated overnight at 4°C. Unlinked biotin and reagents were removed by dialysis against 4 M guanidine hydrochloride followed by three changes of H_2O.

2.4.2.2 Immobilisation of biotinylated hyaluronan onto ELISA plate

L-Sulpho-NHS (0.184 mg/mL) was mixed with 0.2 mg/mL biotinylated hyaluronan (bHA) and 50 µL added to each well of a 96-well covalink-HN plate (Nalgene Nuc, Rochester, NY, USA); each well was coated with 10 µg of HA and 15 µg EDAC and the plate incubated overnight at 4°C. The plates were then washed 3-times in equilibration buffer (2 M NaCl, 50 mM $MgSO_4$, PBS).

2.4.2.3 Assay for hyaluronidase activity

bHA-bound covalink plates (section 2.4.2.2) were equilibrated with 100 µL/well acidic assay buffer (0.1 M formate, pH 3.7, 0.1 M NaCl, 1% (v/v) Triton X-100, 5 mM saccholactone) or neutral assay buffer (0.1 M formate, pH 7.2, 0.1 M NaCl, 1% (v/v) Triton X-100, 5 mM saccholactone). A standard curve was generated using a serial dilution of testicular HYAL that ranged from 78 x 10^{-3} to 1 U. Serial dilutions of the unknown sample were performed across the plate (neat to 10-fold dilution). The plate was incubated at 37°C for 1 h and the reaction stopped by the addition of 120 µL of 6 M guanine-HCl for 5-min at room temperature. The plate was washed 5-times in wash buffer (1 x PBS, 2 M NaCl, 50 mM $MgSO_4$, 0.05% (v/v) Triton X-100). HRP reagent (0.01% (v/v) streptavidin-conjugated HRP (Silneus, Hawthorn, Vic, Australia)/1% (w/v) BSA/PBS) was added and the plate incubated at room temperature for 30-min. The plate was then washed 5-times with wash buffer B and then developed with 100 µL per well with 2, 2 azine-di-3-ethlbenzhiazoline sulphonic acid (ABTS) substrate buffer (0.6 mM ABTS, 50 mM citric acid, 0.03% (v/v) H_2O_2, pH 4) for 15-min and the absorbance read at 415 nm on a Ceres 900 Hdi plate reader (BioTech Instruments Inc, Vermont, USA).

2.4.3 Substrate gel assay

Fifteen μg of the following gags, umbilical cord hyaluronan (HA; ICN, Irvine, CA, USA), desuphated chondroitin (Chon; Seikagaku Corporation, Chuo-ku, Tokyo, Japan), bovine trachea chondroitin sulphate A (C6S; Sigma, St. Louis, MO, USA), porcine intestinal dermatant sulphate (DS; Sigma, St. Louis, MO, USA), Chondroitin sulphate C shark cartilage (C4S; Sigma, St. Louis, MO, USA) , were digested at pH 3.5 (buffer: 20 mM Na acetate, 5 mM NaCl, pH 3.5) or pH 7 (buffer: 20 mM Tris, 5 mM NaCl, pH 7) at 37°C for 16-h. Digestions generally consisting of sample (TNT proteins, concentrated media from transfected cells or Talon-purified; sections 2.2.7, 2.3.1 and 2.3.2), 15 U of testicular HYAL and buffer only were used as postive and negative controls, respectively. Samples were resolved on agarose (section 2.4.3.1) or gradient PAGE (2.4.4).

2.4.3.1 Agarose gel analysis of hyaluronidase digests

HA digests were loaded onto a 0.8% agarose/TAE gel and run for 5-h at 50 V. The HA was stained with 0.005% (w/v) Stains All (3,3'-dimethyl-4,5,4'5-dibenzo-thiacarbocyanine) in 50% ethanol/dH2O for 16-h and destained with H_20 for 30-min. Digital images were generated using a UniPro gel documentation system (Unitec, Cambridge, UK).

2.4.4 Gradient-PAGE analysis of glycosaminoglycan digests

Digested gags were analysed on 30-40% gradient PAGE, as previously described (Turnbull and Gallagher, 1988). Briefly, PAGE gels were produced with a 30-40% gradient (30-40% (w/v) acrylamide, 0.4 M Tris-HCl buffer, pH 8.8) and incorporated a 10% stacking load gel (10 % (w/v) acrylamide, 0.125 M Tris-HCl, pH 6.8). Samples contained 1 μg gag in sample buffer (0.5M Tris HCl, pH 7, 10% (v/v) glycerol, 1%

(w/v) bromophenol blue, 1% (w/v) phenol red). The gels were placed into a Hoefer refrigerated gel apparatus (Hoefer, San Francisco, CA, USA) with gradient-PAGE running buffer (25 mM Tris-HCl, 192 mM glycine, pH 8.3). Samples were run at 100 V for 30-min and then at 350-400 V for 16-h. Gels were fixed in 0.5% (w/v) alcian blue/2% (v/v) acetic acid for 30-min and then destained in 30% (v/v) ethanol/10% (v/v) acetic acid 3-times for 5-min at room temperature. The gels were then washed with H_20 3-times for 5-min at room temperature. A solution of 0.25% (w/v) $AgNO_2$, 0.0175% (v/v) formaldehyde was added and incubated for 30-min at room temperature. The gels were washed twice for 1-min with H_20 at room temperature. Gels were then developed with 3.125% (w/v) Na_2CO_3 0.00875% (v/v) formaldehyde until bands appeared. The reaction was stopped by the addition of 2% (v/v) acetic acid and the gel was stored in H_2O.

2.4.5 Modified hyaluronidase assay

The standard soluble HA assay (section 2.4.3) was performed by the addition of one of the following to the assay mix: 0.1 M, 0.1 mM or 1 μM EDTA, 0.1 M, 0.1 mM or 1 μM cysteine, 0.01% (v/v) Triton X-100, 0.01% (v/v) Chaps, 2 mg/L or 2 g/L BSA, 0.05 M or 0.2 M NaCl, and 0.05 M or 0.2 M $MgCl_2$.

2.4.6 Q-Sepharose anion exchange chromatography

Radiolabelled samples (section 2.5.3) or non-labelled gags (section 2.4.8) were dialysed against 100 mM Tris-HCl, pH 7.5, overnight at 4°C; dialysis was then repeated with two changes of H_2O over night at 4°C. The Tris-HCl buffer was replaced and the sample dialysed for 16-h at 4°C, and repeated once. The samples were then lyophilised and resuspended in 1 mL Q-Sepharose wash buffer (10 M formamide, 50 mM Na acetate, 250 mM NaCl, pH 6). One mL of Q-Sepharose resin (Sigma, St. Louis, MO

USA) was equilibrated in Q-Sepharose wash buffer and the sample was added and incubated for 16-h at 4°C, with rotation. The resin was poured into 5 mL columns and washed with 5 mL Q-Sepharose wash buffer. The column was then eluted 5 times in 1 mL fractions in 2 M NaCl, 10 M formamide, 50 mM Na acetate at pH 6. A Further five 1 mL fractions were eluted with 4 M NaCl, 10 M formamide, 50 mM Na acetate at pH 6. Radiolabelled material was mixed with 4 mL scintillation fluid and analysed on a Wallac scintillation counter for ^{3}H and ^{35}S, non-radioactive gags were quantified using the uronic acid assay (section 2.4.7).

2.4.7 Hydroxydiphenyl estimation of uronic acid

The amount of gag in samples was determined using the hydroxydiphenyl method for estimation of uronic acid (Blumenkrantz and Asboe-Hansen, 1973). Samples were diluted to 200 µL in H_20. D-Glucuronolactone at 1, 2, 5 and 10 µg was used as a standard. Samples were hydrolysed by the addition of 1.2 mL of 0.0125 M sodium tetraborate dissolved in H_2SO_4. Samples were vortexed, incubated at 100°C for 10-min and then chilled on ice. Twenty µL of 0.15% (w/v) meta-hydroxydiphenyl/0.5 % (w/v) NaOH solution was added to the samples and mixed thoroughly. A 200 µL aliquot was placed into a 96-well plate and the absorbance measured at 520 nm on a Ceres 900 Hdi plate reader (BioTech Instruments Inc, Vermont, USA).

2.4.8 Extraction of glycosaminoglycan from mouse tissues

Mouse tissues were collected from mixed-sex 6- and 12-month old mice. The wet weight of tissues was recorded and whole tissue samples lyophilised. Samples were re-suspended in 5 mL of 6 M urea, 0.05 M Na acetate, 0.1 M EDTA, 0.1 M amino caproic acid, pH 6.5, and the tissue extracted for 48-h at 4°C, with rotation. The extracted tissue was clarified by centrifugation at 20000 g for 30-min. The supernatant was diluted to 50

mL with Q-Sepharose wash buffer (10 M formamide, 50 mM Na acetate, 250 mM NaCl, pH 6) and 1 mL of equilibrated Q-Sepharose (section 2.4.6) added. Extracts and resin were incubated for 24-h at 4°C and the gags then eluted, as previously described (section 2.4.6). The amount of gag present in each elution fraction was determined by uronic acid assay (section 2.4.7).

2.5 Osteoblast methods

2.5.1 Mineralising osteoblast tissue culture

MG63 cells were seeded onto 6-well plates at a density of 150000 cells per cm^2 and grown in DMEM supplemented with 10% (v/v) FBS, 50 U/mL penicillin and 5 μg/mL streptomycin. Cells were induced to mineralise by the addition of 100 μM ascorbate-2-phosphate, 10 mM β-glycerol phosphate and 1 μg/mL dexamethasone. Media was changed-weekly for up to 5-weeks. Each experiment was performed on cells using three different culture conditions: 24-h in media (control-week 0); 5-weeks in standard media (control-week 5) and 5-weeks in the mineral-inducing media (mineralising 5-week).

2.5.2 von Kossa staining

Cells were grown under control or mineralising conditions (section 2.5.1) and fixed at time points of 24-h, 3-weeks and 5-weeks. At each time point the media was removed and the cells were washed twice with PBS. Cells were then fixed in 1% formaldehyde in PBS for 30-min at 4°C. Fixed cells were then washed twice in methanol and air-dried. The mineral matrix of fixed cells was stained by the von Kossa method (Bills *et al.*, 1971). Briefly, the cells were flooded with 1% (w/v) silver nitrate and exposed to ultra-violet light for 10- to 15-min. Cells were washed with three changes of distilled water and then treated with 5% (w/v) sodium thiosulphate for 30-sec. Cells were then washed with water and counterstained with 1% (w/v) neutral red for 5-min. Cells were washed

with water and dehydrated through a series of ethanol and xylene. Cells were then covered in DPX mounting solution (BDH Laboratory Supplies, Poole, UK), cover-slipped and examined by light microscopy at 100-times magnification.

2.5.3 Radio-isotope incorporation into glycosaminoglycan

Triplicate cultures of MG63 cells were performed in 6-well plates as described in section 2.2.2.3. Cells were labelled after 24-h in standard culture media (control 24-h), after 5-weeks in standard culture media (control week 5) or 5-weeks after the addition of mineralising additives to the media (mineralising week 5). At the chosen time points cells were washed 3-times with PBS and labelled with 5 μCi/mL ^{3}H-glucosamine and 50 μCi/mL ^{35}S-sulphate in low-sulphate DMEM media supplemented with 10% (v/v) FBS; mineralising additives were added to the media of mineralising cells (100 μM ascorbate-2-phosphate, 10 mM β-glycerol phosphate and 1 μg/mL dexamethasone). Cells were incubated with isotope for 24-h; the media was then harvested, cells washed 3-times with PBS and the cell layer harvested in 2 mL of PG extraction buffer to which protease inhibitors had been added (4 M guanidine hydrochloride, 100 mM Na acetate, 50 mM Tris-HCl, 10 mM Na_2 EDTA, 100 mM amino caproic acid, 5 mM benzamidine, 0.5 mM phenylmethylsulphonylfluoride, 10 mM N-ethyl-maleamide, pH 5.8). The PGs were extracted by rotating the cell layer lysate for 24-h at 4°C and the specific gag types determined (section 2.5.4)

2.5.4 Characterisation of glycosaminoglycan type

Radiolabelled samples of both cells and media (section 2.5.3) were dialysed in 15kDa tubing (Selby Scientific Ltd, Clayton, Vic, Australia) against in 100 mM Tris, pH 7.5, for 16-h at 4°C. The Tris buffer was then replaced with H_20 and the samples dialysed

for 16-h at 4°C; the dialysis against H_2O was repeated. Gag samples were isolated using Q-Sepharose chromatography (section 2.4.6).

Triplicate samples of Q-Sepharose-purified gags were dialysed in 15kDa tubing (Selby Scientific Ltd, Clayton, Vic, Australia) against 100 mM Tris-HCl, pH 7.5, for 24-h, followed by dialysis against H_2O for a further 48-h at 4°C. Samples were lyophilised and resuspended in H_2O. Aliquots were made to 20 mM Na acetate, 150 mM NaCl, pH 6, and digested with 10 U of *Streptomyces* HYAL (ICN, Irvine, CA, USA) for 45-min at 60°C. A further aliquot was made to 0.1 M Tris acetate, pH 7.5, and digested with 0.1 U of chondroitinase ABC (ICN, Irvine, CA, USA) for 45-min at 37°C. Both digests were terminated by heating the samples to 85°C for 15 min.

Undigested and digested gag fractions were run on a BioGel P6 (BioRad, Hercules, CA, USA) equilibrated in 0.2 M Na acetate, 0.25 M NaCl, pH 7.4, in the presence of 100 μg of carrier gag (produced by digestion of chondroitin-4-sulphate (C4S) with chondroitinase ABC) and 500 μg of A1D1 PG (gift from Dr Sharon Byers). The radioactivity in each fraction was determined. The amount of gag digestion was determined from the proportion of each sample eluting at or near the Vt of the column after enzyme digestion compared to the undigested control. Data from cell layers and corresponding media was pooled to give the total incorporation of isotype for each of the triplicate repeats.

2.6 RNA methods

2.6.1 RNA harvest from osteoblasts

RNA was extracted from osteoblasts using an adapted version of the standard TRIzol method for cultured cells recommended by the manufacturer's (Gibco BRL, Rockville,

MD, USA). Media was removed from a single T_{75} flask and cells lysed in 1 mL TRIzol buffer for 5 min. The cells were then dislodged with a cell scraper and harvested. The lysate was centrifuged at 13000 g for 5-min and the supernatant extracted with 100 µL choloroform; centrifugation at 13000 g for 5 min was then repeated. The aqueous phase was removed and mixed with 1 mL isopropanol, and incubated at room temperature for 5-min to precipitate the RNA, then centrifuged at 13000 g for 10 min. The pellet was air-dried and resuspended in 20 µL of diethylpyrocarbonate-treated RNA'se-free H_2O.

RNA was treated with RNA'se-free DNAse I (Roche, Basel, Switzerland) according to the manufacturer's instructions. RNA was further purified using the RNEasy mini kit according to the manufacturer's instructions (Qiagen, Hilden, Germany). Spectrophotometry was used to estimate the amount of RNA ($OD_{AB}260$ x 40 x dilution factor = RNA µg). Five µg of RNA was resolved on an RNA gel to determine the quality of the RNA (section 2.6.2).

2.6.2 RNA MOPS gel

RNA samples were prepared by diluting 5 - 10 µg of RNA in 22.5 µL sample buffer (50% (v/v) formamide, 5% (v/v) formaldehyde, 3-[N-morpholino] propanesulphonic acid (MOPS) buffer (20 mM MOPS, 1.0 mM EDTA, 5.0 mM Na acetate). Samples were heated at 60°C for 5-min and quenched on ice, mixed with 2.5 µL of 10 times FDE loading dye (10 mM EDTA, 90% (v/v) formamide, 0.1% (w/v) bromophenol blue) and loaded onto a 1.2% (w/v) agarose, MOPS gel (1.2% agarose (w/v), 20 mM MOPS, 1.0 mM EDTA, 5.0 mM Na acetate, 5 % (v/v) formaldehyde, pH 7).

The gel was run at 80 V for 100-min in MOPS buffer. The gel was stained with 0.1M ammonium acetate, 100 mM β-mercaptoethanol, 0.0001% (w/v) ethidium bromide for

30-min and destained in DEPC-treated water for 30-min to 2-h. The RNA was then visualised under UV light and the image recorded using the Unipro gel documentation system (Unitec, Cambridge, UK).

2.6.3 RNA quantification

RNA was quantified using the A 260 Ribogreen RNA Quantification Assay (Molecular Probes, Eugene, OR, USA), following the manufacturer's instructions.

2.6.4 cDNA synthesis

cDNA was synthesised from 2 μg RNA (section 2.2.8) using the Super Script II First Strand cDNA Synthesis Kit (Intvitrogen, Carlsbad, CA, USA) according to the manufacturer's instructions

2.6.5 Standard reverse transcription-polymerisation chain reaction

Standard reverse transcription-polymerisation chain reaction (RT-PCR) was performed using 2 μL of cDNA (section 2.6.4). Negative "no RT " cDNA controls were set up for each gene-specific PCR. The PCR mixtures consisted of 5 μM of each dNTP (CTP, ATP, GTP and TTP), 1x PCR buffer (Roche, Basel, Switzerland), 1 mM $MgCl_2$ and 0.5 U Taq polymerase (Roche, Basel, Switzerland) made up to 48 μL with water. Ten pM of each gene-specific primer pair (section 2.6.5.2) was added to the reaction mix and the reaction was covered with mineral oil. PCR was performed to the following specifications: 94°C for 2-min for 1 cycle; 95°C for 2 min; 55°C for 30-sec; 72°C for 1-min for 35 cycles and 72°C for 5-min for 1 cycle. One-tenth of the PCR product was then analysed by 2% agarose gel electrophoresis (section 2.2.3.5).

2.6.5.1 Reverse transcriprion–polymerisation chain reaction primers

Primer	Sequence	Sense (+) or
HAS-1 - A	CACCAACCGCATGCTCAGCAT	+
HAS-2 - A	ACTCCATGGTTGGAGGTGTTG	+
HAS-2 - B	TCTTGGCGGGAAGTAAACTACG	-
HAS-3 - A	TCTGACACTGTGCTGGAATCAA	+
HAS-3 - B	GGCAGAAGGCTGGACATATAG	-
HYAL-1 - A	AGCTGGGAAATACAAGAACC	+
HYAL-1 - B	TGAGCTGGATGGAGAAACTGG	-
HYAL-2 - A	GAGTTCGCAGCACAGCAGTTC	+
HYAL-2 - B	CACCCCAGAGGATGACACCAG	-
HYAL-3 -.A	CCGCCTCCAGTGCCCTCTTCC	+
HYAL-3 - B	AGCCCAGCCCCAGTAACAGTG.	-
HYAL-4 - A	TTCCTGTGATTGGAAGCCCAC	+
HYAL-4 - B	CCAAGGCAGCACTTTCTCCTA	-
PH20 - A	GTACAACTTAGTCTCACAGAG	+
PH20 - B	TACTTCGCATTATACTGAGGG	-
GAPDH - A	TGGTATCGTGGAAGGACTCAT	+
GAPDH - B	GTGGGTGTCGCTGTTGAAGTC	-

2.6.6 Real time reverse transcription polymerisation chain reaction

Real time reverse transcription-polymerisation chain reaction (Real Time-RT-PCR) was performed using 1 μL of cDNA mixture (section 2.6.4) or "no RT" cDNA controls for each primer set. The PCR mixtures consisted of 1x syber green (Applied biosystems, Foster City, CA, USA), 1x AmpliTaq gold PCR buffer, 5 μM each NTPs (CTP, ATP, GTP and TTP), 3 mM $MgCl_2$, 0.5 U of AmpliTaq gold (Applied Biosystems, Foster City, CA, USA) made up to 25 μL with H_2O. Ten pM of gene-specific primer pairs (section 2.6.7.2) were added to the PCR reaction mixes. All PCRs were performed in duplicate. PCR reactions were carried out in the Corbett 2000 72-well rotor (Corbett, Mortlake, NSW, Australia) with the following specifications: 94°C for 10-min for 1 cycle; 95°C for 2-min; 60°C for 30-sec, 72°C for 1-min for 45 cycles and 72°C for 5min for 1 cycle. Data were analysed using Rotor-gene 5 software (Corbett Research, Mortlake, NSW, Australia). For each set of experiments cyclophilin-A was used to normalise data for a single RNA sample. Individual data points were the average of

duplicate samples; standard error was determined from experimental triplicates. A change in gene expression was determined using the comparative ΔΔCt method, which describes the cycle number at which a PCR product in a linear phase of duplication changes between culture conditions. Any change in cycle number was normalised to the expression of the control gene, cyclophillin-A (cyc-A), for a given culture condition (ΔCt). Change in ΔCT between different culture conditions (ΔΔCt) was used to determine the fold change in gene expression according to the equation $2^{-\Delta\Delta CT}$.

2.6.6.1 Real time reverse transcrition–polymerisation chain reaction primers

Primer	Sequence	Sense (+) or Anti sense (-)
CY-A - F	GGTTGGATGGCAAGCATGTG	+
CY-A - R	TGCTGGTCTTGCCATTCCTG	-
HYAL-1 - F	AGTTTCTCCATCCAGCTCACG	+
HYAL-1 - R	ACATTGAACTCCACAGCCATC	-
HYAL-2 - F	CCTGCATCTCAGCACCAACAG	+
HYAL-2 - R	TCAATGTCGGCCCAACTGAGC	-
HYAL-3 - F	TCATGGAGATGCCAGCATCC	+
HYAL-3 - R	GTCCATTGGTGTGAGTGCAGC	-
HYAL-4 - F	AACTGCATCCAAGGCCAACTG	+
HYAL-4 - R	TGCATACCTCAGCAGCTCTGG	-
PH20 - F	GCGAACTGTTGCTCTGGGTG	+
PH20 - R	CCATGTAATTGTCTAGGAGCAAGC	-
HAS-1 - F	TACCAAGTACACCTCCAGGTC	+
HAS-1 - R	CGGAAGTACACCTCCAGGTC	-
HAS-2 - F	ACAAACATCACTTGTGGATGACC	+
HAS-2 - R	TTACCCCGGTAGAAGAGCTGG	-
HAS-3 - F	CCAGCAGTTCCTGGAGGACTG	+
HAS-3 - R	CCAAGGCTCAGGACTCGGTTG	-

Chapter 3

Bioinformatic analysis of the hyaluronidases

3.1 Introduction

Bioinformatics can be used to predict the biochemical characteristics of a protein *in silico*. Using the primary DNA sequence possible structural and functional domains of the encoded protein can be inferred. Recombinant proteins can be used to confirm or refute these predictions. Native HYAL-3 is only classed as a HYAL because of its sequence similarity to HYAL-1 and PH20, enzymes that have been biochemically shown to have a HYAL activity (Frost *et al.*, 1997; Gmachl *et al.*, 1993).

Bioinformatics has previously been used to compare the HYAL in bee venom (Bee HYAL) to the human testicular (PH20) and plasma HYAL (HYAL-1) (Markovic-Housley *et al.*, 2000). Bee HYAL has been thoroughly characterised, with the gene cloned, recombinant protein expressed (Gmachl and Kreil, 1993) and a crystal structure determined (Markovic-Housley *et al.*, 2000). Bee HYAL shows strong similarity to PH20 and HYAL-1 (Markovic-Housley *et al.*, 2000) and it is likely that these HYALs share structural and functional features, such as the $(\alpha/\beta)_8$ Tim barrel structure and the acid-base substrate-assisted catalytic mechanism that has been proposed for Bee HYAL (Markovic-Housley *et al.*, 2000).

Site-directed mutagenesis of the predicted active site residues of PH20 abolished its activity (Arming *et al.*, 1997), experimentally confirming the bioinformatics analysis that suggested PH20 shares a catalytic mechanism with Bee HYAL (Arming *et al.*, 1997).

The genomic arrangement of the homologous HYALs is conserved in humans and mice. In humans, the six paralogous HYALs are clustered into two groups of three at loci 3p21.3 and 7q31.3 (Figure 3.1). This genomic arrangement is paralleled in mice, with the mouse homologues of these HYALs found on syntenic regions of mouse chromosomes, at 9F1-F2 (Csoka *et al.*, 1998) and 6A2 (Csoka *et al.*, 2001). Further analysis of the genomic arrangement of HYALs present in other species has not been performed.

This chapter discusses the use of bioinformatics to analyse all the human HYALs and further characterises the similarity between HYALs present in other species.

3.2 Hyaluronidase gene and protein sequence comparisons

The human HYALs, - HYAL-1,HYAL-2, HYAL-3, HYAL-4, HYAL-P1 and PH20 - (GenBank sequences; Appendix II), were analysed using "clustalW" (http://angis.org.au). The similarities between genes and proteins were determined using "Homologies" (http://angis.org.au) (Table 3.1).

The HYAL-3 gene was most similar to HYAL-1 (26.5 %) and HYAL-2 (24.9 %) (Table 3.1A). Analyses of the amino acid sequence revealed that HYAL-3 was most similar to HYAL-1 (37.1%) and HYAL-2 (36.5 %, Table 3.1B).

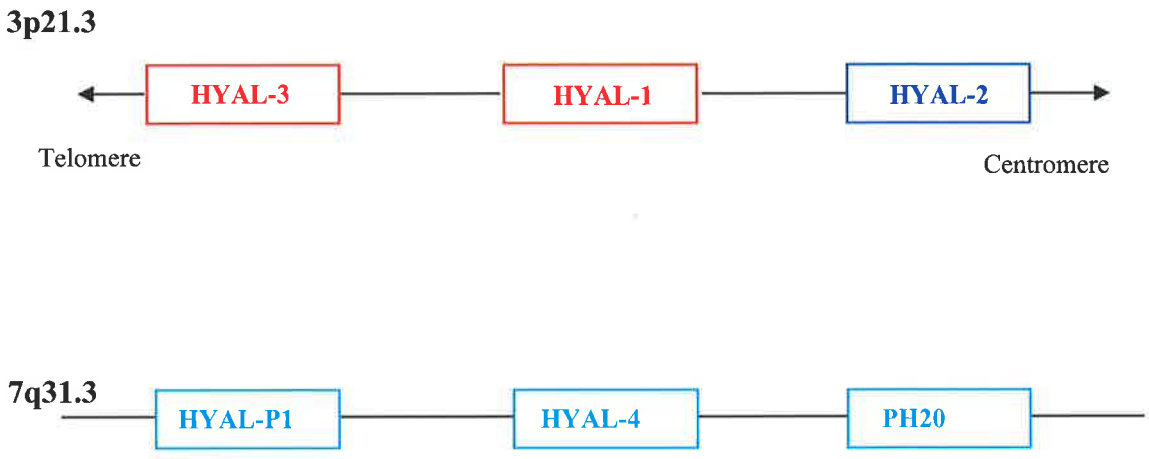

Figure 3.1 Chromosomal location human hyaluronidase genes

The chromosomal orientation of the six paralogous human HYALs is at the two loci shown. While the relative order of genes on chromosome 7 is known, their orientation relative to the telomere and centromere has not been established. The three genes on chromosome 7 generally have larger and additional introns to those on chromosome 3 (Csoka *et al.*, 2001). Colour corresponds to the phylogenetic relationship found through analysis of gene sequence similarity (Figure 3.3). This Figure is adapted from Csoka *et al.* (2001) and is not to scale.

A (% similarity)

(% similarity)	HYAL-3	HYAL-1	HYAL-2	HYAL-4	PH20	HYAL-P1
HYAL-3	100	26.5	24.9	21.9	21.1	17.5
HYAL-1		100	22.1	23.0	20.4	18.6
HYAL-2			100	24.7	22.1	27.2
HYAL-4				100	33.7	15.8
PH20					100	15.3
HYAL-P1						100

B (% similarity)

(% similarity)	HYAL-3	HYAL-1	HYAL-2	HYAL-4	PH20	HYAL-P1
HYAL-3	100	37.1	36.5	31.0	29.7	18.3
HYAL-1		100	37	36.7	32.4	20.3
HYAL-2			100	34.8	31.6	18.6
HYAL-4				100	40.5	19.3
PH20					100	16.3
HYAL-P1						100

Table 3.1 Similarity between human hyaluronidase genes and proteins

Similarity between HYALs is shown for the coding sequences (A) and encoded amino acid protein sequences (B). Sequences (GenBank sequences; Appendix II) were aligned using "E cluster" and the percentage identity at each nucleotide or residue was calculated using "Homologies (http://www.angis.org.au).

3.3 Analysis of protein sequences

3.3.1 Conserved protein motifs

The human HYALs, HYAL-1, HYAL-2, HYAL-3, HYAL-4, HYAL-1P and PH20 (GenBank sequences: Appendix II) were analysed for the presence of protein domains using "Scan Prosite" (http://www.expassy.org).

The human HYALs were found to possess at least one fully conserved and one partially conserved potential glycosylation site (Table 3.2). Each HYAL possessed at least one additional glycoylation-site that is specific for each enzyme, with HYAL-4 having a total of eight (Table 3.2).

3.3.2 Determining molecular mass of hyaluronidases

The predicted molecular weight of the translation product of each human HYAL gene (GenBank sequences; Appendix II) was determined using "Pepstats" (http://angis.org.au).

The predicted molecular mass of the human HYALs falls in the range 48-52 kDa, except for HYAL-P1 (Table 3.3). HYAL-P1 possesses a premature stop codon and translation would result in a non-functional truncated protein of 28.9 kDa. However, the DNA sequence maintains its homology beyond the stop codon. HYAL-P1 most likely represents a pseudo-gene.

3.3.3 Prediction of signal peptide cleavage of hyaluronidases

The N-terminus of each of the human HYAL protein sequences was analysed for the presence of a peptide signal cleavage site using "SignalP" (http://www.cbs.dk/services/signalP/). This method incorporates a prediction of cleavage sites and a signal peptide/non-signal peptide prediction based on neural networks and hidden Markov models (Bendtsen *et al.*, 2004).

Enzyme	Conserved site 1	Conserved site 2	Additional sites
HYAL-1	99NAS	350NVT	216NYT
HYAL-2	103NVS	356NVS	103NVS
HYAL-3		348NVT	69NMT, 348NVT
HYAL-4	115NTS	368NVT	86NVT,177NVS,262NYS, 253NSS, 343NLT, 350NCT
HYAL-P1	103NVS	356NVT	153NHS, 188 NIT
PH20		368NVT	82NAT, 166 NRS, 225NGS 254 NES, 393NSS

Table 3.2 Potential N-glycosylation sites

Human HYAL protein sequences (GenBank sequences; Appendix II) were analysed for the N-glycosylation motif N-X-S/T ("Scan Prosite", http://www.expassy.org). Two sites were found to be conserved in most of the HYALs (sites 1 and 2). Additional potential glycosylation sites were observed that varied between the HYALs; each site is listed with its position and amino acid sequence.

3.3.4 Prediction of GPI anchor for hyaluronidases

The C terminal of the human HYAL protein sequences was analysed for the presence of cleavage sites of GPI anchor using DGPI (http://www.129/194.186.123/GPIanchor/index_en.htmL) to identify whether the protein was membrane-bound.

HYAL-2, HYAL-4 and PH20 were predicted to be GPI-anchored proteins (Table 3.3). If utilised, GPI anchors could attach these proteins to the cell surface.

3.3.5 Alignment of hyaluronidases

Alignment of the human, mouse and frog complete sequences (GenBank sequences; Appendix II) was performed using "clusterW" and visualised using "pretty box plot" (http:www.angis.org.au).

The highly conserved regions between species are highlighted (Figure 3.2). The two conserved potential N-glycosylation sites are shown and were found across many species, indicating that the carbohydrate motif could have a role in the function or structure of HYALs in general (Figure 3.2).

Four cysteine residues found to be important in the crystal structure of Bee HYAL were also found to be conserved across all species (Figure 3.2). These cysteine residues are thought to be involved in the formation of disulphide bridges that would be important for the structural integrity of the HYALs (Markovic-Housley *et al.*, 2000). Analysis of HYAL alignment revealed that the active site residues of PH20 - Asp111, Glu 113 and Glu247 - , were also conserved across all the species (Figure 3.2).

Enzyme	Molecular Weight (kDa)	Signal peptide cleavage (aa)	GPI anchor cleavage (aa)
HYAL-1	48.4	21 – 22	None
HYAL-2	53.3	20 – 21	445
HYAL-3	46.5	20 – 21	None
HYAL-4	54.3	34 – 35	463
HYAL-P1	28.9*	21 – 22	None
PH20	57.9	35 – 36	483

* HYAL-P1 is a pseudo gene, which if translated, would result in a truncated protein due to a premature stop codon.

Table 3.3 Molecular weight, signal peptide and GPI anchor of human hyaluronidases

The expected molecular mass of HYAL protein sequences was derived from the human gene sequences (Appendix II: GenBank sequences) using "Pepstats" (http://angis.org.au). The N-terminal of the protein sequences was analysed for the presence of peptide signal cleavage sites using "SignalP" (http://www.cbs.dk/services/signalP/). The C terminal was analysed for the presence and cleavage of a GPI anchor using "DGPI" (http://www.129/194.186.123/GPI-anchor/index_en.htmL).

3.4 Phylogenetic analysis of hyaluronidases

Phylogenetic analysis of the "clusterW" alignment of the HYALs was performed using "ProtPars" (http://ww,angis.org.au/bioNavigator) to produce a rooted tree (Figure 3.3). The invertebrate Bee HYAL was used as an out-group for rooting the tree.

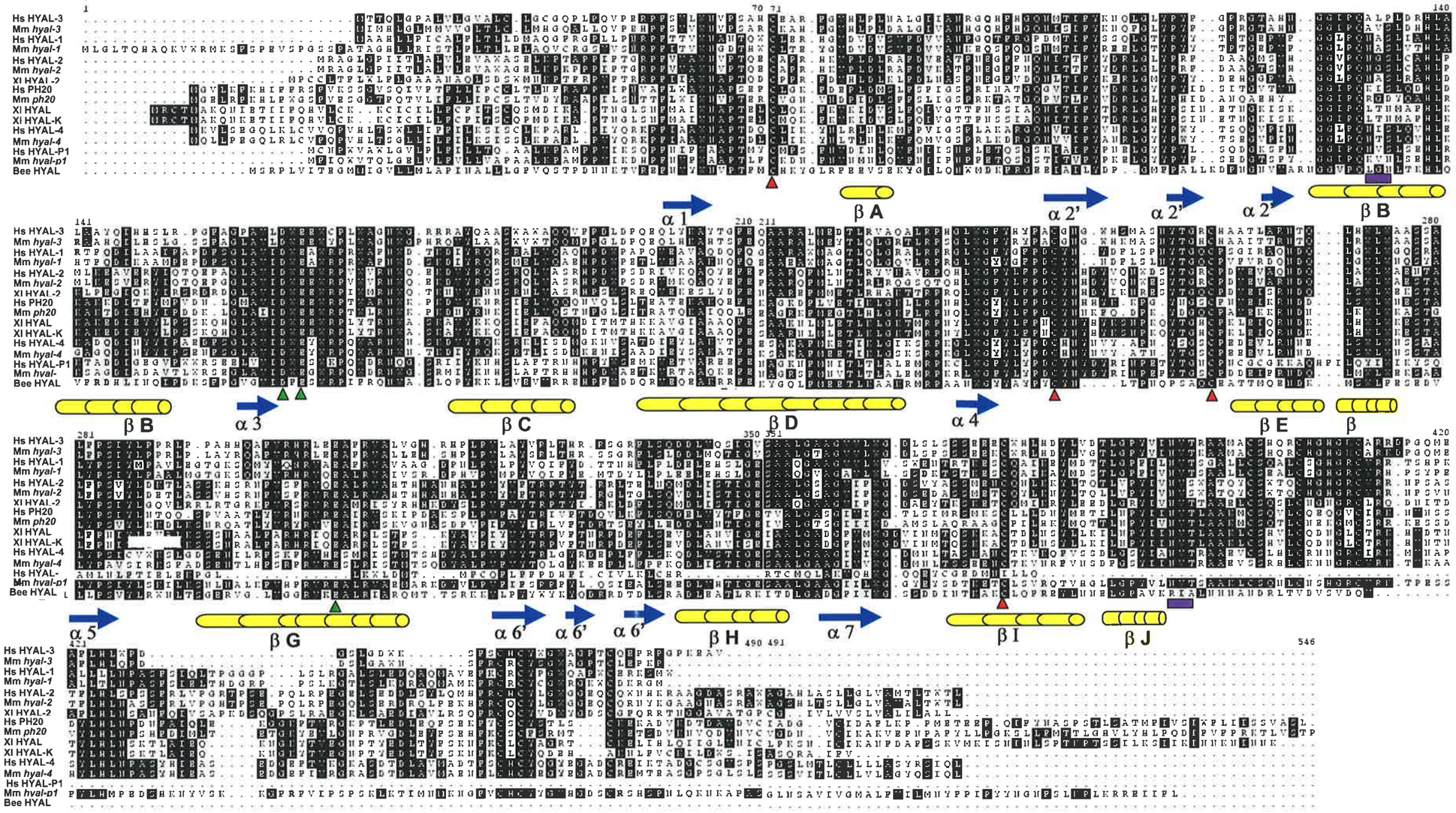

Figure 3.2 Alignment of hyaluronidases

The alignment of HYALs from mouse (Mm), human (Hs), frog (Xl) and bee venom (Bee) show distinct similarity in their sequence, which places them in glycosyl hydrolyase family 56. Fully conserved amino acids are shown in black (■), while partially conserved amino acids are in grey (■). The crystal structure of Bee HYAL identified a number of important residues that are conserved in this alignment (Markovic-Housley *et al.,* 2000). The potential active site residues of Bee HYAL, Asp111, Glu113 and Glu247, are marked by a green triangle (▲). Four conserved cysteine residue that form two disulphide bridges, Bee HYAL Cys22-Cys313 and Csys189-Cys201, are marked by a red triangle (▲). Two conserved regions that may encode N-glycosylation sites are marked by a filled rectangle (▬). Blue arrows represent β strands (⟶ 1 – 7), and yellow cylinders represent α helices (A -J). GenBank sequences (Appendix II) were aligned using "clusterW", and a figure prepared using "PrettyBox (GCG)" (http://www.angis.org.au/BioNavigator/).

This phylogeny shows that true homologues are present across the species (Figure 3.3), with the branch points of the human, frog and mouse displaying homologues that cluster together. Distinct branching occurs with the human and mouse genes to coincide with their synergistic chromosomal arrangements. The HYAL-1 and HYAL-3 genes cluster together as the closest relatives of each other on human chromosome 3 (red), while HYAL-2 (dark blue) is more closely related to the genes of chromosome 7 (light blue).

3.5 Discussion

Bioinformatics is a useful tool to predict the structural features and biochemical properties of enzyme families. The mammalian HYAL protein sequences were aligned to sequences of other species and analysed for structural and functional regions of conservation. Experimental data present in the literature was then correlated to the bioinformatic predictions and used to outline the expected properties and function of HYAL-1 and HYAL-3.

The similarities between the six human HYAL sequences (Table 3.3) show a conserved family of genes that are all members of the glycohydrolase 56 family of carbohydrate-degrading proteins (Henrissat and Bairoch, 1993). HYAL-3 showed greatest amino acid similarity to HYAL-1 (37.1%) and HYAL-2 (36.5 %).

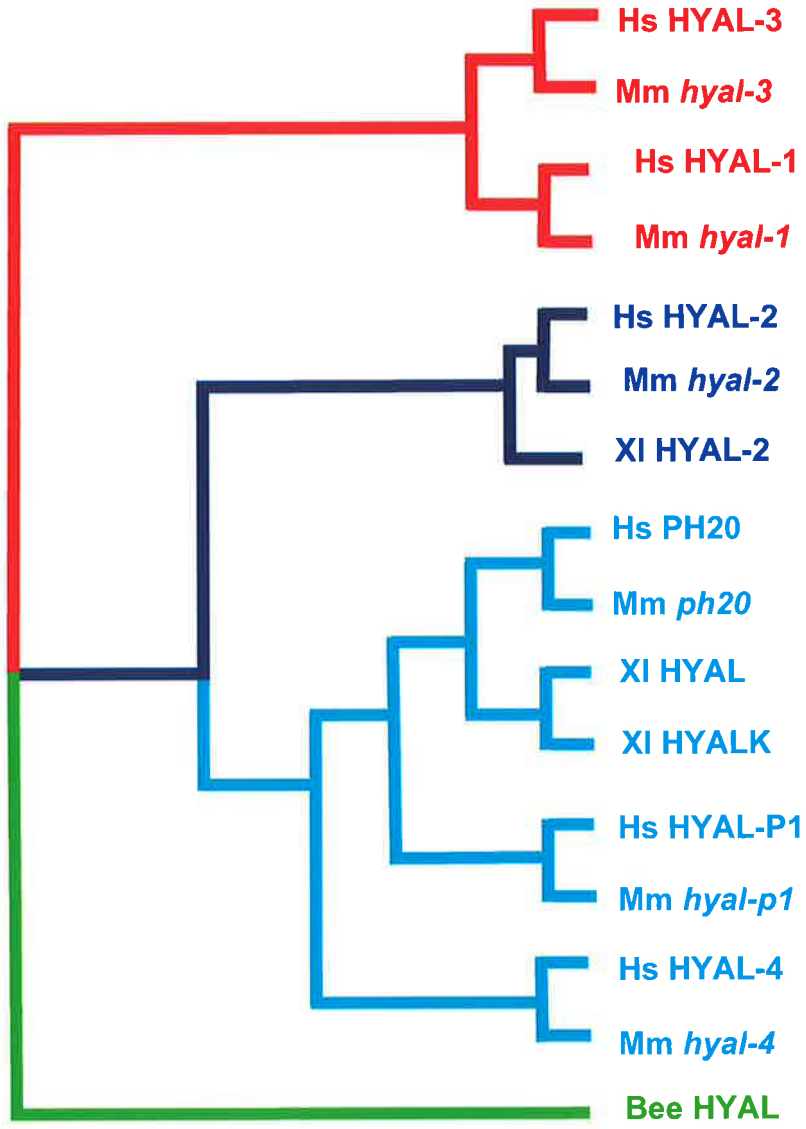

Figure 3.3 Phylogenetic analysis of hyaluronidases

HYALs from mouse (Mm), human (Hs), frog (Xl) and bee venom (Bee) were aligned using "clusterW", and a rooted tree drawn using "ProtPars" (http://www.angis.org.au/BioNavigator). Homologous genes cluster from nodes, i.e. all HYAL-2 genes clusted together. HYAL-2 genes (dark blue) branched firstly from the genes on chromosome-3; HYAL-1 and HYAL-3 (red), then branch later from the genes of chromosome 7; HYAL-P1 , PH20 and HYAL-4 (light blue) that they are more closely related to. The tree is rooted by using invertebrate Bee HYAL gene (green).

HYAL-3 should therefore share characteristics of these enzymes, such as an ability to degrade HA at an acidic pH optimum (Frost *et al.*, 1997, Lepperdinger *et al.*, 1998). Thus, investigation into the function of HYAL-3 was performed with the expectation of characterising an acidic-acting HYAL (chapter 4).

3.5.1 Conservation of amino acids in the hyaluronidases across species

Key amino acids that are conserved across species have previously been shown to be important in the generation of structural disulphide bridges, as the sites of N-glycosylation and active site residues in Bee HYAL.

Cysteine residues that have been shown to participate in disulphide bridge formation in the crystal structure of Bee HYAL were found to be conserved across the species examined (Markovic-Housley *et al.*, 2000). The importance of these disulphide bridges has also been shown experimentally for PH20, with the reduction of the enzyme completely inhibiting its activity (Li *et al.*, 2002). These data highlight the importance of the conserved cysteine residues and disulphide bridges in the general structure of HYALs, implicating their importance in the structure of HYAL-1 and HYAL-3.

Assuming that the HYALs use a similar acid-base catalytic mechanism to other glycohydrolases such as lysozyme chitinases and xylanases (Withers and Aebersold, 1995), the putative amino acids of the active site have been identified (Arming *et al.*, 1997). These amino acids were conserved in HYALs across the species examined (Figure 3.1). Site-directed mutagenesis of the active site residues in recombinant PH20 (Asp111 and Glu113) results in a decrease in activity to 1-3% of wild type (Arming *et al.*, 1997). The co-crystallisation of Bee HYAL with the HA substrate revealed that the

homologous active site residues in Bee HYAL are in the substrate-binding groove and are positioned to play a role in catalysis of substrate (Markovic-Housley *et al.*, 2000). These active site residues were also conserved in HYAL-1 and HYAL-3 (Figure 3.2), indicating that these enzymes should possess HYAL activity or at least general gylcohydrolase activity.

Two theoretical N-glycosylation sites have been conserved amongst the sequences of the HYAL gene across all species examined (Table 3.2; Figure 3.1). Experimental confirmation that glycosylation does occur in HYALs was found in the crystal structure of bee venom (Markovic-Housley *et al.*, 2000) and in the glycosylation of HYALs extracted from different somatic tissues and body fluids (Fiszer-Szafarz *et al.*, 2000).

The functional importance of glycosylation in HYAL was demonstrated by the de-glycosylation of Macaque sperm PH20; this resulted in a loss of enzymatic activity (Li *et al.*, 2002). N-Linked glycosylation in HYALs could function to target enzyme to the lysosome. The incorporation of mannose-6-phosphate residues onto N-link glycosylation would allow HYALs to use the mannose-6-phophate receptor-mediated pathway, a well characterised mechanism for targeting other glycohydrolases to the lysosome (Hille-Rehfeld, 1995). However, the precise function of glycosylation in HYALs remains unclear. In other enzymes glycosylation modulates protein-protein interactions (Ji and Ji, 1990; Zhang *et al.*, 1991), protein folding (Lis and Sharon, 1993; Varki 1993; Parodi, 2000), enzyme activity (Cumming, 1991; Howard *et al.*, 1991) and enzyme proteolysis (Kretz *et al.*, 1990). The purpose of glycosylation in HYALs could involve any of these functions and will thus be further investigated in recombinant HYAL-1 and HYAL-3 (chapter 4).

3.5.2 Signal peptide in mammalian hyaluronidases

N-Terminal sequencing of recombinant PH20, HYAL-1 and HYAL-2 proteins demonstrates that the signal peptide predicted from gene sequences (Table 3.2) is cleaved in the production of recombinant protein in mammalian cells (Csoka *et al.*, 1999). HYAL-3 and HYAL-4 are also predicted to have a signal peptide (Table 3.2), however experimental confirmation is required to define whether the predicted signal peptides are cleaved. The general purpose of signal peptides is to direct protein across the ER to specific organelles for secretion (Wilkinson *et al.*, 1997). Lysosomal glycohydrolases are generally transported though the vesicular transport system (Rouille *et al.*, 2000; Rohn *et al.*, 2000) that can result in both secreted and lysosomal distribution of the proteins (Hasilik, 1992). Thus, the presence of a signal peptide may play an important role in the transport of HYAL through the ER and ultimate lysosomal localisation.

3.5.3 GPI anchors in mammalian hyaluronidases

HYAL-2 and PH20 were predicted to be GPI-anchored (Table 3.2) and this has been shown experimentally with both proteins existing as a cell surface GPI-anchored variant and non-GPI-anchored intra-cellular variant (Rai *et al.*, 2001; Thaler and Cardullo, 1995). HYAL-4 was also predicted to be a GPI-anchored protein, but this has not yet been confirmed. Therefore, when over-expressing recombinant HYAL-4 it will be important to not only determine whether there is secreted protein in the media, but also to examine membrane preparations for GPI-anchored variants of HYAL-4 (Csoka *et al.*, 1999). HYAL-3 and HYAL-1 are not predicted to be GPI-anchored, thus recombinant over-expression in mammalian cells should saturate any intra-cellular targeting and result in secretion of the protein into the media.

3.5.4 Evolutionary analysis of hyaluronidases

Analysis of the phylogenetic tree reveals that the homology between the orthologous mouse and human genes is greater than the similarity that exists between the paralogous genes of each species. The phylogenetic relationship of the HYALs, coupled with knowledge of the chromosomal clustering of these genes, gives an insight into the evolutionary origin of the mammalian HYALs. Genes at the human loci 7.q23 most likely result from an initial cross-chromosome duplication event involving an ancestral gene most similar to HYAL-2, and then the successive duplication at this site. HYAL-1 and HYAL-3 branch together, representing an intra-chromosomal duplication. This chromosomal clustering is conserved between mouse and humans, revealing that the duplication events that gave rise to the paralogous HYAL genes occurred before the divergence of human and mouse, around 80 million years ago (Csoka *et al.*, 2001).

The evolutionary divergent origin of the HYAL genes suggests a complex array of enzymes that can catabolise this simple sugar chain of the most basic repeating disaccharide structure. Through variations in amnio acid sequence the HYALs can alter their substrate specificity: HYALs such as HYAL-1 and PH20 can degrade other non-HA gags such as CS (Byers *et al.*, 2005; Knudson *et al.*, 1984), whilst other HYALs such as HYAL-2 exclusively degrade HA (Lepperdinger *et al.*, 1998).

3.5.5 Conclusion

Many of the predictions made through bioinformatics correlate with the experimental evidence from the well-characterised HYAL-1, HYAL-2 and PH20 enzymes, validating the use of bioinformatics as the first step in characterising novel HYAL genes.

HYALs vary in their tissue expression profiles, indicating that some HYALs may possess unique tissue-specific functions (Csoka *et al.*, 2001). HYAL-3 was most similar to HYAL-1, and both enzymes were further investigated for HYAL activity through the characterisation of rHYAL-1 and rHYAL-3 proteins (chapter 4).

Chapter 4

Characterisation of recombinant hyaluronidase-1 and -3

4.1 Introduction

HYALs are a class of endo-glycohydrolases that degrade not only HA but are active towards the unsulphated regions of CS (Knudson *et al.*, 1984; Byers *et al.*, 2005). The gene and protein sequences of HYAL-3 are very similar to the other HYALs (section 3.2) and show a tissue expression pattern that is restricted to testis, bone marrow and cartilage (Csoka *et al.*, 1999, Flannery *et al.*, 1998). rHYAL-3 protein produced in a cell-free system has previously been demonstrated to exhibit HYAL activity (Lokeshwar *et al.*, 2002).

The attempts to express recombinant protein for the other mammalian HYALs has given some insight into the expected problems, activities and methods required to produce an active rHYAL-3. The only cloned and characterised mammalian HYALs are PH20 (Gmachl and Kreil, 1993), HYAL-1 (Frost *et al.*, 1997) and HYAL-2 (Lepperdinger *et al.*, 1998).

PH20 was first identified as the sperm receptor for the zona pellucida (Myles *et al.*, 1987; Primakoff *et al.*, 1985). Recombinant PH20 was expressed in RK13 cells using a vaccinia virus expression system and the protein confirmed to be a HYAL (Gmachl *et al.*, 1993).

HYAL-1 protein was isolated from plasma (Frost *et al.*, 1997) and the gene that encoded the isolated HYAL-1 protein was subsequently cloned. rHYAL-1 protein was expressed in HEK-293 cells. rHYAL-1 has a pH optimum of 3.5, suggesting that it functions in acidified organelles such as the lysosome.

HYAL-2 was first cloned and expressed using a vaccinia virus expression vector in both a HYAL-deficient C6 glioma cell line and in HeLa cells, this protein was demonsated to

be a lysosomal hyaluronidase (Lepperdinger *et al.*, 1998). HYAL-2 protein was also produced using NIH3T3 cells and a Moloney murine leukaemia virus-based retroviral vector. However, this rHYAL-2 protein did not possess any HYAL activity (Rai *et al.*, 2001) and was demonstrated to be a GPI anchored protein that acted as a receptor for the Jaagsiekte sheep retrovirus (Rai *et al.*, 2001). These conflicting results suggest that HYAL-2 exists both as a GPI anchor protein at the cell surface and as an endohydrolase in the lysosome, but its function and localisation depends upon the cell type in which it is expressed. No study has yet reported the localisation of endogenous HYAL-2 in different tissues, but it would be helpful in clarifying its function. These discrepancies in the role and extent of activity possessed by HYAL-2 highlights the importance of a diversified approach to the production of recombinant production to necessary to produce active enzyme.

The success of these previous expression techniques for the production of recombinant protein for other HYALs led to the use of a similar approach in this study. A pcDNA3.1 vector (Invitrogen, Carlsbad, CA, USA) utilising a CMV promoter was employed to produce rHYAL-3 and rHYAL-1 in the TNT cell-free system (Promega, Madison, WI, USA), by transient expression in 293T cells, and by stable expression in CHO-K1 and COS-7 cells.

Analysis of the putative protein sequence of HYAL-3 reveals a potential signal peptide cleavage site at the N-terminus (Table 3.3). A similar signal peptide sequence site is conserved in HYAL-1, PH20 and HYAL-2, and is cleaved in the production of recombinant proteins (Csoka *et al.*, 1999). Thus, any attempts to tag the recombinant proteins have been restricted to the C terminus, as disruption of the signal peptide would

likely result in aberrant localisation of the chimeric protein or removal of the tag in the normal processing of the pre-protein.

Glycohydrolase activity was examined using zymography, an ELISA-based assay and a soluble substrate assay to assure that the limitations of each assay did not result in false negatives. Given that the other mammalian HYALs showed some diversity in their substrate specificity and optimal pH, HYAL-3 and HYAL-1 was analysed for activity against a range of gag substrates (HA, Chon, C4S, C6S and DS) at both pH 3.5 and 7. This chapter discusses the recombinant expression of HYAL-3 and contrasts it with HYAL-1.

4.2 Construction of recombinant hyaluronidase expression vectors

Three HYAL-3 expression vectors were constructed to encode HYAL-3 non-tagged, HYAL-3-His_6 fusion protein and HYAL-3-GFP fusion protein.

4.2.1 Human hyaluronidase-3 non-tagged vector construction

PCR primers HYAL-3-15 and HYAL-3-17 (section 4.2.2) were designed to the HYAL-3 sequence (GenBank Accession Number AF036035). PCR was performed using Platinum Taq Pfx DNA polymerase (Invitrogen, Carlsbad, CA, USA) and a human testis cDNA library 1000b (ClonTech, Mountain View, CA, USA) as a template, and the gene-specific primers HYAL-3-15 and HYAL-3-17 (Section 2.1.11.1). The annealing temperature was 55°C and all other conditions were as described in section 2.1.2.

The Pfx enzyme has a proof-reading mechanism that removes 5' terminal adenosine residues that are generally maintained using standard non-proof-reading Taq DNA

polymerase. The TOPO cloning system (Invitrogen, Carlsbad, CA, USA) requires overhanging adenosine residue to allow cloning, thus the initial PCR product was incubated with standard non-proof-reading enzyme to attach the required adenosines (section 2.1.9). This adenosine + PCR product was gel-purified (section 2.1.5) and cloned into pcDNA3.1 using the TOPO cloning system (section 2.1.9). The TOPO-cloned vector was electroporated into DH5α electro-competent bacteria (section 2.1.7); and the resulting colonies were picked and plasmid DNA prepared (section 2.1.8.1).

Mini Preps were diagnostically digested for orientation and size of the insert with *Bgl*II (sections 2.1.3 and 2.1.4). MidiPreps were then performed (section 2.1.8.2) and sequenced (section 2.1.11.1). An error-free clone containing the complete HYAL-3 sequence was identified and designated pHYAL-3-no –Tag

4.2.2 Hyaluronidase-3-His_6 expression vector

Site-directed mutagenesis was performed on the pHYAL-3 vector (section 2.1.12.1) using primers HYAL-3-His_6-1 and HYAL-3-His_6-2 (section 2.1.12.1); to removed the native stop codon and produce a vector with the HYAL-3 protein in-frame with a tag of six histidines (His_6).

Colonies isolated from this mutagenesis reaction were sequenced (section 2.1.11) using HYAL-3 sequencing primers (section 2.1.11.2). A continuous error-free clone was obtained. The HYAL-3-His_6 sequenced region was cut from the mutagenic vector using *Bam*HI and *Pme*I enzymes (section 2.1.3), gel purified (section 2.1.5) and re-cloned into the pcDNA3.1 His_6 vector (Invitrogen, Carlsbad, CA, USA) (section 2.1.10). This new vector was transformed into *E. coli* (section 2.1.7) and four plasmid preparations

sequenced (sections 2.1.8 and 2.1.11.1) to isolate a new error-free plasmid that was designated pHYAL-3-His_6.

4.2.3 Hyaluronidase-1-His_6 expression vector

pHYAL-1-His_6 was a gift from Dr Sharon Byers. Briefly, HYAL-1-specific PCR product was cloned into pcDNA3.1/V/His_6.TOPO using the TOPO cloning system (section 2.1.9). This vector was transformed into DH5α *E coli* (section 2.1.7); plasmid Midi Preps were performed (section 2.1.8) and sequenced (section 2.1.11.1) and an error-free clone identified. This vector was designated pHYAL-1-His_6.

4.2.4 Production of hyaluronidase-3-GFP expression vector

Using 1 ng of pHYAL-3 as a template (section 4.2.1), a PCR was performed using primers HYAL-3-GFP-1 and HYAL-3-GFP-2 (Section 2.1.11.2) and Pfx Platinum Taq DNA polymerase, with an annealing temperature of 55°C; all other conditions were as discribed in section 2.1.2. This PCR product and the pGFP-N1 vector (ClonTech, Mountain View, CA, USA) were restricted with *Eco*RI and *Bam*HI restriction endonucleases (section 2.1.3).

The restricted PCR fragment was run on an agrose gel (section 2.1.4); the PCR product was then purified (section 2.1.5) and cloned into the pGFP-N1 vector (Clontech, Mountain View, CA, USA) (section 2.1.10). Ligated vector was transfected into DH5α (section 2.1.7). Mini Preps were performed on colonies (section 2.1.8.2) and diagnostically digested for orientation and size with *Bgl*II (section 2.1.3). Midi Preps were performed on selected clones (section 2.1.8.1) and an error-free clone containing

the complete HYAL-3 sequence was identified by DNA sequencing (section 2.1.11); this vector was designated pHYAL-3-GFP.

4.3 Cell-free translation of hyaluronidase-3-His_6 and hyaluronidase-1-His_6

S^{35}-labelled protein was produced from pHYAL-3-His_6, pHYAL-1-His_6 and empty control vectors using the TNT cell-free transcription and translation system (Promega, Madison, WI, USA; section 2.3.1). The resultant proteins were electrophoresed on 4-20 % SDS–PAGE (section 2.3.4) and assayed for activity by zymography (section 2.4.1). In addition, the cell-free reaction was assayed for activity using an ELISA-based HA assay (section 2.4.2) and a soluble HA assay (section 2.4.3).

A protein of 46 kDa was produced from the pHYAL-3-His_6 vector (Figure 4.1A), which corresponded to the expected size based on the amino acid sequence (Table 3.3). A protein of 56 kDa was produced from the pHYAL-1-His_6 vector (Figure 4.1A), which was higher than the expected band size based on amino acid sequence (Table 3.3).

Commercially available testicular HYAL gave a clear band on zymography at pH 3.5, indicating the presence of HYAL activity (Figure 4.1B). TNT-produced rHYAL-3-His_6, rHYAL-1-His_6 or vector control proteins did not display HYAL activity on the zymograms (Figure 4.1B).

rHYAL-3-His_6, rHYAL-1-His_6 or control proteins from the TNT reaction were incubated with 15 μg HA and the digestion products resolved on a 0.8% agarose gel (sections 2.4.3 and 2.4.3.1). No digestion of HA was observed with either enzyme (Figure 4.1C).

An ELISA-based activity assay (section 2.4.3) employing a biotinylated HA substrate indicated that the proteins produced by rHYAL-3-His_6, rHYAL-1-His_6 and control TNT reactions (section 2.3.1) had the same amount of substrate in the assay wells as the undigested control (Figure 4.1D); indicated that there was no detectable HYAL activity in these samples.

Although the TNT reactions produced proteins, three independent assays indicated that these proteins did not have any detectable HYAL activity under the conditions used.

4.4 Transient expression of hyaluronidase-3-His_6 and hyaluronidase-1-His_6

Transient expression of the plasmid pHYAL-3-His_6 and pHYAL-1-His_6 was performed on the premise that recombinant HYAL enzyme would saturate cellular protein processing and trafficking mechanisms and result in the secretion of active recombinant protein into the cell culture media (Wurm, 2004; 1997; Hunziker and Geuze 1996).

pHYAL-3-His_6 and pHYAL-1-His_6 were transiently-transfected into 293T cells using calcium phosphate co-precipitation (section 2.2.3). Media from pHYAL-3-His_6 transfected, pHYAL-1-His_6-transfected and untransfected control cells was concentrated (section 2.2.7), examined for protein production by Western blot (section 2.3.4) and for HYAL activity at pH 3.5 in a soluble enzyme assay that employed multiple gag substrates (section 2.4.3), with the reaction products resolved by gradient-PAGE (section 2.4.4).

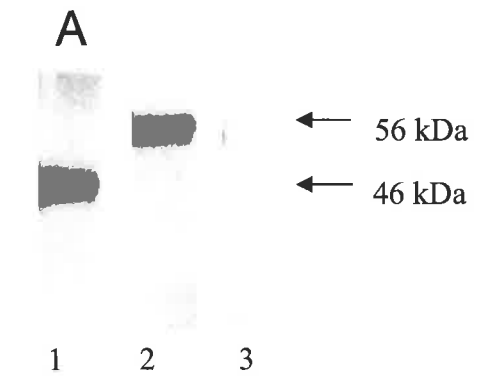

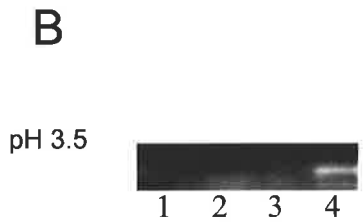

D

TNT-produced protein	Hyaluronidase Activity (U)
pHYAL-3-His_6	0
pHYAL-1-His_6	0
No plasmid control	0

Figure 4.1 Cell free translation of recombinant hyaluronidase-3-His_6 and hyaluronidase-1-His_6 and assay of activity

^{35}S-Methionine labelled proteins produced by TNT reaction were run on 4-20% SDS-PAGE (panel A). The resultant proteins were assayed for HYAL activity by zymography (panel B) using a soluble HA substrate assay (panel C) and a ELISA-based assay (panel D). For assays gel based assays (panels A-C) the TNT produced proteins were run with; Lane 1: pHYAL-3-His[6]; lane 2: pHYAL-1-His_6 and lane 3: control. The zymogram contains the additional of a testicular HYAL positive control (panel B, lane 4).

Western blot of concentrated media from 293T cells that were transiently-transfected with the pHYAL-1-His_6 construct contained a 53 kDa protein, whereas no protein was detected in the 293T cells that were transiently-transfected with HYAL-3-His_6 (Figure 4.2). Concentrated media from untransfected 293T cells showed no detectable His_6-tagged proteins (Figure 4.2).

Concentrated media from pHYAL-3-His_6-transfected cells showed no activity against HA, Chon, C4S, C6S or DS in the soluble assay at pH 3.5 (Figure 4.3).

In contrast, concentrated media from pHYAL-1-His_6-transfected 293T cells showed greatest activity against HA, which was digested to small saccharides that were not visualised on the gel (Figure 4.3A). When comparing the activity of HYAL-1-His_6 against the Chon gags the greatest activity was seen against the sulphated gag C4S, the enzyme completely digesting the high molecular weight gags (Figure 4.3C lane 2).

C6S was degraded to a lesser extent than C4S, forming a high molecular weight smear and a ladder of smaller gag fragments (Figures 4.3D). Degradation of desulphated Chon with rHYAL-1-His_6 removed most of the higher molecular weight gag, but the small gag fragments produced were much fainter than those produced in the digestion of the sulphated Chons (Figure 4.3C and Figure 4.3D). Silver staining was more effective on the sulphated Chon than de-sulphated Chon species because the latter are not highly charged. rHYAL-1-His_6 showed the least activity toward DS, degrading some material to small fragments but much of the high molecular weight gag was still present (Figure 4.3E). Concentrated media from control 293T cells showed no activity against HA, Chon, C4S, C6S or DS (Figure 4.3).

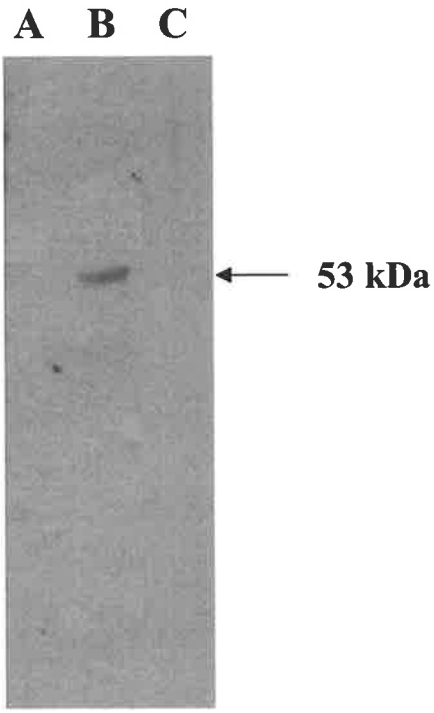

Figure 4.2 Western blot analysis of transiently-transfected 293T cells

Concentrated media from control 293T cells (A) and 293T cells transiently-transfected with pHYAL-1-His_6 (B) and pHYAL-3-His_6 (C) were electrophoresed on 10% SDS-PAGE and transferred to a PVDF membrane. Western blot analysis of protein was performed with primary mouse anti-His_6, secondary sheep anti-mouse HRP antibodies (section 2.3.4).

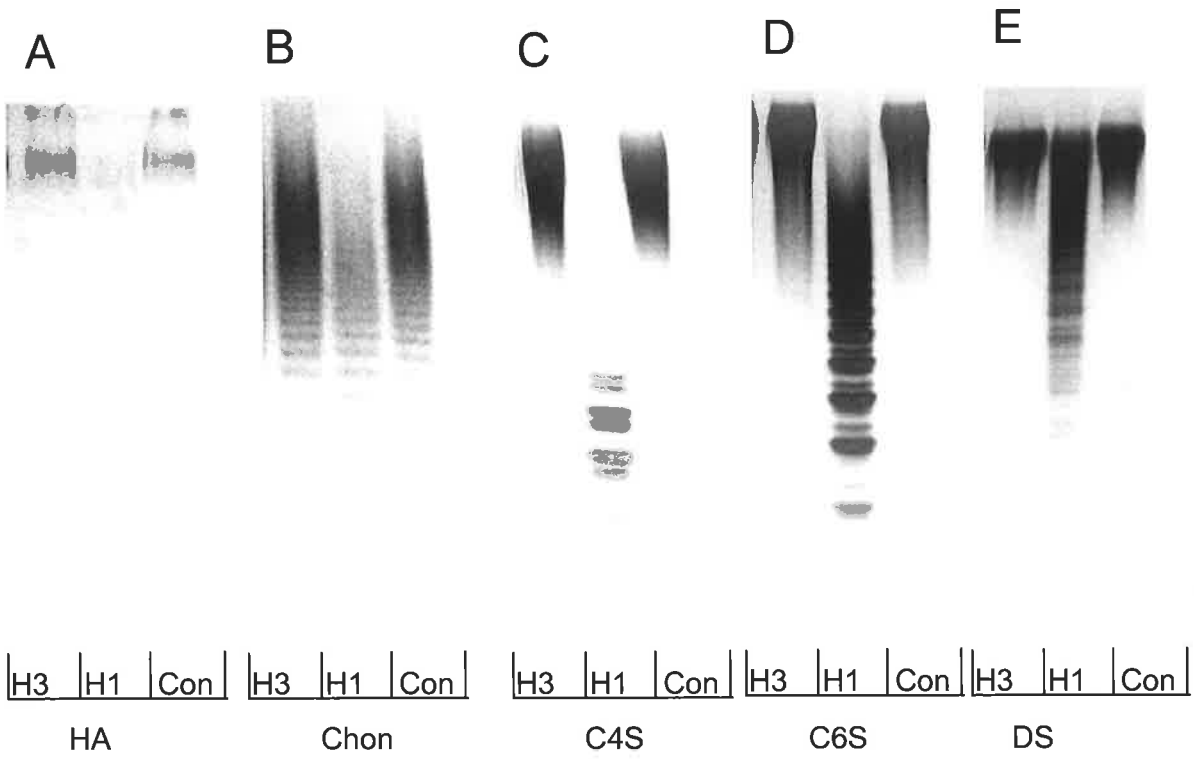

Figure 4.3 Glycohydrolase activity assay for transiently-transfected 293T cells

The substrates HA (A), Chon (B), C4S (C), C6S (D) and DS (E) were each digested at pH 3.5 for 16-h with concentrated media from 293T cells transfected with pHYAL-3-His_6 (lane 1), pHYAL-1-His_6 (lane 2) and control (untransfected) 293T cells (lane 3). Digested samples were resolved on a 30-40% gradient PAGE gel and gags visualised with silver staining.

4.5 Stable expression of recombinant hyaluronidase-3-His_6

4.5.1 Isolation of a stable hyaluronidase-3-His_6-expressing cell line

Stable expression of pHYAL-3-His_6 vector was performed in CHO-K1 cells with the aim of producing a high-yielding rHYAL-3-His_6 cell factory system. Recombinant HYAL enzyme is expected to saturate the cellular mechanisms of protein processing and trafficking, resulting in the secretion of active recombinant protein into the growth media (Wurm, 1997; 2004; Hunziker and Geuze, 1996).Recombinant protein could then be easily collected, concentrated, purified and assayed for protein amount and activity. The advantage of stable expression above transient is the ability to easily scale-up protein production.

CHO-K1 cells were grown to 80% confluence and transfected with pHYAL-3-His_6 using the Fugene6 (Roche, Basel, Switzerland) mammalian transfection reagent, and a HYAL-3-His_6-expressing cell line was isolated after three rounds of cloning by limiting dilution in a 96-well plate (section 2.2.4). The cell line that was expressing the highest amount of recombinant protein was determined by analysis of intra-cellular His_6-tagged protein by immunofluorescence (see below).

His_6 proteins were detected in fixed cells using mouse anti-His_6 and sheep anti-mouse FITC-conjugated-secondary antibody (section 2.2.5). His_6-specific immunofluroscence allowed the visualisation of rHYAL-3-His_6 in discrete vesicular particles within the cell (Figure 4.4). Using nuclear staining to determine cell number, the percentage of strong HYAL-3-His_6 cells was used as the basis for selecting a high expression cell line (Figure 4.4). The clonal cell line chosen had 43 ± 7% cells expressing rHYAL-3-His_6 (n=3).

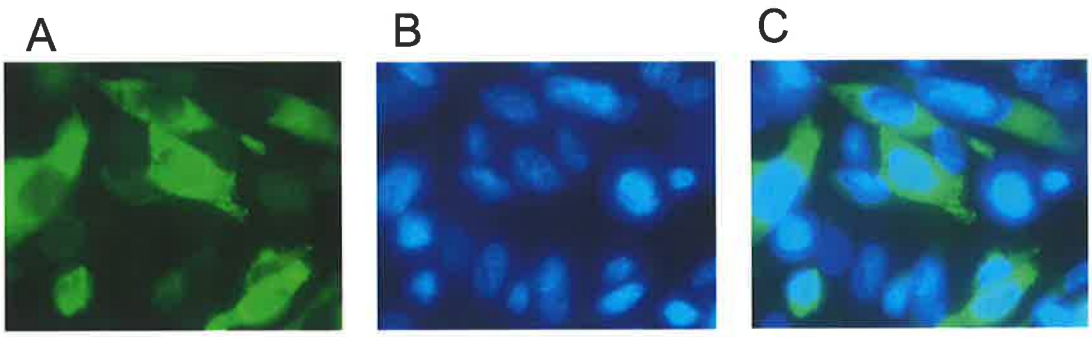

Figure 4.4 Immunolocalisation of HYAL-3-His$_6$

The stable rHYAL-3-His$_6$-expressing CHO-K1 cells were fixed in formaldehyde. rHYAL-3-His$_6$ was localised with primary mouse anti-His$_6$ antibody, secondary sheep anti-mouse FITC-conjugated antibody and visualised under a NB filter (A). Cells were co-incubated with DAPI to stain nuclei and were visualised under a WU filter (B). Panel C is a merge of panels A and B. Cell are shown at 400x magnification.

4.6 Intra-cellular localisation of recombinant hyaluronidase-3-GFP

The intra-cellular localisation of rHYAL-3-$His_6$to discrete vesicular particles within the cell was further investigated in live cells by expression of a rHYAL-3-GFP fusion protein and tracker dye to locate organelles of interest (section 4.6).

rHYAL-3-GFP showed distinct localisation to intra-cellular vesicles using fixed cells;, further investigation into the localisation of rHYAL-3 was therefore performed using pHYAL-3-GFP and organelle tracker dyes on live cells.

CHO-K1 cells grown to 80% confluence (section 2.2.1) and transfected with pGFP-N1 or pHYAL-3-GFP (section 2.2) using the Fugene6 (Roche, Basel, Switzerland) mammalian transfection reagent (section 2.2.4) were allowed to divide and were then placed into G418 selective media for 2-weeks to isolate a GFP-expressing cell line (section 2.2.4). Cell were grown on slides and examined under a fluorescent light microscope using a specific narrow band NB (DM500) filter.

Cells transfected with pGFP-N1 displayed diffuse staining throughout the cell (Figure 4.5A), whereas pHYAL-3-GFP (Figure 4.5B) showed a staining pattern very similar to pHYAL-3-His_6 (Figure 4.4), with rHYAL-3-GFP localising to distinct punctate vesicles (Figure 4.5B).

The HYAL-3-GFP stable expression cell line was co-labelled with various organelle markers to determine the intra-cellular localisation of rHYAL-3 (section 2.2.6). HYAL-3-GFP (Figure 4.6A) did not co-localise with the Golgi-specific marker BoDiPy-C5 (Figure 4.6B). Distinct GFP-labelled vesicles were observed in the merged image, particularly those surrounding the unstained nucleus (Figure 4.6C).

A

B

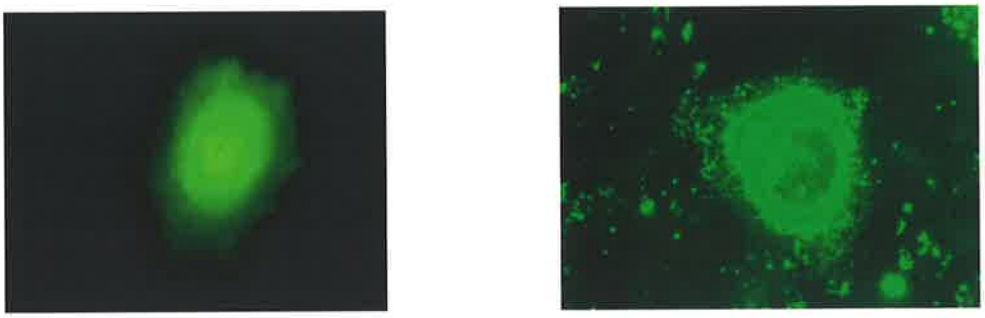

Figure 4.5 Localisation of hyaluronidase-3-GFP in CHO-K1 cells

CHO-K1 cultured cells transfected with (A) pEGFP-N1 and (B) pHYAL-3-GFP. Cell are shown at 1000x magnification under a NB filter.

HYAL-3-GFP (Figure 4.6D) did not co-localise with the Mitotracker (Figure 4.6E). The merged image shows that the green rHYAL-3-GFP-containing vesicles are separated from the red-labelled mitochondria, and do not overlap completely (Figure 4.6F).

HYAL-3-GFP (Figure 4.6G) co-localised with the Lysotracker Red (Figure 4.6H). The merged image shows distinct yellow vesicles (Figure 4.6I), however rHYAL-3-GFP is also observed in other organelles that are Lysotracker-negative (Figure 4.6I).

HYAL-3-GFP co-localised (Figure 4.6J) with ER Tracker blue/white (Figure 4.6K). The merged image shows that the bulk of the green rHYAL-3-labelled vesicles turned white as they co-localised with blue vesicles stained with the ER Tracker blue/white (Figure 4.6L).

4.7 Stable expression of recombinant hyaluronidase-1-His_6

The HYAL-1-His_6 expressing cell line was available in the laboratory. This cell line was made by transfection of CHO-K1 cells with pHYAL-1-His_6; a clonal cell was then isolated by serial dilutions.

4.8 Production and purification of recombinant hyaluronidase-3-His_6 and hyaluronidase -1-His_6 proteins

Cell lines that stably-expressed rHYAL-3 and rHYAL-1 proteins were used to produce conditioned media. This was concentrated and His_6-tagged recombinant protein was enriched over an immobilised ion affinity "Talon" column (Clontech, Mountain View, CA, USA) (section 2.3.2). Purified protein was then analysed by Western blot and HYAL activity assay.

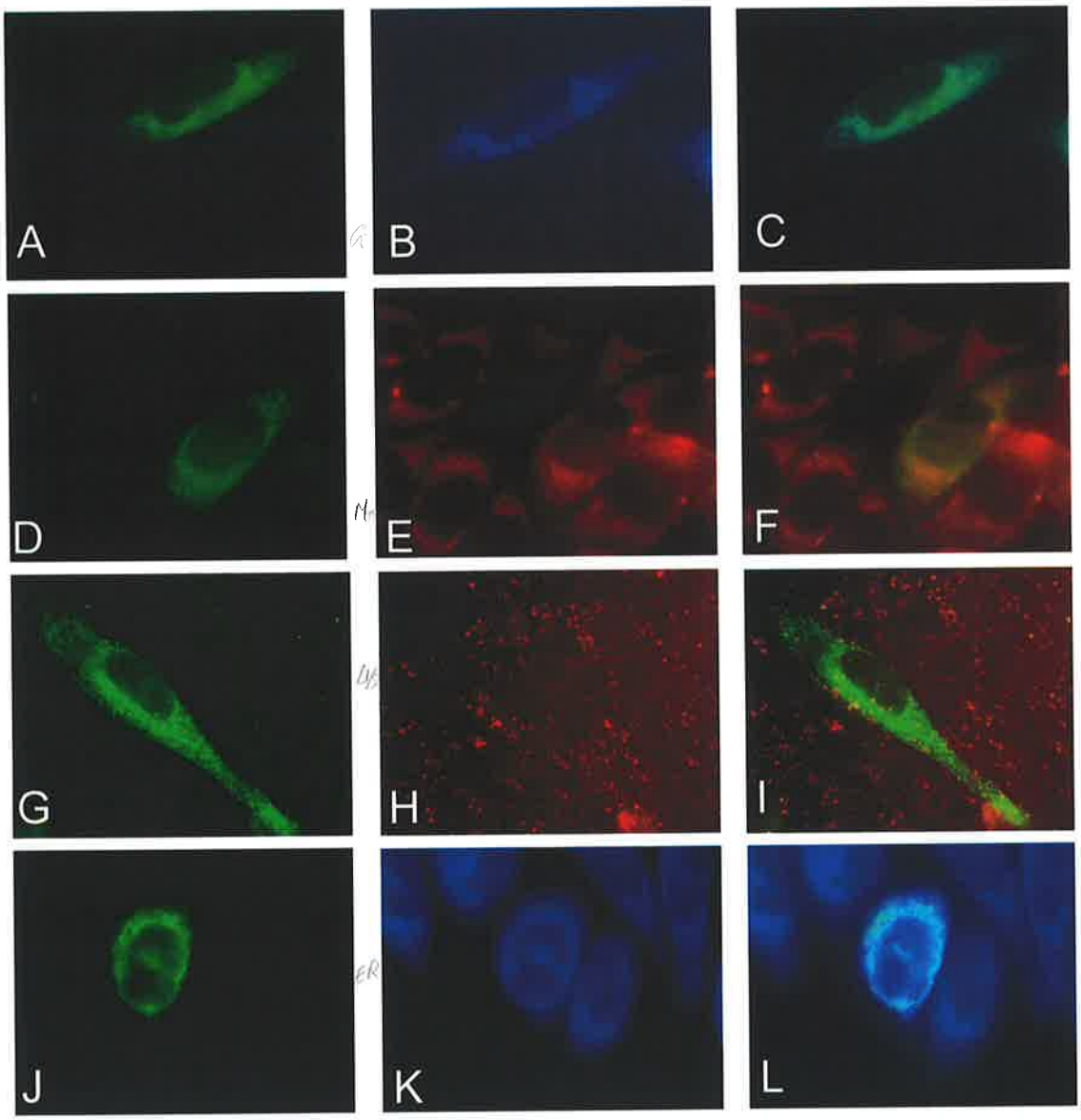

Figure 4.6 Intra-cellular localisation of hyaluronidase-3-GFP

CHO-K1 cells were transfected with pHYAL-3-GFP and fluorescent recombinant protein was visualised under a NB filter on live cells (panels A,D,G,J). Intra-cellular organelles were stained with Golgi specific ceramide BODiPy-C5 (panel B), Mitotracker red (panel E), Lysotracker red (panel H) and ER Tracker blue/white (panel K). Panels B and K were visualised under WU filter, panels E and H were visualised under an NE filter; Panel C is a merger of A and B; panels F is a merger of D and E; panel I is a merger of panels G and H; and panel L is a merger of panels J and K. All images are at x1000 magnification.

Western blot analysis with an anti-His_6 antibody (section 2.3.4) revealed three bands in the Talon column elution from untransfected CHO-K1 cell-conditioned media, that were 30 kDa and 13/12 kDa (Figure 4.7A; lanes 3 - 6). In addition to these non-specific bands, CHO-K1 cells transfected with pHYAL-3-His_6-secreted a protein of 46 kDa into the cell culture media (Figure 4.7B; lanes 4 - 6). CHO-K1 cells transfected with pHYAL-1-His_6 secreted a protein of 57 kDa into the cell culture media in addition to the non-specific bands (Figure 4.7C lanes 5 - 7). HYAL-1 and HYAL-3 were only apparent in elutions of the Talon purification and were not observed in unpurified concentrated media.

Coomassie staining of the Talon column process (section 2.3.5) allowed the visualisation of all non-specific proteins (Figure 4.7; panels E, F and G; lanes 1 - 7). In addition to the three His_6-tagged proteins many other proteins of varied sizes remained in the Talon-purified elutions (Figure 4.7; panels E, F and G; lanes 3 - 7).

4.9 Glycosylation of recombinant hyaluronidase-1-His_6 and hyaluronidase-3-His_6

Media collected from the stable cell lines expressing either rHYAL-3-His_6, rHYAL-1-His_6 or a CHO-K1 control cell line was concentrated (section 2.2.7) and His_6 proteins purified using the Talon column (section 2.3.2). These Talon-purified His_6-tagged proteins were then digested with PNG'ase-F to remove N-linked carbohydrates (section 2.3.6). The molecular weight of rHYAL-3-His_6 decreased from 46 to 37 kDa on digestion with PNG'ase F (Figure 4.8). The molecular weight of HYAL-1-His_6 decreased from 57 to 47 kDa on digestion with PNG'ase-F (Figure 4.8). Digestion of the co-purified proteins with PNG'ase-F did not alter their molecular weights and they remained at 30 and 12/13 kDa.

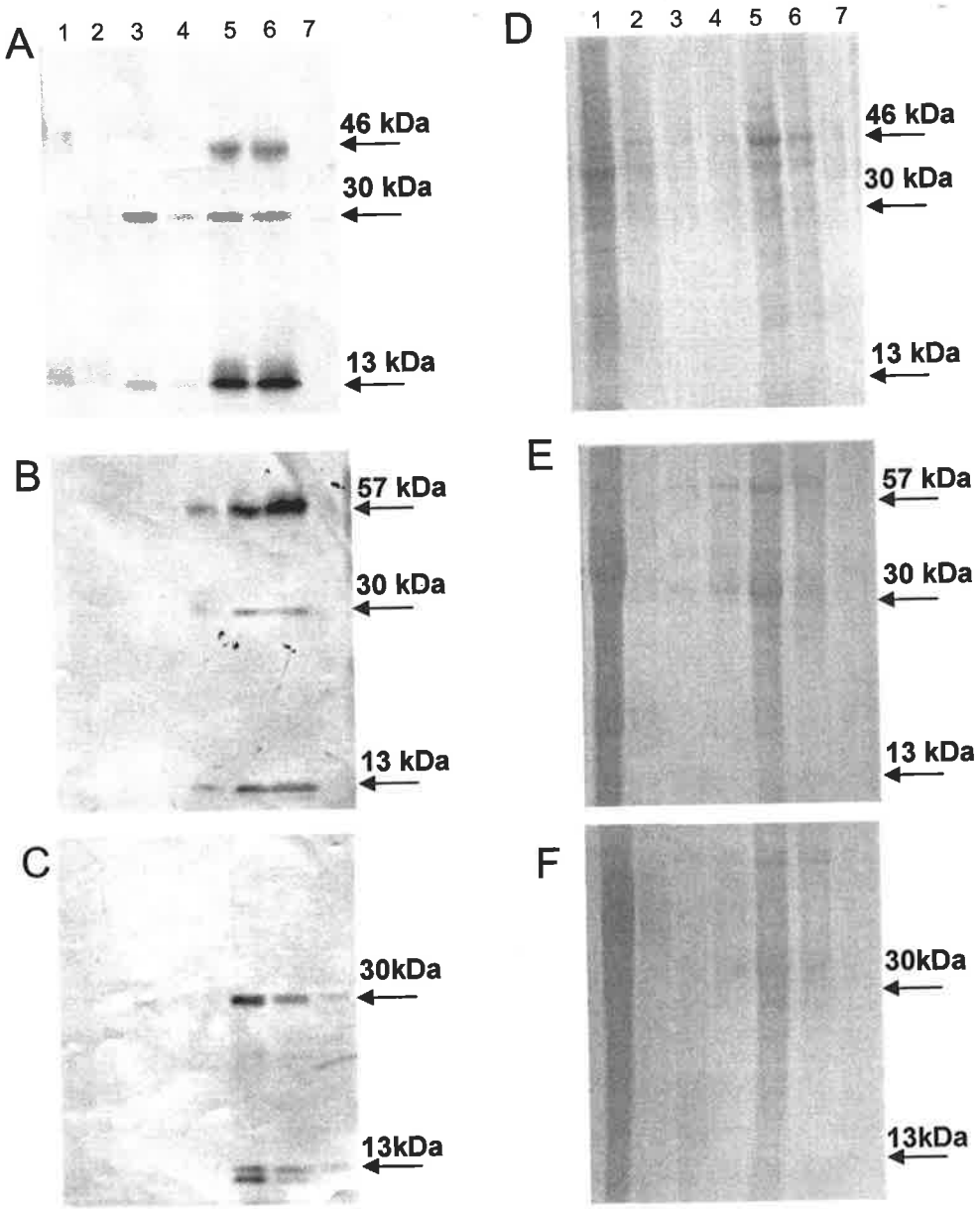

Figure 4.7 Western blot analysis of Talon-purified recombinant hyaluronidases

Talon-purified rHYAL-3- His_6 (A, D), rHYAL-1His_6 His (B, E) and control CHO-K1 proteins (C, F) were run on 10% SDS-PAGE and transferred to a PVDF membrane. Western blot of protein was performed with primary mouse anti-His_6, secondary sheep anti-mouse HRP and subsequent color reaction to the HRP (A-C). For each gel, lane 1: concentrated media; lane 2: Talon column wash; lanes 3 - 7: Talon column elutions 1 – 5. Proteins were also non-specifically stained on non transferred gels with Commassie blue (D-F).

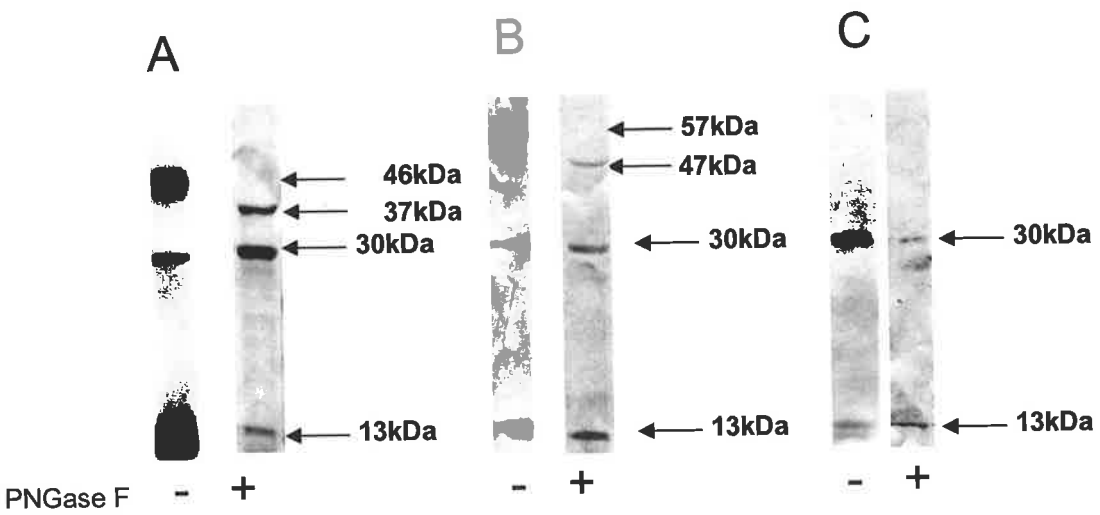

Figure 4.8 Glycanase-F treatment of recombinant hyaluronidases

Talon-purified rHYAL-3-His_6 (panel A), rHYAL-1-His_6 (panel B), and control CHOK1 cells (panel C) were incubated with (+) or without (-) PNGase-F. Proteins were then run on a 10% SDS-PAGE and transferred to a PVDF membrane. Protein was detected with primary mouse anti-His_6 antibody, secondary sheep anti-mouse HRP-conjugated antibody and subsequent colour reaction to HRP.

4.10 Glycohydrolase activity of recombinant hyaluronidase-1-His_6 and hyaluronidase-3-His_6

The activity of Talon-purified rHYAL-1 and rHYAL-3 toward HA (section 4.10.1) and the effect of additives to the soluble HYAL assay were examined (4.10.2). The activity of Talon-purified rHYAL-1 and rHYAL-3 toward other gag substrates was also examined using a soluble substrate assay (section 4.10.3).

4.10.1 Activity of recombinant hyaluronidase-3-His_6 and hyaluronidase-1-His_6 toward hyaluronan

The Talon column system (section 2.3.2) was used to purify His_6-specific proteins from concentrated media collected from cells expressing rHYAL-3-His_6, rHYAL-1-His_6 and non-tranfected CHO-K1 control cells (section 2.2.7).

HA activity in the concentrated media before purification, and in the Talon column elutions, was assayed using a natural substrate assay (section 2.4.3). Concentrated media from untransfected cells showed activity against HA at pH 3.5, as the HA was degraded to a lower molecular weight smear (Figure 4.9A lane 5) when compared to an undigested HA control (Figure 4.9A lane 8). This endogenous activity is removed though purification of the media with the Talon column, as activity is not seen in the control CHO-K1 elution (Figure 4.9A lane 6).

The Talon column-purified rHYAL-3-His_6 protein showed no activity against HA at either pH 3.5 or pH 7 (Figure 4.9A lane2 and 4.9B lane 2), as the size and amount of HA remained constant when compared to the negative no-enzyme controls (Figure 4.9A lane 8 and 4.9B lane 8).

rHYAL-1 His_6 showed activity against HA at pH 3.5 (Figure 4.9A lane 4), but no activity was observed at pH 7 (Figure 4.9B lane 4). Bovine testicular HYAL was active at both pH's, as it completely digested the HA to small molecular weight fragments that were undetectable by 0.8% agarose gel electrophoresis (Figure 4.9 A lane7 and 4.9 B lane7).

4.10.2 Hyaluronidase activity assay with additives

BSA (Maingonnat *et al.*, 1999; Afify *et al.*, 1993; Myer and Rapport, 1952) cysteine (Myer and Rapport, 1952), sodium ions (Afify *et al.*, 1993; Myer and Rapport, 1952), magnesium (Afify *et al.*, 1993), detergents (Maingonnat *et al.*, 1999) and EDTA (Krishnapillai *et al.*, 1999) have previously been shown to affect HYAL activity or stability.

Talon column-purified HYAL-3-His_6, HYAL-1-His_6 and control CHO-K1 proteins (section 2.4.8) were examined for HYAL activity in a soluble HA assay; BSA, cysteine, detergents, sodium ions, magnesium ions and EDTA were added and assessed to determine whether they had an effect on rHYAL-3-His_6 or rHYAL-3-His_6 (section 2.4.5). The HA digestions were resolved on 0.8% agarose and HA stained with Stains All (section 2.4.3).

No additive had any discernible effect on the activity of Talon-purified rHYAL-3-His_6 or CHO-K1 control proteins, as digests resolved on agarose gel retained the same size and amount of HA irrespective of the additive (Figure 4.10A and C).

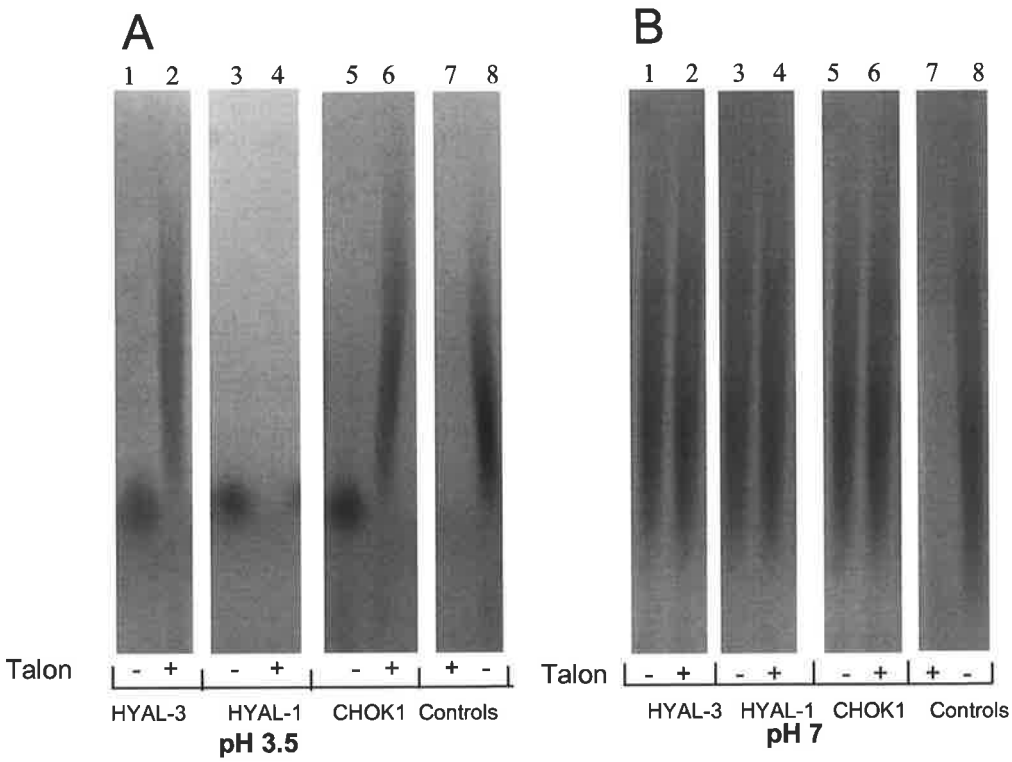

Figure 4.9 Hyaluronidase activity assays on Talon-purified recombinant hyaluronidase-3-His_6 and hyaluronidase-1-His_6

The soluble HYAL assay was performed at pH 3.5 (panel A) and pH 7 (panel B) using non-purified concentrated media (-) and Talon column-purified protein (+). Each gel shows digestion with pHYAL-3-His_6 stably-transfected CHO-K1 cells (lane 1 and 2); pHYAL-1-His_6 stably transfected CHO-K1 (lanes 3 and 4) and control CHOK1 cells (lanes 5 and 6). Positive control digests of testicular HYAL (lane 7: +) and no-enzyme control (lane 8: -) are also shown. Digested samples were resolved on 0.8% agarose and stained with Stains All.

High concentrations of EDTA, sodium and magnesium were found to have an inhibitory effect on rHYAL-1-His_6 in a soluble assays resolved on agarose gel showed an increase in the size and amount of HA when compared to the control reaction without additives (Figure 4.10B). BSA, cysteine, Triton X-100, CHAPS or low concentrations of EDTA, sodium or magnesium, had no effect on rHYAL-1-His_6 activity; samples resolved on agarose gels showed that all HA was digested to small undetectable saccharide fragments, leaving a clear lane in the gel (Figure 4.10B). However, positive effect for rHYAL-1-His_6 would not have been detected in this assay, because samples digested under the standard reaction conditions demonstrated total digestion that leaves a clear lane in the gel (Figure 4.10B).

4.10.3 Hyaluronidase activity toward other glycosaminoglycans

The Talon column system (section 2.4.3) was used to purify His_6-specific proteins from concentrated media collected from cells expressing rHYAL-3-His_6, rHYAL-1-His_6 and CHO-K1 control proteins (section 2.4.8). The Talon column eluates were examined for activity against natural substrate in a soluble gag assay with the reaction products resolved on gradient-PAGE (sections 2.4.3 and 2.4.4). Degradation was determined as a shift in the banding pattern towards smaller molecular weight oligosaccharides when compared to the negative (no enzyme) control (Figure 4.11).

Talon-purified rHYAL-3-His_6 and control untransfected CHO-K1 proteins showed no activity against HA, Chon, C4S, C6S or DS at either pH 3.5 or pH 7 (Figure 4.11). No alteration in the size or concentration of gag substrate was observed in the presence of Talon-purified rHYAL-3 or untransfected CHO-K1 cells. rHYAL-1-His_6 showed activity against HA, C4S, C6S and DS at pH 3.5, but not at pH 7 (Figure 4.11).

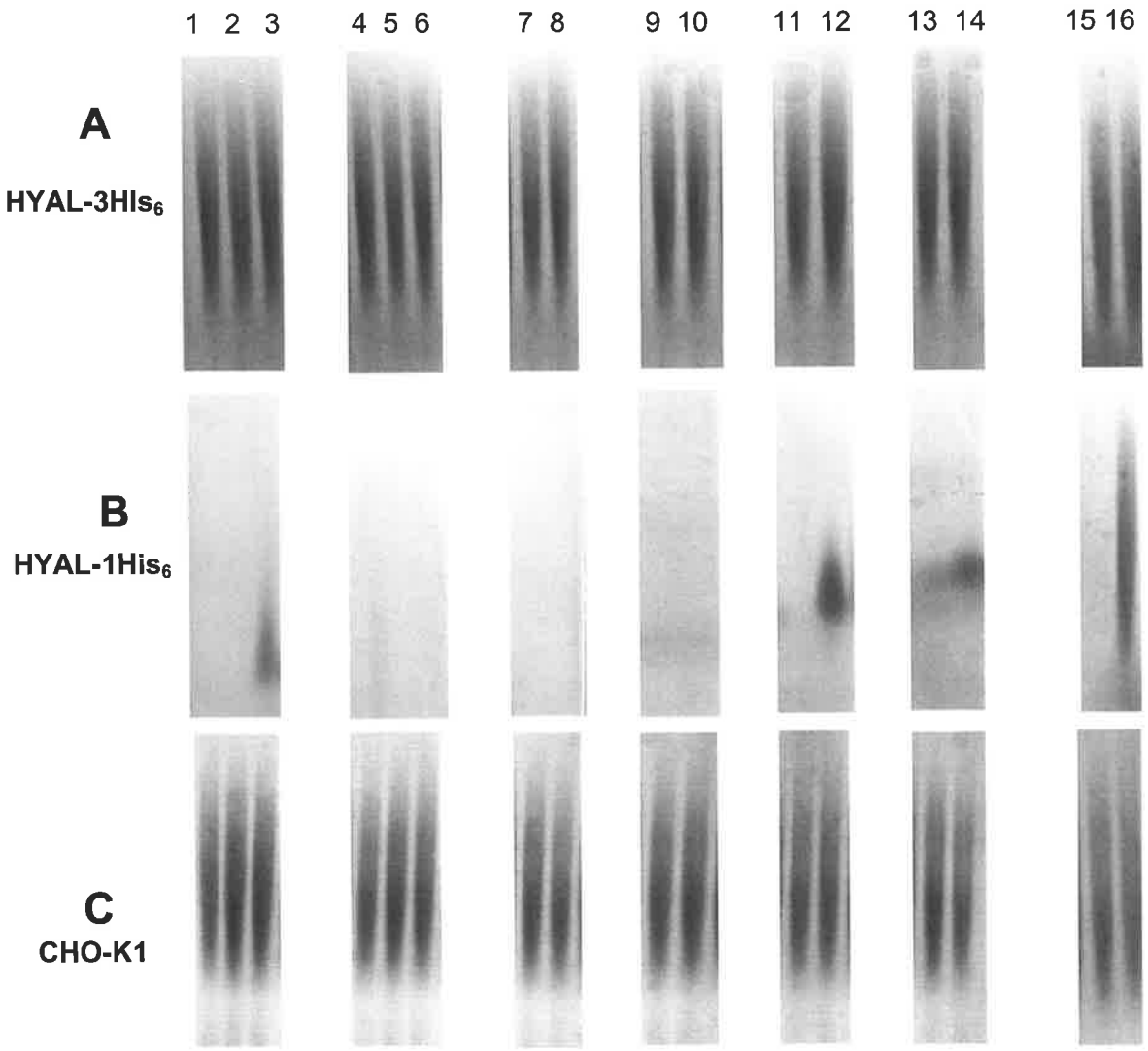

Figure 4.10 Hyaluronidase agarose activity assays with additives

Agarose HYAL activitys assays were performed using the Talon column purified proteins from cells stably-expressing pHYAL-3-His_6 (panel A), pHYAL-1-His_6 (panel B) or untransfected control CHO-K1 cells (panel C). The standard soluble HA assay was performed by the addition of 1 μM, 0.1 mM and 0.1 M EDTA (lanes 1, 2, 3); 1 μM, 0.1 mM and 0.1 M cysteine (lanes 4, 5, 6); 0.01% (v/v) Triton X-100 (lane 7); 0.01% (v/v) CHAPS (lane 8); 2 mg/L and 2 g/L BSA (lanes 9, 10); 0.05 M and 0.2M NaCl (lanes 11, 12); 0.05 M and 0.2M $MgCl_2$ (lanes 13, 14); standard HYAL reaction conditions (lane 15) and non-digested HA control (lane 16).

The activity of rHYAL-1 at pH 3.5 was visible, as the high molecular weight gag at the top of the gels decreased, while the low molecular weight gag at the base on the gel increased (Figure 4.11). The results of stable CHO-K1 produced protein echoed that found for rHYAL-1-His_6 produced by transient expression in 293T cells: the rHYAL-1 enzyme was again able to degrade the sulphated gags. At pH 7 no HYAL activity was observed for rHYAL-1, as the size and concentration of gags of resolved samples appeared the same whether they were incubated with rHYAL-1 or controls

4.11 Analysis of non-tagged recombinant hyaluronidase-3

No gag-degrading activity was observed with rHYAL-3-His_6 protein under any assay condition. rHYAL-3 protein without a His_6 tag (rHYAL-3 non-tagged) was produced to investigate whether the His_6 tag had an inhibitory effect on rHYAL-3 activity.

4.11.1 TNT protein production of non-tagged hyaluronidase-3

Non-tagged HYAL-3 was produced in a cell-free transient system, as previously described for HYAL-3-His_6 (section 2.3.1).Using the pHYAL-3 non-tagged plasmid the TNT system produced a protein of 46 kDa, which is the expected size for non-tagged rHYAL-3 (Figure 4.12).

4.11.2 Transient expression of non-tagged hyaluronidase-3

pHYAL-3 non-tagged was transiently-transfected into 293T cells using calcium phosphate precipitation (section 2.2.3).

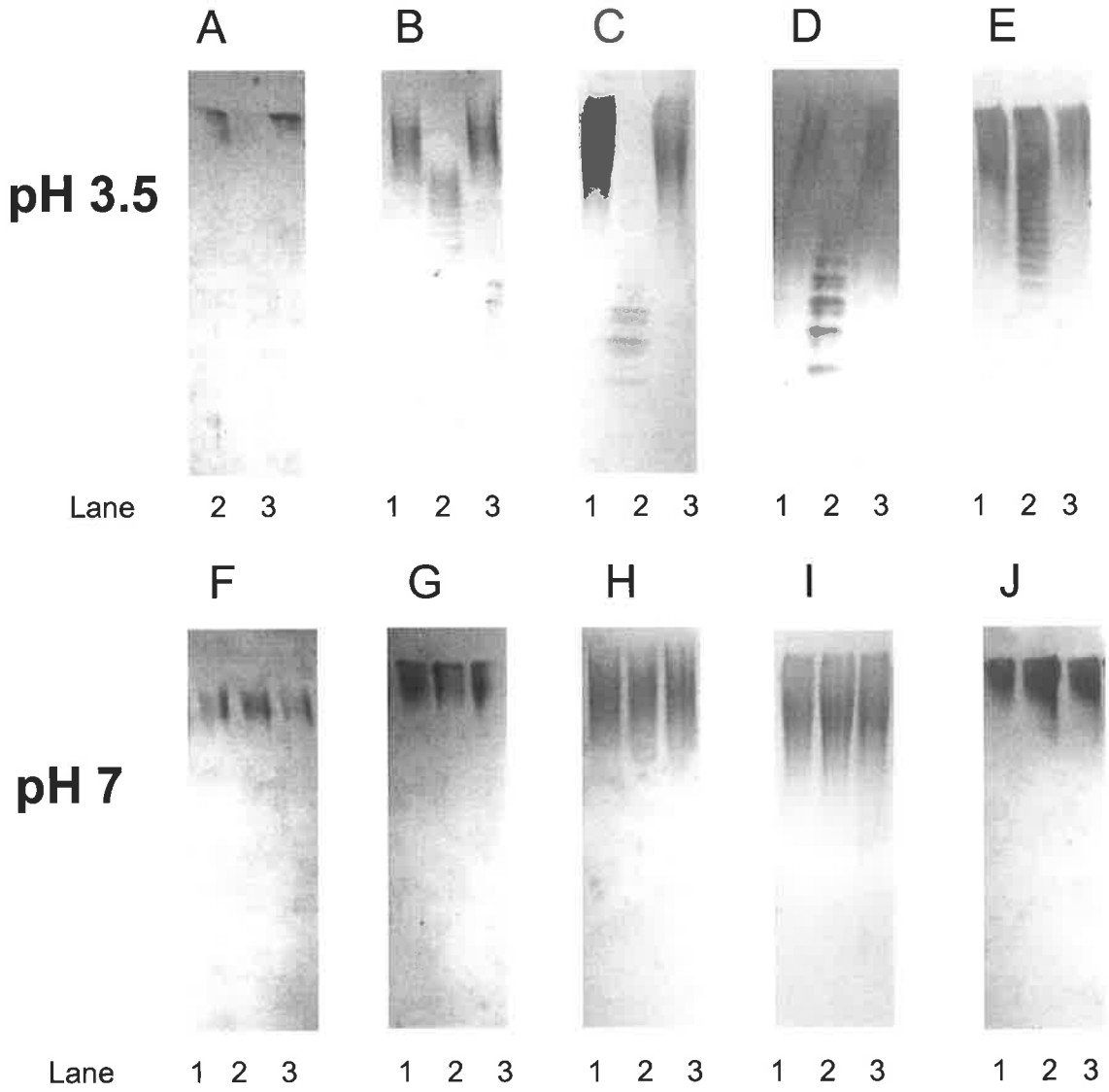

Figure 4.11 Glycohydrolase activity assay for recombinant hyaluronidase-3-His_6 and hyaluronidase-1-His_6 from stably transfected CHO-K1 cells

Digests were performed using CHO-K1 Talon-purified proteins rHYAL-3-His_6 (lane 1), rHYAL-1-His_6 (lane 2) and untransfected control (lane 3). Substrates of HA (panels A and F), Chon (panels B and G), C4S (panels C & H), C6S and (panels D and I) and DS (panels E and J) were each digested at pH 3.5 (panels A - D) and pH 7 (panels E - J). Digested samples were resolved on a 30-40% gradient PAGE and gags visualised by silver staining.

Figure 4.12 TNT produce recombinant non-tagged hyaluronidase-3 protein

^{35}S-methionine-labelled recombinant HYAL-3 non-tagged protein was produced by TNT reaction and resolved by 4-20% SDS-PAGE: lane 1; pHYAL-3; lane 2: control.

Media from pHYAL-3 and control non-transfected cells was concentrated (section 2.2.7.) and examined for HYAL activity through a zymography assay (section 2.4.1), an ELISA-based HYAL assay (section 2.4.2) and a natural substrate assay in which reaction products were resolved by agarose electrophoresis (section 2.4.3).

The ELISA-based HYAL assay showed that the amount of biotin-labelled HA detected in the assay wells remained unchanged irrespective of whether the well had been incubated with concentrated media from pHYAL-3 non-tagged transfected 293T cells or negative untransfected control 293T cells (Figure 4.13). Similarly, no HYAL activity was observed in the soluble natural substrate assay (Figure 4.13).

The amount and size of HA remained the same irrespective of whether it was incubated with concentrated media from 293T cells transfected with pHYAL-3 non-tagged, untransfected 293T cells or negative (no enzyme) control (Figure 4.13). Zymogram analysis showed a clearing of HA in the testicular HYAL-positive control, however concentrated media from 293T cells expressing pHYAL-3 non-tagged and 293T untransfected negative controls showed no HYAL activity.

4.11.3 Stable expression of recombinant hyaluronidase-3 non-tagged in COS-7 cells

The finding that CHO-K1 cells exhibited endogenous HYAL activity in concentrated media (Figure 4.9) indicated that an alternate system was required in the use of the pHYAL-3 non-tagged plasmid; it did not possess a His_6 tag and therefore could not be purified using the Talon column system. Accordingly, COS-7 cells were chosen as an alternative stable expression line since they did not possess any endogenous activity (Figure 4.14).

A

1 2

B

293T concentrated media	Hyaluronidase Activity (U)
pHYAL-1-non-tagged	0
No plasmid control	0

C

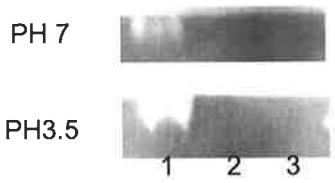

Figure 4.13 Hyaluronidase activity in media from 293T cells transiently expressing non-tagged recombinant hyaluronidase-3

Concentrated media from 293T cells transiently-transfected with pHYAL-3 (1) or non–transfected controls (2) were assayed in a soluble HYAL assay at pH 3.5, digests were resolved on 0.8% agarose and visualised with Stains All (panel A). An ELISA based HYAL assay was performed on concentrated media from 293T cells transiently-transfected with pHYAL-3 non-tagged or non–transfected control 293T cells (panel B). Zymography (panel C) was performed with: testicular positive controls (1); concentrated 293T media (2); and concentrated media from 293T cells transfected with pHYAL-3 non-tagged (3).

COS-7 cells were grown to 80% confluence and transfected with pHYAL-3 non-tagged using the Fugene6 mammalian transfection reagent (Roche, Basel, Switzerland,-section 2.2.4). Cells were selected with G418 for 2-weeks. A rHYAL-3 non-tagged expressing cell line was isolated by twice cloning out the cells with serial dilution. Media collected from the rHYAL non-tagged stably-expressing COS-7 cell line and control non-transfected cell line was collected, concentrated (section 2.2.7) and assayed for HYAL activity in an ELISA-based HYAL assay (section 2.4.2) and a soluble natural substrate assay (section 2.4.3).

Neither the concentrated media from COS-7 control cells nor the COS-7 cells stably-transfected with pHYAL-3 non-tagged, had detectable HYAL activity in the soluble natural substrate assay (Figure 4.14).No change in the electrophoretic pattern of HA was observed between the negative (no enzyme) control and the HA incubated with concentrated media from untransfected or HYAL-3-transfected COS-7 cells (Figure 4.14). The same result was observed in an ELISA-based HYAL assay, with the same amount of biotinylated HA detected in wells incubated with concentrated media collected from untransfected, pHYAL-3-non-tagged transfected cells and undigested negative controls (Figure 4.14), indicating that there was no HYAL activity in these samples. The lack of HYAL activity under transient and stable expression of non-tagged rHYAL-3 indicates that the His_6 tag is unlikely to affect HYAL-3-His_6 activity.

A

1 2

B

COS-7 concentrated media	Hyaluronidase Activity (U)
pHYAL-1 non-tag	0
No plasmid control	0

Figure 4.14 Hyaluronidase activity assay in media from COS-7 cells stably expressing non tagged recombinant hyaluronidase-3

Concentrated media from COS-7 cells transiently-transfected with pHYAL-3 non-tagged (1) or untransfected control COS-7 cells (2) were assayed in a soluble HYAL assay at pH 3.5; digests were resolved on 0.8% agarose stained with Stains All (panel A). An ELISA-based HYAL assay was performed on concentrated media from COS-7 cells stably-transfected with pHYAL-3 non-tagged or non–transfected control COS-7 cells (panel B).

4.12 Analysis of glycosaminoglycans in hyaluronidase-3 knock-out mouse tissues

A HYAL-3 knock-out mouse model has been generated which shows no gross morphological changes and appears phenotypically normal (Triggs-Raine personal communication).

Tissue from 6- and 12-month-old *hyal*-3 knock-out (*hyal*-$3^{-/-}$) heterozygote (*hyal*-$3^{-/+}$) and normal (*hyal*-$3^{+/+}$) mice were kindly donated by Dr Triggs-Raine. A list of mouse genotype and tissue type is shown in Table 4.1. Gags were extracted from these tissues using 8 M urea extraction buffer (section 2.4.8) and purified using Q-Sepharose anion-exchange chromatography (section 2.4.6). Gag concentration was determined by uronic acid assay (section 2.4.7).

The amount of uronic acid in organs of *hyal*-$3^{-/+}$ and *hyal*-$3^{+/+}$ animals was not significantly different (ANOVA $p>0.05$); these data were therefore pooled (Figure 4.15).

The amount of uronic acid in 6-month-old *hyal*-$3^{-/-}$ mice increased 4-fold in the liver (ANOVA $p<0.05$) and 7-fold in the testis (Figure 4.15) compared to heterozygotes and unaffected control animals. No significant difference in the amount of uronic acid between the *hyal*-$3^{-/-}$, *hyal*-$3^{+/+}$ and *hyal*-$3^{-/+}$ mice was observed in all other tissues tested from 6- or 12-month old mice (Figure 4.15).

	Mice per group			
	6-month		12-month	
Tissue	*hyal*-3$^{+/-}$and *hyal*-3$^{+/+}$	*hyal*-3$^{-/-}$	*hyal*-3$^{+/-}$ and *hyal*-3$^{+/+}$	*hyal*-3$^{-/-}$
Brain	5	3	5	2
Heart	5	3	5	2
Lung	5	1	5	2
Kidney	5	3	5	2
Liver	5	3	5	2
Muscle	5	1	5	1
Fat	5	3	5	2
Skin	1	1	1	2
Testsis	1	1	1	1
Ovaries	NA	NA	5	1

Table 4.1 Mice used for glycosaminoglycan extraction

The type and number of tissues that were used to determine gag amounts are listed for the 6- and 12-month-old hyaluronidase-3 knock-out (*hyal*-3$^{-/-}$), heterozygote (*hyal*-3 $^{-/+)}$ and normal (*hyal*-3$^{+/+}$) mice. The amount of uronic acid in organs of *hyal*-3$^{-/+}$ and *hyal*-3$^{+/+}$ animals was not significantly different (ANOVA $p>0.05$); therefore these data were pooled (Figure 4.15).

In 12-month-old animals the difference in gag accumulation between *hyal*-$3^{-/-}$ or *hyal*-$3^{+/+}$/*hyal*-$3^{-/+}$ had changed, with only a 5-fold increase of uronic acid in the testis of *hyal*-$3^{-/-}$ mice (Figure 4.14) and no significant difference in the liver (ANOVA $p>0.05$). In 12-month-old mice the amount of uronic acid was found to be 5-fold greater in the muscle of *hyal*-$3^{-/-}$ than in the *hyal*-$3^{+/+}$/*hyal*-$3^{-/+}$ (Figure 4.15). For all other tissues at 12-months there was no significant difference was obsevered in the amount of accumulated uronic acid in *hyal*-$3^{-/-}$ mice compared to *hyal*-$3^{+/+}$/*hyal*-$3^{-/+}$ mice (Figure 4.15).

4.13 Discussion

Recombinant protein technology provides a means for analysing the structure and activity of HYAL enzymes. HYAL1 mammalian expression vector was already available in Byers laboratory (Byers *et al.*, 2005), in this study vector that encoded HYAL-3 was created. HYAL-1 and HYAL3 fusion proteins were produced with a C-terminal His_6 tag to aid in purification, and the localisation of HYAL-3 was further investergated by the encorporation of a C-terminal GFP tag .

4.13.1 Production of recombinant protein

pHYAL-1-His_6 and HYAL-3-His_6 vectors were expressed in cell-free translation system, transient mammalian system and a stable mammalian system. The resulting proteins were characterised and their activities examined.

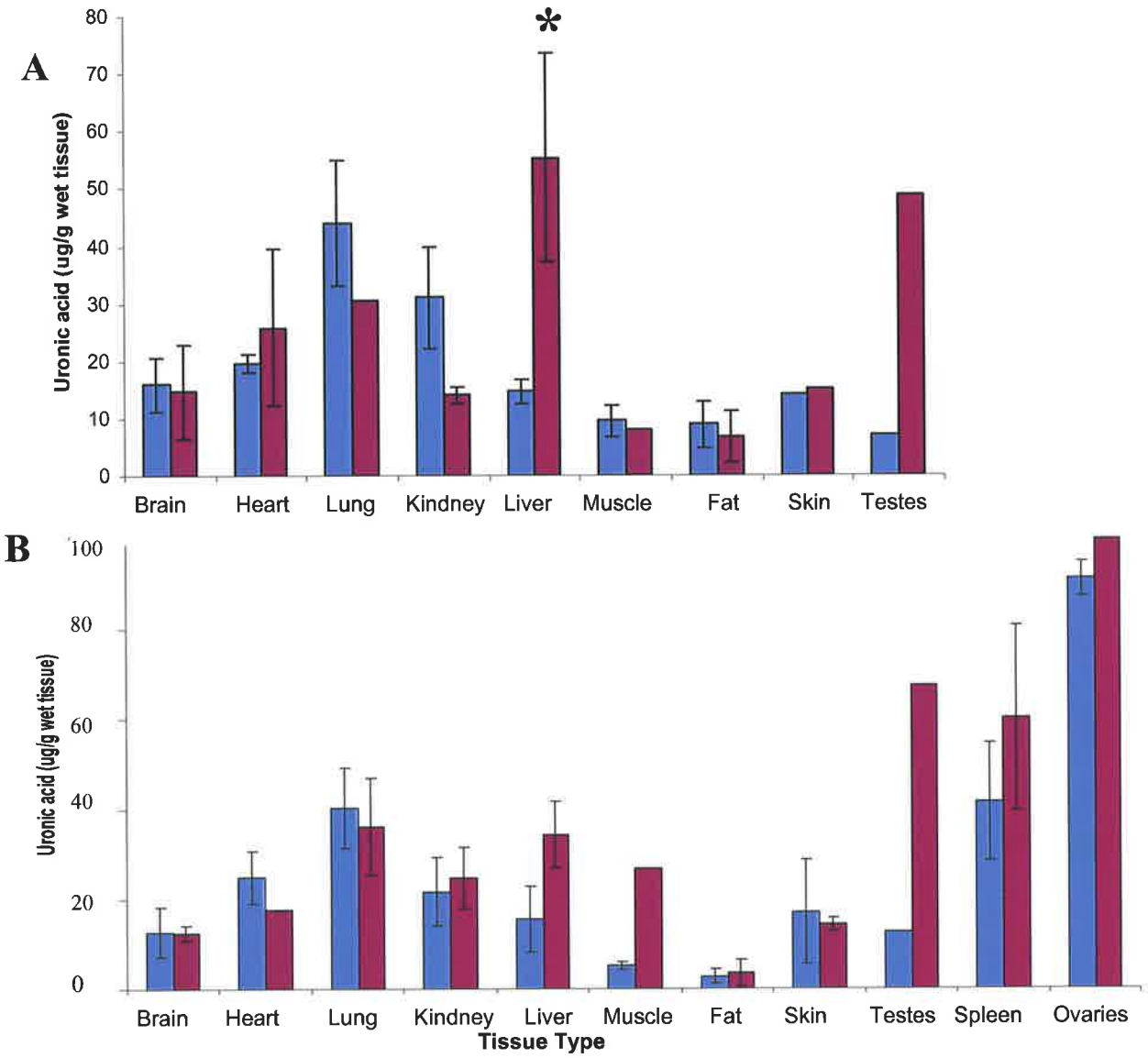

Figure 4.15 Quantitation of glycosaminoglycans in hyaluronidase-3 knock-out mice

Using Q-Sepharose chromatography gags were purified from tissues of 6-month (panel A) and 12-month old (panel B) mice. The amount of uronic acid purified from combined data from normal (*hyal*-$3^{+/+}$)/heterozygote (*hyal*-$3^{-/+}$) mice are shown in blue (■) and *hyal*-3 knock-out mice (*hyal*-$3^{-/-}$) in purple (■). For Details as to the numbers of mice per group see table 4.1. * denotes ANOVA P>0.05 between *hyal*-3 knock-out mice and (*hyal*-$3^{-/-}$).normal (*hyal*-$3^{+/+}$)/heterozygote (*hyal*-$3^{-/+}$) mice.

4.13.1.1 Cell-free expression of hyaluronidase-1 and hyaluronidase-3

The cell-free TNT translation system produced proteins of the predicted size, demonstrating the integrity of the plasmid sequences generated. However, no activity was observed for either HYAL-1 or HYAL-3 in the cell-free system using three independent assays. Cell-free *in vitro* production of both HYAL-1 and HYAL-3 was previously shown to produce an active HYAL (Lokeshwar *et al.*, 2002). Using the same method of TNT protein production (Promeg Madison, WI, USA) and a ELISA-based HYAL assay (section 2.4.2; Frost and Stern, 1997). As discussed below, the pHYAL-1-His_6 vector was capable of producing an active enzyme in either the transient or stable cell lines that were produced, suggesting that lack of activity for HYAL-1 produced by the cell-free TNT system was not a problem associated with the expression vector or assays. The reason for the conflicting data is unclear, as the experiments were identical to those published and used the same HYAL-3 sequence, expression vector, assay and TNT protein production system (Lokeshwar *et al.*, 2002). Contrary to the published data (Lokeshwar *et al.*, 2002) the experimental evidence presented in this thesis suggests that the cell-free TNT system is not an effective method for the production of active HYAL protein.

4.13.1.2 Transient expression of recombinant hyaluronidase-1 and hyaluronidase-3

Western blot of the concentrated culture media from 293T cells transiently-transfected with pHYAL-1-His_6 revealed a 53 kDa His_6-specific protein and the concentrated media was able to degrade HA, Chon, C4S, C6S and DS. No His_6-specific protein or glycohydrolase activity at pH 3.5 was detected in the culture media of cells transfected with pHYAL-3-His_6 or untransfected 293T cells. These results indicate that active rHYAL-1-His_6 can be isolated through transient expression. However, expression of

HYAL-3-His_6 protein was only successfully isolated after changing to a stable expression system.

4.13.1.3 Stable expression of recombinant hyaluronidase-1 and hyaluronidase-3

Stable cell lines that express a recombinant protein can be expected to generate higher amounts of protein over time than can be achieved with transient systems; therefore HYAL-1 and HYAL-3 were expressed in stable CHO-K1 cell lines. Clones stably-expressing the HYAL of interest were selected by immunostaining with anti-His_6 antibody, and His_6-tagged protein was enriched by Talon affinity chromatography.

rHYAL-1-His_6 purified from CHO-K1 cell culture media by Talon affinity column chromatography was found to have a molecular weight of 57 kDa, identical to the published data for the pre-protein of HYAL-1 (Csoka *et al.*, 1997; 2001). Removal of the carbohydrate structures from rHYAL-1-His_6 revealed a core protein of 47 kDa, similar to the 46.4 kDa mass that was predicted by bioinformatics (Table 3.3). These data demonstrate that the rHYAL-1 produced in these experiments was similar to the pre-protein form of HYAL-1 found in serum and not the processed form found in urine that has as 100 amino acid cleaved from the C-terminus to leave a core protein of 35.4 kDa (Csoka *et al.*, 1997).

HYAL-3-His_6 was stably transfected into CHO-K1 cells. Immunostaining of the clonal cell line with anti-His_6 antibody revealed that only 47% of cells were expressing a detectable amount of His_6-tagged protein (Figure 4.4); this did not increase after three rounds of cloning by limiting dilution. The problem may be associated with the detection system; however, HYAL-1-His_6 had clearly shown much greater transfection

efficiency using the same methods indicate (Byers *et al.*, 2005), suggesting that there is a novel problem with cell lines that over-express rHYAL-3. Variability in clone expression is thought to involve either (i) gene expression being turned off; (ii) unstable insertion of the expressed gene; or (iii) the presence of non-transformed cells (Barnes *et al.*, 2003). An inability to obtain a truly clonal rHYAL-3-expressing cell line affects the capacity to scale-up protein production since not all cells produce the protein.

rHYAL-3-His_6 was enriched from the culture media of the CHO-K1 stable expression cell line using the Talon column. rHYAL-3-His_6 had a molecular weight of 46 kDa (Figure 4.1), of which 37 kDa was core protein, as shown by PNGase-F digestion to remove carbohydrate; this was smaller than the expected size based on the amino acid sequence predicted by the HYAL-3 gene (47.5 kDa). One explanation for this discrepancy is that HYAL-3 might undergo C-terminal processing, analogous to that found for urinary HYAL-1 (Csoka et al., 1997) where an 11 kDa fragment is lost from the protein. Therefore, glycosylation and proteolytic cleavage must have occurred in the production of rHYAL-3-His_6.

4.13.2 Activity of recombinant hyaluronidase-1.

rHYAL-1-His_6 displayed greatest activity against HA, which it digested to small saccharides that were not detected on gradient-PAGE (Figures 4.3 and 4.11); it also digested the related gag structure, Chon (desulphayed CS), but to a lesser extent, resulting in a ladder of high to low molecular weight fragments (Figures 4.3 and 4.11). Activity was observed only at acid pH. Thus, rHYAL-1-His_6 displays a substrate preference towards the *N*-acetylglucosamine (β1-3) glucuronic linkage in HA over the N-acetylgalactosamine (β1-3) glucuronic linkage in Chon.

rHYAL-1-His_6 also showed activity against C4S and C6S and, to a lesser extent, DS (Figures 4.3 and 4.11). The sulphated gags have a heterogeneous structure that is not uniformly sulphated and is variably epimerised. Unsulphated residues of *N*-acetylgalactosamine (β1-3) glucuronic acid within the C4S, C6S and DS chains may be more susceptible to HYAL-1 cleavage in a manner analogous to the activity of PH20 (Knudson *et al.*, 1984). The sulphation of gag substrates has also been shown to be important for the activity of other endoglycosidases such as bacterial HYALs (Takagaki *et al.*, 2000; Pritchard *et al.*, 1994) and heparanase (Freeman and Parish, 1998). The variability of rHYAL-1 to degrade these sulphated gags highlights the importance of gag composition, in particular sulphation patterns, for the activity of HYAL-1.

4.13.3 Activity of recombinant hyaluronidase-3

No activity was observed for rHYAL-3-His_6 against any of the gag substrates at either acidic or neutral pH. Three different assay systems were employed to measure HYAL activity: a soluble ELISA-based assay, zymography and HA agarose gel electrophoresis. A possible explanation for the lack of activity displayed by rHYAL-3-His_6 may be found in the areas of protein expression, protein purification or enzymatic assay conditions.

4.13.3.1 Protein expression

Problems associated with protein expression occur because the recombinant expression system is unable to mimic the production of an active protein, as would occur in native systems. This can result in the accumulation of protein throughout different compartments of the cell and may result in a mis-folded protein that is active and/or targeted for degradation.

The core protein size of rHYAL-3 was different from the predicted size, indicating that proteolysis had occurred. Thus, the lack of activity for HYAL-3 could be due to the enzyme not receiving the correct post-translational modification. Recombinant protein production can cause slight aberrations in protein folding (Schwarz *et al.*, 1996) and glycosylation (Bhatia and Mukhopadhyay, 1999) that can result in mis-targeting, loss of activity and incorrect post-translational modification.

rHYAL-3-GFP was observed in the lysosome, as expected, and the function of lysosomal HYAL-3 will be discussed in chapter 6. Large amounts of rHYAL-3-GFP were also found in the ER, this may reflect the normal localisation of HYAL-3. For example, HYAL-3 in the ER could act as a transglycosylase or HA-binding protein. Testicular HYAL not only degrades gags, but also possesses a transglycosylation activity that allows the enzyme to synthesise and/or alter the sequence of gags (Takagaki *et al.*, 1994; Hoffman *et al.*, 1956). Further investigation is required to determine wether rHYAL-3 possess these alternative functions.

Alternatively, the localisation of rHYAL-3-GFP to the ER could represent an artefact of the recombinant expression system. Overexpression of HYAL-3 may result in enzyme accumulating in the ER prior to the tranfer to the lysosome or secretion into the cell cellture media.. rHYAL-3 within the ER can alternatively represent a saturation of the protein expression system, resulting in mis-folded protein that is trapped in the endoplasmic system and targeted for degradation (Schmitz and Herzog, 2004; Jorgensen *et al.*, 2003). Thus, likely problems with HYAL-3 expression are that (i) insufficient protein is properly-secreted; and (ii) the isolated protein may be in an inactive form.

4.13.3.2 Protein purification

Problems associated with the purification of HYAL-3-His_6 are associated with either the fusion of the His_6 tag to the recombinant protein or the Talon affinity column used for purification.

4.13.3.2.1 His_6 tag interference

His_6 tags have previously been shown to cause aggregation of the recombinant protein, affecting protein folding, protein stability, post-translational modification, and causing simple steric hindrance that disrupts the active site (Ramage *et al.*, 2002). HYAL-1 was expressed as an active His_6-tagged protein; HYAL-2 (Lepperdinger *et al.*, 1998) and Bee HYAL (Markovic-Housley *et al.*, 2000) also retained their activities when expressed as tagged proteins. Since the C terminal tagging does not disrupt these other HYAL enzymes, which are similar in protein sequence to HYAL-3, the utilisation of a His_6 tag was not expected to alter the properties of the enzyme. Untagged rHYAL-3 produced in cell-free, transient and stable systems also lacked HYAL activity. These results suggest that the His_6 tag was not the reason why HYAL activity was not associated with rHYAL-3-His_6.

4.13.3.2.2 Talon purification column

The immobilised metal ion absorption chromatography method of protein purification (Talon column) has previously been shown to oxidise and destabilise proteins due to the leaching effect of metal ions (Ramage *et al.*, 2002). Active rHYAL-1-His_6 was purified using the Talon column, indicating the suitability of this system for the isolation of mammalian HYALs. Transiently-expressed rHYAL-3-His_6 and untagged rHYAL-3, which were not exposed to the Talon column, showed no activity, indicating that the

Talon column was unlikely to be the cause of the lack of activity associated with rHYAL-3-His_6 enzymes.

Talon column purification enriched the stably-expressed His_6-tagged protein, removing many of the proteins present in the concentrated media. However, other non-HYAL proteins of various sizes were still present (Figure 4.7). These co-purified proteins could inhibit the activity of rHYAL-3-His_6. However, any inhibition was specific to rHYAL-3-His_6 and was not a general inhibitor of all HYALs, as these co-purified proteins were present in preparations of HYAL-1-His_6 and did not inhibit the activity of this enzyme.

4.13.3.3 Enzymatic assay conditions

High concentrations of EDTA, Na^+ and Mg^{++} had an inhibitory effect on HYAL-1 activity, while lower concentrations did not. This concurs with previously published data (Maingonnat *et al.*, 1999; Afify *et al.*, 1993; Myer and Rapport, 1952; Krishnapillai *et al.*, 1999). Additives, such as low concentrations of BSA, cysteine, EDTA, Na and Mg, have previously been shown to increase HYAL activity (Maingonnat *et al.*, 1999; Afify *et al.*, 1993; Myer and Rapport 1952; Krishnapillai *et al.*, 1999). These additives did not induce activity with rHYAL-3-His_6. HYAL-3 may require some other co-factor, such as a specific ion, buffering condition or other peptides to simulate its activity.

The activity of rHYAL-1 validated the methods of production, purification and reaction conditions used in these assays, confirming that it is intrinsically difficult to produce active HYAL-3 rather than a problem with the production of the mammalian HYALs in general. The specific substrate requirements of rHYAL-3, such as size and sulphation of gag or enzymatic conditions, have not been represented by the assays used.

Alternatively, the specific activity of HYAL-3 could be much lower than HYAL-1, such that the level of rHYAL-3 expression was below the level of detection.

4.13.4 Glycosaminoglycan accumulation in the hyaluronidase-3 knock-out mouse

Evidence for HYAL-3 as a gylcohydrolase can be found in the accumulation of gags in the tissues of 6- and 12-month-old *hyal*-3 knock-out mice (section 4.5.6). Increased storage in testis is consistent with the known expression of HYAL-3 in the testis (Csoka *et al.*, 1999), and HYAL-3 may play a specific role in specialised turnover of gags in this organ. Gag that was accumulating in the liver of *hyal*-3 knock-out mice at 6-months had decreased towards normal by 12-months, indicating a redundancy of function for HYAL-3. Initially, HYAL-3 was required to degrade gags in liver, hence storage, but by 12-months other HYALs or enzymes appear to be compensating. Alternatively, the substrate for HYAL-3 enzyme may no longer be synthesised in these tissues during the later stages of a mouse's life, therefore the amount of gag accumulation decreases as other enzymes compensate. The redundancy of HYAL-3 is also evident through the apparent lack of pathology in the *hyal*-3 knock-out mice (Triggs-Raine, personal communication); other enzymes must overlap in function with HYAL-3 such that knocking this gene out has no adverse effects.

4.13.5 Conclusions

rHYAL-1 was shown to be more diverse than an enzyme that exclusively degrades HA, with a substrate specificity toward the sulphated gags. Thus HYAL-1 is proposed to be involved in the endolytic turnover of CS and DS gags from PG, much like the role of heparanase on the turnover of HS gag chains from HS PGs. However, the precise role that HYAL-3 plays in cellular processes remains unknown. Bioinformatic analysis

suggests that it is a member of the mammalian HYAL family, although experimental data using the recombinant HYAL-3 protein did not produce any evidence of a HYAL activity. However, the discovery of gag storage in the tissues of the *hyal*-3 knock-out implys that HYAL-3 plays a role in gag turnover; any glycohydrolase activity possessed by HYAL-3 must be highly specific to the primary stored substrates of the *hyal*-3 knock-out mouse. Only a very low number tissues were obtained from the newly established HYAL-3 knock-out mouse colony (Table 4.4); if greater numbers of mice become available, the HYAL assays should be repeated using gags isolated from the appropriate knock-out mouse tissues.

Chapter 5

Hyaluronan metabolism in mineralising osteoblasts

5.1 Introduction

In bone, 3% of the total gag content is represented by HA (Hjertquist and Vejlens 1968). The precise role of HA in the formation and maintenance of bone is unknown, although it has been implicated in various diverse mechanisms, such as intra-cellular signalling and as a structural organiser of the ECM (section 1.4). The addition of HA to the media of mineralising bone cell culture has an osteo-inductive effect, increasing total mineral content and the number of bone-forming colonies in an *in vitro* cell culture assay (Pilloni and Bernard, 1998). HA can act as a scaffold for nucleators of bone formation (Fisher, 1985) or act as a integral part of ECM organisation.

The immortalised human osteoblast cell line MG63 was originally derived from a human osteosarcoma (Franceschi *et al.*, 1985, 1988) and is thought to represent a relatively immature osteoblast (Boyan *et al.*, 1989a). MG63 cells display many of the characteristics of an osteoblast, such as an ability to synthesise osteoid and respond to $1\alpha,25\text{-}(OH)_2D3$, a metabolite of vitamin D3, with an increase in alkaline phosphatase and osteocalcin production (Franceschi *et al.*, 1985; Bonewald *et al.*, 1992; Boyan *et al.*, 1989b). Thus, MG63 cells were chosen as an *in vitro* model of a mineralising osteoblast to study HA turnover.

The expression of HYAL by RT-PCR has previously been performed in cartilage, but not in bone (Caterson *et al.*, 2000). HAS expression has been examined in osteoblasts, with HAS-2 identified as the most abundant HAS in MG63 cells (Recklies *et al.*, 2001).

This chapter examines changes in the expression of HASs and HYALs in MG63 cells as they are induced to undergo mineralisation (Adams *et al.*, 2006). Gag

synthesis, as determined by the incorporation of ^{3}H-glucosamine and $^{35}SO_4$ into gags, was also assessed (Adams *et al.,* 2006).

5.2 Histology of mineralising osteoblasts

MG63 cells were maintained in culture for up to 5-weeks under control and mineralising culture conditions (section 2.5.1). After 24-h, 3-weeks and 5-weeks cells were fixed and stained with von Kossa (section 2.5.2) to assess mineral deposition.

No mineral deposition was observed in freshly-plated 24-h cultures (Figure 5.1A) or in 3 or 5-week cultures grown under control conditions (Figures 5.1B and C). Mineral deposition, as defined by von Kossa staining, was first observed after 3-weeks in mineralising media (Figure 5.1E). By 5-weeks the matrix surrounding the cells grown under mineralising conditions was extensively mineralised (Figure 5.1F).

5.3 RT-PCR in mineralising osteoblasts

RT-PCR was performed to determine which of the HAS and HYAL genes were being expressed in the mineralising and control non-mineralising osteoblast cultures (Adams and Byers, 2005). HYAL-P1 is a pseudo-gene (section 1.3.2.5) that could not have a direct effect on HA turnover and was therefore excluded from the analysis. The expression of MGEA-5 in mineralising osteoblasts was not pursued in this thesis because it was not possible to discern differences in MGEA-5 function as either a HYAL or O-GlcNase by the analysis of gene expression (section 1.2.2.6).

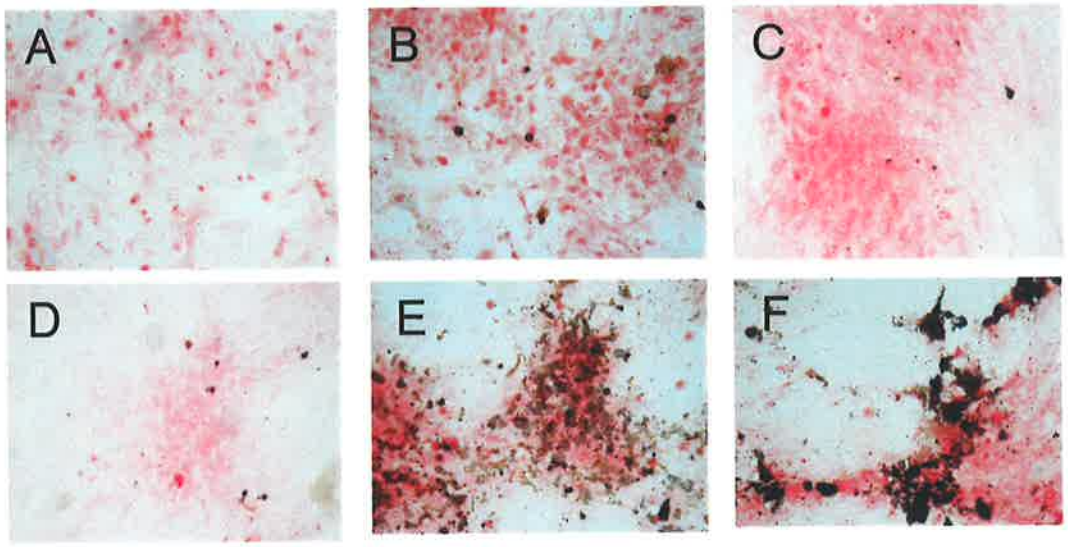

Figure 5.1 Mineralisation of MG63 osteoblast cultures

von Kossa staining of control MG63 cells (panels A, B, C) cultured in DMEM + 10% FBS. Mineralising MG63 osteoblasts were cultured in DMEM + 10% FBS, 100 μM abscorbate-2-phosphate, 10 mM β–glycerophosphate and 4 μg/mL dexamethasone (panels D, E, F). Cells were fixed 24-h after plating (panels A and D), 3-weeks (panels B and E) or after 5-weeks in culture (panels C and F). All cells are shown at x100 magnification.

RNA was purified from the MG63 cells (section 2.6.1) at 24-h and after 5-weeks under control or mineralising culture conditions (section 2.5.1). RNA quality was checked by gel electrophoresis (section 2.6.2) and the amount quantified (section 2.6.3). Purified RNA was used as a template to produce cDNA (section 2.6.4), that was subsequently used for gene-specific PCR (section 2.6.5). PCR products were then resolved on an agarose gel to determine size and intensity (section 2.1.4).

The expression of the control gene, glyceraldehyde-3-phosphate dehydrogenase (GAPDH), remained relatively constant irrespective of culture conditions (Figure 5.2). Abundant PCR products of the expected size were found for both HAS-2 and HAS-3 (Figure 5.2); HAS-1 expression was not detected; HYAL-2 and HYAL-3 expression was similar undear all conditions; whereas HYAL-4 expression was up-regulated under mineralising conditions (Figure 5.2). These initial investigations show that HAS and HYAL could be detected by PCR in this model system of mineralisation and led to the quantification of HAS and HYAL expression by real time RT-PCR (section 5.4).

5.4 Real time reverse transription-PCR in mineralising osteoblasts

HYALs and HAS expression was quantified using real time RT-PCR. RNA was harvested from triplicate cultures of MG63 cells (section 2.6.1) that were maintained either under control conditions for 24-h, control conditions for 5-weeks or mineralising conditions for 5-weeks (section 2.5.1). RNA was checked for quality (section 2.6.2), quantity (section 2.6.3) and then used as a template in reverse transcription reactions to produce cDNA (section 2.6.4). cDNA was subsequently used as a template for gene-specific real time RT-PCR (2.6.6). Any change in cycle number for a gene was normalised to the change in cycle number of a control gene, cyclophilin-A (cyc-A).

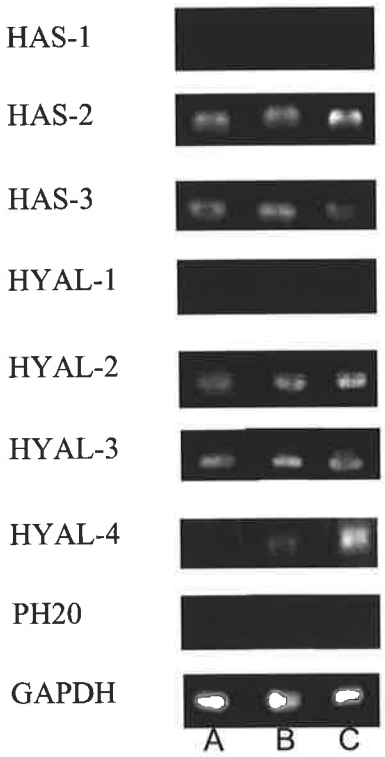

Figure 5.2 Reverse Transcription-PCR on mineralising MG63 cells

Gene-specific RT-PCR was performed on RNA isolated from MG63 osteoblasts that were cultured under control conditions for 24-h (lane A), control conditions for 5-weeks (lane B) and mineralising conditions for 5-weeks (lane C). GAPDH expression was used as an internal control as it is expressed constitutively irrespective of culture condition or time in culture. The expression of HAS-1, HAS-2, HAS-3, HYAL-1, HYAL-2, HYAL-3, HYAL-4 and PH20 was examined.

HAS-2 and HAS-3 but not HAS-1 were expressed by MG63 cells. Gene expression of HAS-2 did not change significantly with time in culture over the 5-weeks period under either control or mineralising conditions (Figure 5.3.A). However, a 13-fold down regulation of HAS-3 expression was observed in mineralising cultures; whereas HAS-2 expression did not significantly change under mineralising conditions (Figure 5.3A).

HYAL-2; HYAL-3 and HYAL-4, but not HYAL-1 or PH20, were expressed by MG63 cells (Figure 5.3B). Time in culture had no significant effect on the HYALs expression, with no change in expression observed over the 5-weeks culture period in the non-mineralising cultures (Figure 5.3B). In cells induced to undergo mineralisation, HYAL-2 expression increased 62-fold, HYAL-3 expression increased 13-fold and HYAL-4 expression increased 3-fold, when compared to the non-mineralising control 5-week cultures (Figure 5.3B). However, only the changes in HYAL-2 RNA levels were significant ($P < 0.05$).

5.5 Mineralising MG63 osteoblast cultures

The type of gags produced by the MG63 osteoblast cultures was determined by their susceptibility to digestion by specific enzymes. The triplicate samples of Q-Sepharose-isolated macromolecules from each culture condition were digested with either *Streptomyces* HYAL (i.e. HA) or chondroitinase ABC (i.e. DS, CS) (section 2.5.4). Undigested and digested samples were separated by size exclusion chromatography on a Bio-Gel P6 column (section 2.5.4). An example of the results obtained for determining the amount and type of gag is shown for the cell layer extracted from control 24-h cells (Figure 5.4).

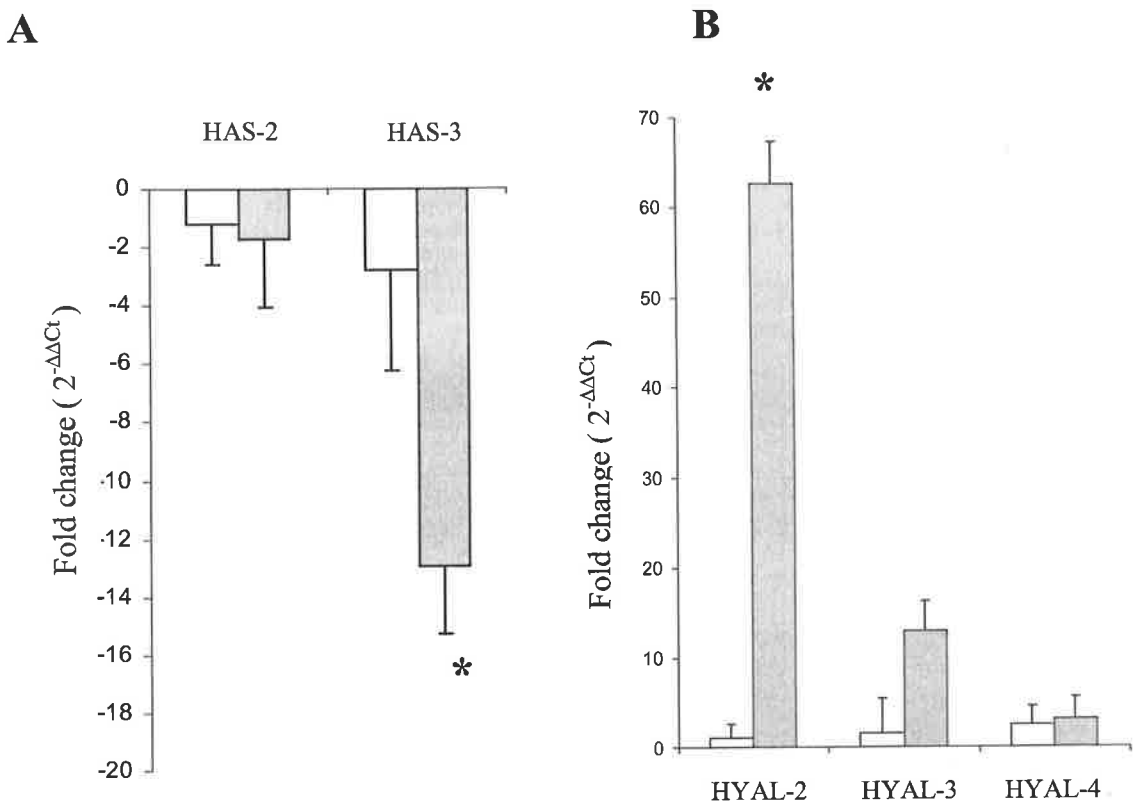

Figure 5.3. Analysis of hyaluronan synthases and hyaluronidase gene expression in mineralising osteoblasts

HAS (A) and HYAL (B) expression was determined by real-time PCR and normalised to cyclophilin-A. The normalized fold-change ($2^{-\Delta\Delta Ct}$) in gene expression between 24-h and 5-weeks in non-mineralising cultures is denoted by the clear boxes. The normalized fold-change ($2^{-\Delta\Delta Ct}$) in gene expression between mineralising and non-mineralising cultures at 5-weeks is denoted by the grey boxes. Results are the mean and standard deviation of n=3 replicates.

* Denotes $P < 0.05$ using one way ANOVA for the comparison of change in expression between 5-week mineralising culture conditions versus 5-week control conditions.

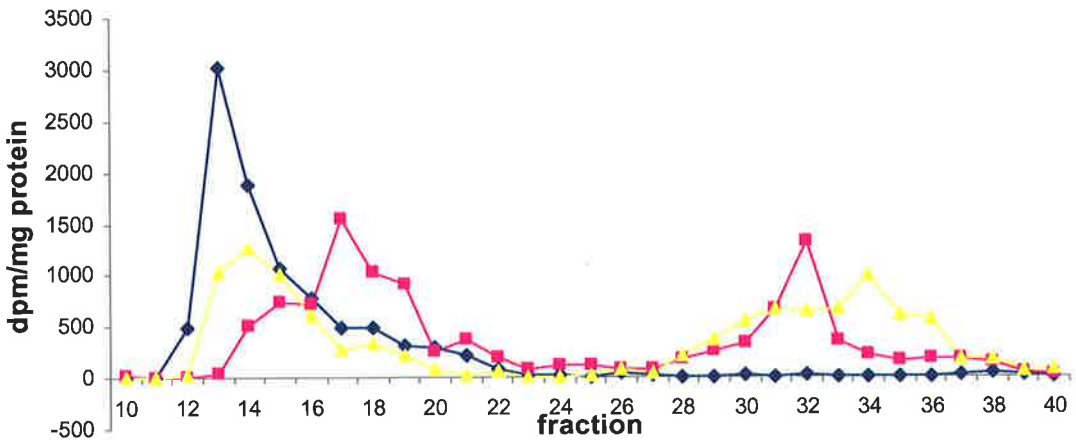

Figure 5.4 BioGel P6 chromatography of digested glycosaminoglycans.

The sub-type of gag present in radio-labelled samples was determined by digestion with specific enzymes followed by chromatography to separate digested and undigested components. The graph shows data from a control 24-hr cell layer demonstrates a typical BioGel P6 profile of ^{3}H-glucosamine labelled samples run prior to digestion (◆) or after digestion with *Streptomyces* HYAL (■) or chondroitinase ABC (△).

5.6 Total glycosaminoglycan synthesis in mineralising MG63 osteoblast cultures

MG63 osteoblast cells were cultured for 24-h or 5-weeks under control and mineralising conditions respectively (section 2.5.2). Triplicate wells were then labelled with 5 μCi ^{3}H-glucosamine and 50 μCi ^{35}S-sulphate (section 2.5.3) for 24-h. Unincorporated radiolabel was removed by dialysis and components of the cell layer and media were isolated by Q-Sepharose anion exchange chromatography (section 2.5.4).

The total amount (media and cell layer) of ^{3}H-glucosamine incorporated into the Q-Sepharose-purified macromolecules showed little change with time in culture, as the amount of ^{3}H-glucosamine incorporated into control 24-h samples was similar to the amount in control 5-week samples (Figure 5.5 A). The total amount of ^{3}H-glucosamine incorporation into mineralising 5-week cultures showed a 2- to 3-fold increase when compared to the non-mineralising 5-weeks cultured cells (Figure 5.5A). Similarly, the total amount (media and cell layer) of ^{35}S-sulphate incorporated into charged macromolecules isolated by Q-Sepharose also showed little change with time in culture. Although the mineralising weeks-5 cultures showed a 2- to 3-fold increase in total ^{35}S–sulphate incorporation when compared to the control non-mineralising cultures.

The incorporation of ^{3}H-glucosamine into HA, CS/DS or other non-gag macromolecules did not change with time in culture (Figure 5.5A). The incorporation of ^{3}H-glucosamine into HA was 5- to 7-fold lower in the weeks-5 mineralising cells when compared to the non-mineralising controls (Figure 5.5A). In addition, a 2- to 3- fold increase in ^{3}H-glucosamine incorporation into CS/DS gags, and a 10- to 12-fold increase into material that was not digested with either *Streptomyces* HYAL or

chondroitinase ABC (i.e. HS or glycoprotein) was observed in the 5-week mineralising cells compared to the non-mineralising controls (Figure 5.5A).

The incorporation of ^{35}S-label into HA, CS/DS or other macromolecules did not significantly change with time in culture, with no change observed when control 24-h samples were compared to the control weeks-5 samples (Figure 5.5B). Mineralisation resulted in a 3- to 5-fold increase in incorporation ^{35}S-label into CS/DS and a 2- to 3-fold increase in macromolecules that were not digested with either enzyme tested, as determined by comparing the weeks-5 mineralising material to the non-mineralising control material (Figure 5.5B). A small amount of $^{35}SO_4$ (less than 8% of the total) was associated with the HA fraction that did not change with time in culture. This most likely represents a low level of carry-over of sulphated gags from the Q-Sepharose columns.

5.7 Discussion

This study examined the expression of HAS and HYAL enzymes in the human osteoblast cell line, MG63, under both control and mineralising conditions. Control MG63 cells express HAS-2, HAS-3, HYAL-2, HYAL-3 and HYAL-4 but not HAS-1, HYAL-1 or PH20. The expression of HASs and HYALs did not change with time in culture. However, when MG63 cells were induced to mineralise by the addition of ascorbate-2-phosphate, β-glycerophosphate and dexamethasone to the culture media, a down-regulation of HAS-3 and an up-regulation of HYAL-2, HYAL-3 and HYAL-4 was observed. This coincided with a decrease in ^{3}H-glucosamine incorporation into HA under mineralising conditions. In contrast, the amount of CS/DS PGs and other non-digestible macromolecules increased in mineralising cultures.

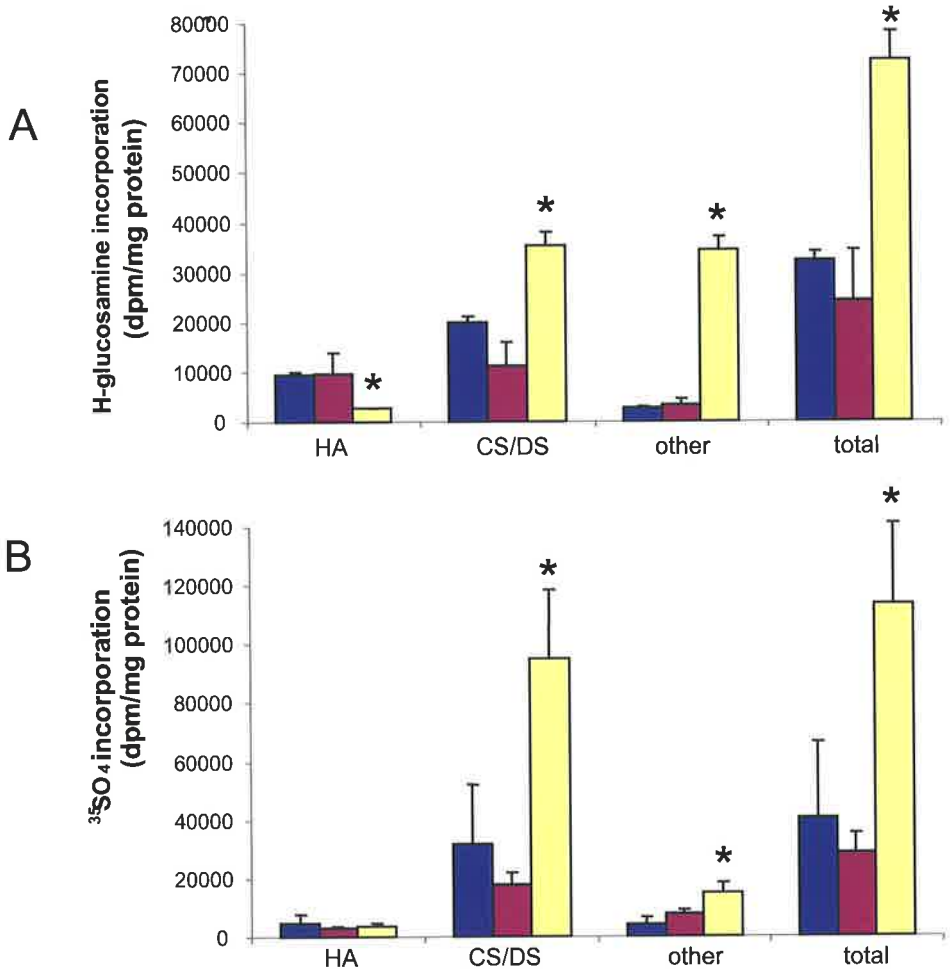

Figure 5.5 Q-Sepharose chromatography of radiolabelled macromolecules

MG63 cultures were grown under non-mineralising (24-h ■; 5-weeks ■) or mineralising conditions (5-weeks ■) and labelled with ^{3}H-glucosamine (panel A) or $^{35}SO_4$ sulphate (panel B). The total amount of radioactive macromolecules was normalised to cell protein (n=3). Total denotes the total amount of radioactive label incorporated prior to digestion; HA denotes the portion of sample that was susceptible to digestion with *Streptomyces* HYAL; CS/DS denotes the portion of sample that was susceptible to digestion with chondroitinase ABC; and other denotes the portion of sample that was not digested with either enzyme. Results are expressed as the mean ± standard deviation of n=3 replicates. * denotes P>0.05, 5-week mineralising culture conditions versus 24-h or 5-week control conditions.

5.7.1 HAS during mineralisation

MG63 cells synthesise HA using HAS-2 and HAS-3 enzymes but not HAS-1 (Recklies *et al.*, 2001). The HASs have different inherent properties, including enzyme stability, the rate of HA elongation and the size distribution of HA produced (Itano *et al.*, 1999). HAS-2 produces HA of a considerably larger size than HAS-3 (greater then 2 x 10^6 Da) and at a much faster rate (Itano *et al.*, 1999). Large molecular weight HA acts as a scaffold for PG assembly in the ECM (Weibkin and Muir, 1977). Anti-sense inhibition of HAS-2 in chondrocytes results in a reduced in PG retention (Nishida *et al.*, 1999). The HA produced by HAS-2 and HAS-3 may have a similar role in osteoblast matrix assembly, capturing space destined to become bone (Fisher, 1985). The control of HAS-3 expression may be crucial in the expansion process that occurs before bone formation by modulation of the PG binding capacity of matrix components. Consistent with the decrease in HAS-3 expression, HA synthesis also decreased during mineralisation, as measured by the incorporation of ^{3}H-glucosamine into *Streptomyces* HYAL susceptible material,

5.7.2 Hyaluronidase during mineralisation

All HYALs produced by MG63 cells were up-regulated in the mineralised cells. In particular, HYAL-2 expression increased 62-fold when cells were cultured in mineralising media. HYAL-2 is generally thought to degrade HA to a specific 20 kDa intermediate, with no activity towards other gags (Lepperdinger *et al.*, 1998). The up-regulation of HYAL-2 may represent an increase in the amount of intermediate-sized HA fragments that are involved in intra-cellular signalling cascades during mineralisation to promote bone formation (Deed *et al.*, 1997; Pilloni and Bernard 1998).

The major tissue form of HYAL, HYAL-1, was absent in MG63 cells. HYAL-1 is generally thought to be a ubiquitous HYAL that degrades the intermediate-sized fragments of HA digestion produced by HYAL-2 to tetrasaccharides. These are subsequently degraded to monosaccharides by the lysosomal exo-hydrolases, β-hexosaminidase and β-glucuronidase (Stern *et al.,* 2004). The absence of HYAL-1 in bone would suggest that either; (i) HYAL-2, HYAL-3 or HYAL-4 can compensate for HYAL-1 activity, or (ii) the accumulation of larger HA fragments in the endolytic pathway has a biological function during mineralisation.

A 13-fold increase in HYAL-3 and a 3-fold increase in HYAL-4 were also observed on mineralisation. The activity of these HYALs is poorly characterised: HYAL-3 has been shown to degrade HA in a cell-free translation system (Lokeshwar *et al.*, 2002) and HYAL-4 is reported as a "chondroitinase" with preferential activity towards CS rather than HA (Csoka *et al.*, 2001); neither of these activities has been independently confirmed and clarification of their role in bone mineralisation awaits a fuller understanding of their individual function.

RT-PCR analysis of HYAL-4 showed an increasing intensity in PCR product after 5-weeks of culture under mineralising conditions when compared to the non-mineralising sample (Figure 5.2), which translated to a 3-fold difference on real time RT-PCR quantification that was not significant (Figure 5.3). Genes that showed a much greater difference in real time RT-PCR, such a HYAL-2, showed no difference in PCR product intensity with the standard PCR method. These different PCR experiments were performed using different primers, amplicons, enzymes and reaction conditions. The results highlight the importance of performing a validated, quantitated experiment to

determine gene expression. Standard RT-PCR remains a useful tool to determine the presence or absence of a gene's expression, but is not a satisfactory method by which to to accurately determine the magnitude of expression.

5.7.3 Changes in glycosaminoglycan macromolecules during mineralisation

In contrast to the decrease in HA production, CS/DS gag synthesis increased in mineralising MG63 cells. While some PGs have previously been shown to inhibit mineralisation (Tenenbaum and Hunter, 1987), others such as decorin and biglycan have been isolated from bone cultures and shown to act as modulators of mineralisation (Boskey *et al.*, 1997; Waddington *et al.*, 2003). The gag chains of decorin and biglycan also change under mineralising conditions (Sugars *et al.*, 2003). The modulation of mineralisation can be controlled by a specific subset of PGs and glycoproteins that increase in amount as mineralisation progresses (Boskey *et al.*, 1997; Sugars *et al.*, 2003; Waddington *et al.*, 2003; Midura *et al.*, 1990; Bianco *et al.*, 1991; Termine *et al.*, 1981). The highly charged gag side chains have been shown to act as a reservoir for the calcium used in bone formation (Embery *et al.*, 1998) and PGs also mediate growth factor and intra-cellular signalling (Bertolami and Messadi, 1994; Yamaguchi *et al.*, 1990; Couchman and Woods, 1993). PGs may therefore also play a role in the cellular initiation of bone formation rather than just a structural role at the site of mineral deposition.

5.7.4 Changes in non-glycosaminoglycan macromolecules during mineralisation

An increase in the amount of ^{3}H-glucosamine and $^{35}SO_4$ incorporation into molecules not susceptible to *Streptomyces* HYAL or chondroitinase ABC digestion could represent non-gag glycoproteins or non-CS/DS gags, respectively.

A number of glycoproteins contribute to bone matrix organisation and mineralisation. Osteonectin (Termine *et al.*, 1981) and bone sialoprotein (Bianco *et al.*, 1991; Hunter and Goldberg, 1993; Midura *et al.*, 1990) are present in osteoblast cell cultures and may act as nucleators or modulators of bone formation. The increase in non-HA gag and glycoprotein production highlights the metabolic activity still present in these cultured osteoblasts and the fact that bone formation is not the passive deposition of mineral on cells, but a highly regulated and controlled process that is organised by the osteoblasts.

5.7.5 Role of hyaluronan in the mineralising matrix

HA is initially present in the maturing matrix that surrounds osteoblasts, where it performs a structural role in expanding the space between cells that is destined to become bone (Fisher, 1985). HA can also act as a scaffold for PG that can modulate mineralisation. It has been shown to both inhibit (Chen *et al.*, 1984; Chen and Boskey 1985) and stimulate bone formation (Sugars *et al.*, 2003; Boskey *et al.*, 1997). HA not only has the ability to act as a structural component of the ECM but also to function as an intra-cellular signal (Lee and Spicer, 2000). HA fragments have been shown to have an osteo-inductive effect, thus the removal of HA in the mineralising matrix may be a mineralisation nucleation signal to the cell rather than a simple effect of structural matrix alteration.

5.7.6 Model for the changes in the mineralising osteoblast extra-cellular matrix

This study was restricted to examining the changes that occurred in the transition between a mature and mineralised matrix (Figure 5.6). During mineralisation there is a change in HA metabolism to a state of higher turnover, with an up-regulation of HYAL-2 and HYAL-3 and a down regulation of HAS-3 (Figure 5.6).

Degradation of HA would produce HA fragments that have osteo-inductive properties (Pilloni and Bernard, 1998; Huang *et al.*, 2003). As the matrix surrounding osteoblast begins to mineralise mineralization the cells begin to produce more CS/DS-containing PGs and other bone-specific glycoproteins (Figure 5.5).

5.8 Conclusion

These results support a role for HA in the early stages of bone formation rather than during the mineralisation phase of bone formation. HA is decreased in the mineralising osteoblast by a combination of decreased synthesis (as shown by the down-regulation of HAS-3 and the decreased rate of ^{3}H-glucosamine incorporation into HA) and increased turnover, as shown by the up-regulation of HYALs. HA may be required for the initiation of mineralisation, in roles such as space capture and/or matrix organisation. However, as mineralisation progresses a lower amount of large molecular weight HA is produced by HAS-3 and any HA present has increased amount of HYAL enzymes acting upon it.

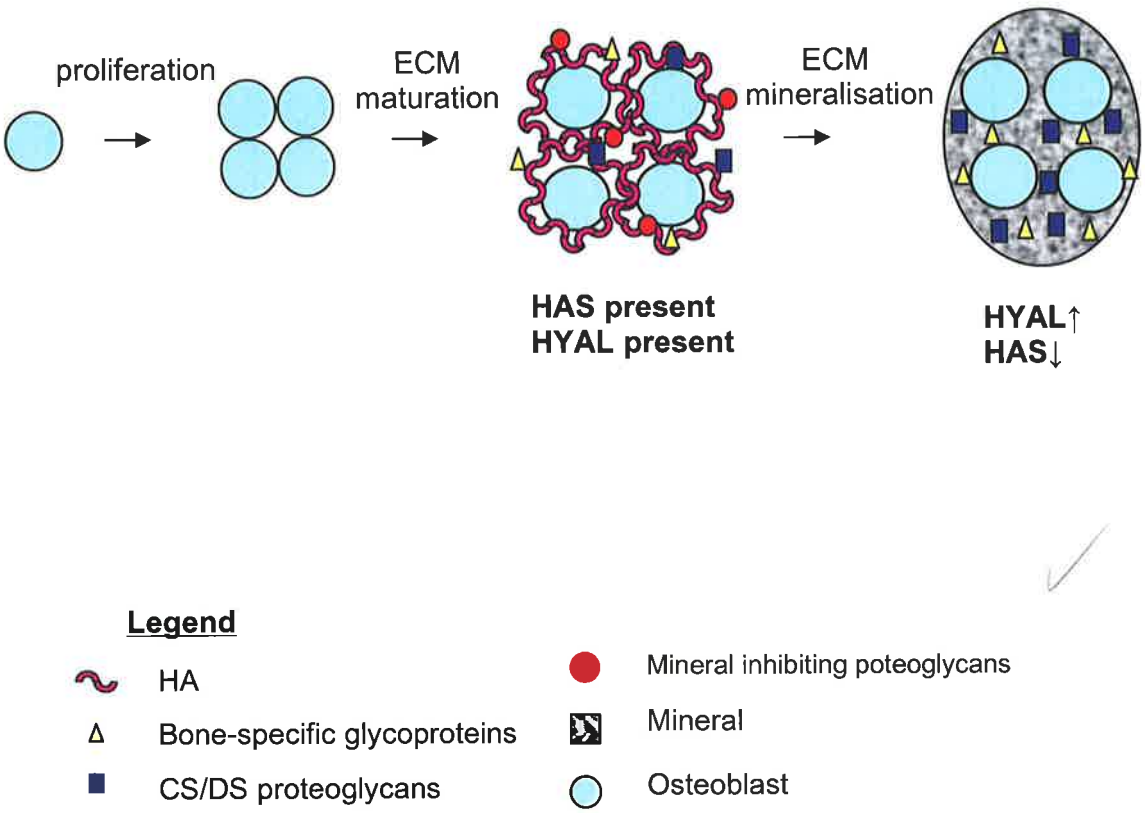

Figure 5.6 Model of mineralisation

Osteoblasts are initially in a matrix maturation process , abundant HA is present, which expands the space between cells that is destined to become bone; HA acts as a scaffold for PG that can inhibit mineralisation. As osteoblasts are induced to mineralise HA is removed through a co-ordinate down-regulation of HAS and an up regulation of HYALs. At the onset of mineral deposition the osteoblast have increased production of CS/DS PGs and other bone-specific glycoproteins.

Chapter 6

Conclusions

6.1 Bioinformatic predictions of recombinant hyaluronidase

The use of bioinformatics to discern the conserved features of the HYALs gave an indication of their functional characteristics. HYAL-3 and HYAL-1 were predicted to be proteins of 46 kDa and 57 kDa, possessing a signal peptide and possible N-glycosylation. N-Glycoslyation of recombinant HYAL-1 and HYAL-3 was confirmed by PNG'ase-F digestion (section 4.9). N-Terminal sequencing of recombinant HYAL-1, HYAL-2 and PH20 has been previously published (Csoka *et al.*, 1999), experimentally confirming the predicted signal peptide for these proteins. Thus the predictions made through bioinformatics correlated with the experimental evidence obtained from the recombinant HYAL's.

6.2 Function of hyaluronidase-1

A model for HYAL-1 in HA degradation has been proposed (Stern, 2003; 2004), whereby HA is internalised and degraded in the lysosome (Figure 6.1). The initial cleavage occurs through the action of HYAL-2, which degrades HA to 20 kDa intermediates (Lepperdinger *et al.*, 1998). HYAL-1 then degrades the intermediate to smaller oligosaccharide fragments that are sequentially degraded to monosaccharides by the exohydrolases β-hexosaminidase and β-glucuronidase (Stern, 2003; 2004).

In this study rHYAL-1 was shown to degrade the sulphated gags CS and DS and could therefore function in a manner analogous to a role that heparanase plays in HS degradation. HS degradation is well characterised and occurs though the action of heparanase to generate HS fragments of intermediate size, followed by exolytic digestion of each fragment by lysosomal hydrolases (Freeman and Hopwood, 1992). A model for the degradation of gag from small CS- and DS-containing PGs begins with

endocytosis of the small PGs into the cell (Schaefer *et al.*, 1998; Hausser *et al.*, 1992). Not all PGs follow this route of degradation, as large aggregating PGs are degraded in the matrix through the action of matrix metallo proteinases (Samiric *et al.*, 2004; Caterson *et al.*, 2000). However, the model presented in this thesis concentrates on the pathway of small endocytosed PGs, with gag degradation beginning with the initial action of the endolytic enzymes HYAL-1 and/or HYAL-4 (Figure 6.2), which has previously been defined as a specific chondroitinase (Csoka *et al.*, 2001). The fragments produced by endolytic digestion of the sulphated gags are subsequently degraded to monosaccharides by an array of specific exoglycosidase enzymes (Neufeld and Muenzer 2001).

Indirect evidence for the presence of an endolytic enzyme that acts on CS and DS is seen in the MPS (Neufeld and Muenzer 2001). The MPS are a sub-class of LSD that occur because of a deficiency of enzyme involved in gag degradation (Neufeld and Muenzer, 2001). An array of gag fragments of varying size accumulate in the MPS cells and are excreted into the blood and urine, implicating the action of an endolytic enzyme to generate the different sized gag fragments (Byers *et al.*, 1998).

6.3 Possible functions for hyaluronidase-3

Based on the results of experiments performed in this study, three models of HYAL-3 function are possible, which may not be mutually exclusive (Fig 6.1).

1) HYAL-3 is present in the lysosome/endosome, where rather than degrading gag, it is involved in gag binding and transport (Figure 6.1A). HYAL-3 may have lost its ability to degrade gags but has maintained other functions associated with HYALs such as HA

binding, the association with other proteins or synthetic transglycosylation of gags. This model is supported by the localisation of HYAL-3-GFP to the lysosome, the homology that HYAL-3 shares with other HYALs and the apparent total lack of glycohydrolase activity for HYAL-3. The accumulation of gags in the *hyal*-3 knock-out mouse can be explained by the occurrence of a novel disorder of mis-trafficked gag rather than a lack of glycohydrolase activity;

2) HYAL-3 is present in the lysosome, where it acts to degrade a specific sub-set of gags (Figure 6.1B). Although rHYAL-3 did not digest any of the substrates tested, the knock-out *hyal*-3 mouse accumulates gags in the liver at 6-months and testis at all ages when compared to normal. This strongly suggests that knocking-out HYAL-3 causes an aberration in gag metabolism; any activity possessed by HYAL-3 must be highly specific and not against the larger types of gags that were tested in this study. A more stringent assessment of activity will require larger amounts of enzyme and the isolation of greater amounts of the gags that accumulate in specific tissues of *hyal*-3 knock-out mouse; this study was limited to the amount of gag that could be isolated from the recently-created *hyal*-3 knock-out mouse colony.

3) HYAL-3 is located in the ER where it either acts in a synthetic or gag-binding role (Figure 6.1C). HYAL-3-GFP was localised to the ER and possessed no glycohydrolase activity. The similarity between the HYAL-3 protein sequence and other HYALs can result in a protein structure that still possesses a gag-binding groove or may retain alternative enzymatic properties that other HYALs exhibit, such as transglycosylation.

To discriminate these functions of HYAL-3, further investigation is required to experimentally confirm the ability of rHYAL-3 protein to bind gags or display transglycosylase activity.

6.4 Glycosaminoglycan turnover in the mineralising matrix of osteoblasts

The importance of HA in mineralising osteoblasts is shown through the changes in gene expression that result in decreased in HA production. HYAL-1 is not expressed in osteoblasts; consequently, the HA degradation pathway previously proposed by Stern (2003; 2004) cannot occur in these bone cells. Similarly, the absence of HYAL-1 in osteoblasts eliminates the possibility that the newly-proposed pathway of sulphated gag degradation occurs (Figure 6.1). Therefore, in bone an alternative method that does not require HYAL-1 must have evolved that ustilises alternative endo- and exo-hydrolases.

In this study, HYAL-3 and HYAL-4 were expressed in osteoblasts; their regulation during mineralisation implies that they have some function. Although HYAL-3 showed no activity against any gags tested it may have a specific function against gags in bone. HYAL-4 has been referred to as a chondroitinase (Csoka *et al.*, 2001) although no corroborating evidence has been published to support this claim. Thus, HYAL-4 could be a major endo-chondroitinase in osteoblasts.

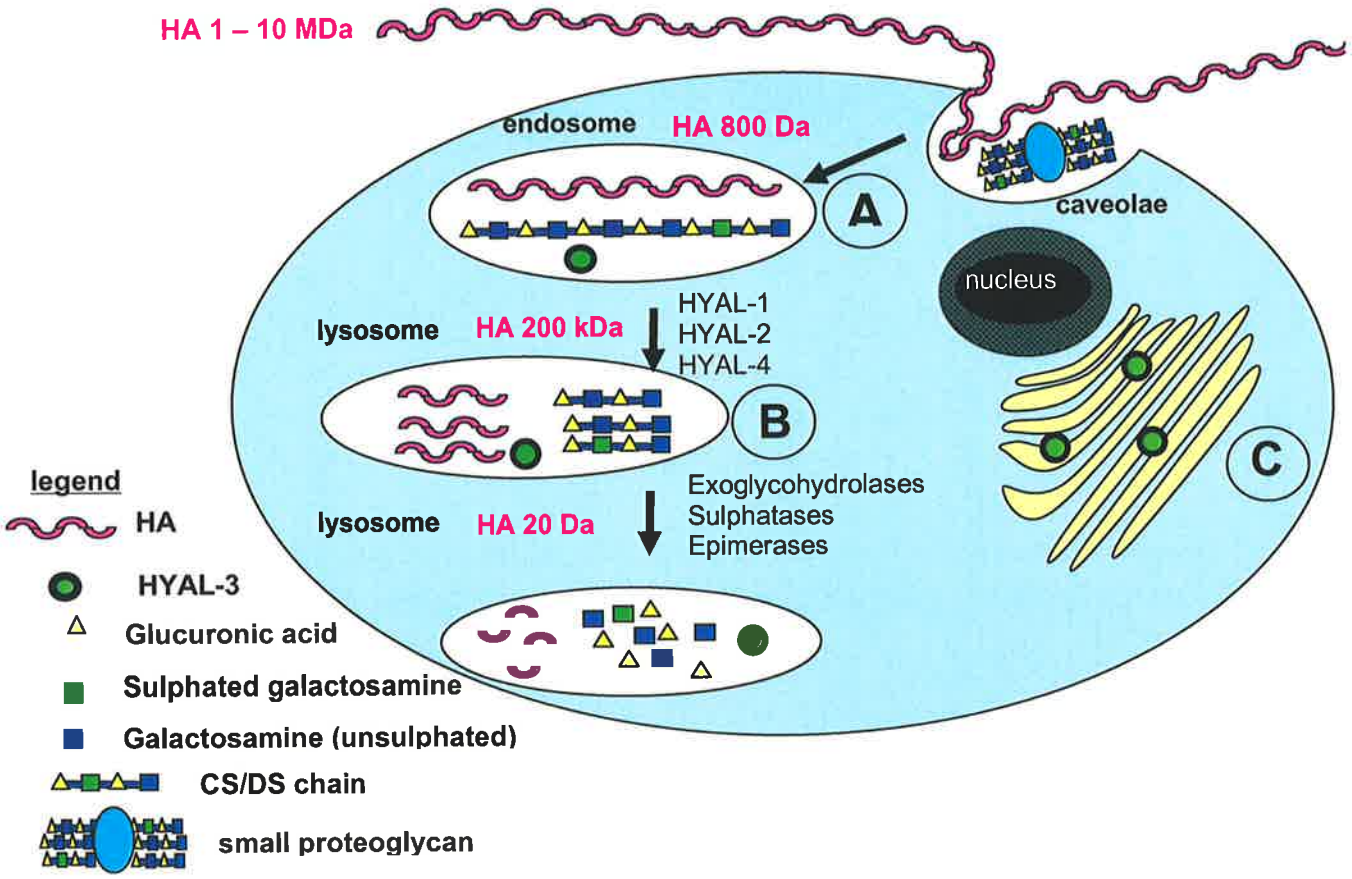

Figure 6.1 Roles of hyaluronidase-3 in the cell
Degradation of gag beings with the internalization of HA or small PGs and subsequent entry into the endosomal/lysosomal system. HYAL-2 degrades the macromolecule HA into 20 kDa intermediate fragments, which are further degraded to tetrasaccharides by HYAL-1, and finally degraded to monosaccharides by exoglycohydrolases. CS and DS gags are susceptible to the activity of the endo-hexosaminidase enzyme, HYAL-1, and the putative chondroitinase HYAL-4. The sulphated gag fragments are then further degraded to monosaccharides through the step-wise action of a series of exolytic sulphatases and glycohydrolases. Roles for HYAL-3 in the cell include: binding and stabilisation of the HA or other gag substrates within the vesicular trafficking and endosome/lysosome pathway (A); as a specific glycohydrolase within the lysosome (B); or as a synthetic or gag binding component of glycoprotein and PG processing in the ER (C). (Figure adapted from Csoka *et al.*, 2001).

6.5 Conclusions and future directions

Bioinformatics is a useful tool for predicting the function of proteins, although the characterisation of recombinant proteins is required to confirm predictions. Further characterisation of the substrate specificity that HYAL-1 shows towards the sulphated gags would allow insight into the fundamental steps of gag degradation.

The classification of HYAL-3 as a "HYAL" implies function and was based on the similarity of its genes sequence to other enzymes that have HYAL activity. Defining HYAL-3 as a HYAL may well prove to be premature, as its function is yet to be demonstrated. However, the gag accumulation in tissues of the *hyal*-3 knock-out mouse complicates the interpretation of the lack of activity observed for rHYAL-3, as it suggests that HYAL-3 may have a highly specific glycohydrolase. Characterisation of the storage material in a larger number of *hyal*-$3^{-/-}$ knock-out mouse tissues would improve understanding of HYAL-3 function, in particularly the sub-cellular fractionation of *hyal*-$3^{-/-}$ knock-out mouse tissues would determine the precise cellular compartment in which gags accumulate.

Localisation of a non-gag-degrading rHYAL-3 to the ER suggests two alternative explanations: (i) it could represent mis-folded protein targeted to the ER for degradation, or (ii) it may have retained some other function associated with HYALs, such as gag binding or transglycosylation, and performs this in the ER. The ability of HYAL-3 to bind or transglycosylate a variety of gag substrates should be tested using techniques that have been established to characterise the transglycosylase activity of PH20 (Shen *et al.*, 2003; Takagaki *et al.*, 1994).

These experiments into the production of rHYAL-3 highlight the problems associated with the age of molecular biology. Recombinant proteins produced by a model system, especially those possessing affinity tags, are not the native protein of the cell. Confirmation of the lack of HYAL activity for HYAL-3 requires a more classical step in biochemistry to purify the enzyme from tissues and assay the native protein; the gag accumulation data from the *hyal*-3 knock-out mouse and previous expression data (Csoka *et al.,* 1999) suggest that the testis should be a likely source.

HA decreases in the mineralisating osteoblast, which corresponds to a general decrease in HASs (HAS-2, HAS-3) and an increase in HYALs (HYAL-2 HYAL-3 HYAL-4). There appears to be coordinate regulation of genes that control the production and catabolism of HA and result in a decrease in HA production. Further characterisation of the size of HA, precise PG core proteins and composition of sulphated gags would give greater insight into the role of gags that undergo regulated changes during mineralisation of the osteoblast matrix.

Chapter 7:

References

7.1 Publications resulting from this work

Book chapters

Adams JRJ and Byers S. Hyaluronan metabolism in the MG63 osteoblast cell line. (2005). In: Balazs EA and Hascall VC (eds), *Hyaluronan: Its Structure, Metabolism, Biological Activities and Therapeutic Applications*. Matrix Biology Insitute Press, New Jeresey, USA pp 459-463.

Peer reviewed journals

Adams JRJ, Sander G and Byers S (2006). Expression of hyaluronan synthases and hyaluronidases in the MG63 osteoblast cell line. *Matrix Biol.* **25**(1):40-6.

Abstracts

Adams JRJ, Anson DS and Byers S (2003). Metabolism of hyaluronan in mineralising MG63 osteoblast. *Proceedings of the Matrix Biology Society Australia and New Zealand* **27**: 34.

Adams JRJ, Dunning KR, Thomas BJ, Litjens T, Fietz MJ, Anson DS and Byers S (2002). Molecular cloning and expression of the human hyaluronidases: HYAL-1, HYAL-3 and HYAL-4. *Proceedings of Proceedings of the Matrix Biology Society Australia and New Zealand* **26**: 26.

Adams JRJ, Litjens T and Byers S (2001). RT-PCR analysis to determine the expression of mammalian hyaluronidases in osteoblasts. *Proceedings of the Matrix Biology Society Australia and New Zealand* **25**: 31.

7.2 References

Adams JRJ and Byers S. Hyaluronan metabolism in the MG63 osteoblast cell line. (2005). In: Balazs EA and. Hascall VC (eds), *Hyaluronan: Its Structure, Metabolism, Biological Activities and Therapeutic Applications.* MBI press, Vol 2. pp 459-463.

Adams JRJ, Sander G and Byers S (2006). Expression of hyaluronan synthases and hyaluronidases in the MG63 osteoblast cell line. *Matrix Biol.* **25**(1):40-6.

Afify AM, Stern M, Guntenhoner M and Stern R (1993). Purification and characterization of human serum hyaluronidase. *Arch Biochem Biophys* **305**: 434-41.

Aikawa J and Esko JD (1999). Molecular cloning and expression of a third member of the heparan sulfate/heparin GlcNAc N-deacetylase/N-sulfotransferase family. *J Biol Chem* **274**: 2690-5.

Akimoto Y, Kreppel L, Hirano H, and Hart G (1999). Localization of the O-linked N-acetylglucosamine transferase in rat pancreas. *Diabetes* **48**: 2407-13.

Anderson HC (1995). Molecular biology of matrix vesicles. *Clin Orthop Relat Res* **314**: 266-80.

Aubin JE, Gupta A, Zirngibl R and Rossant J (1996). Knockout mice lacking bone sialoprotein expression have bone abnormalities. *J Bone Mineral Res* **11**: S102.

Arming S, Strobl B, Wechselberger C and Kreil G (1997). In vitro mutagenesis of PH-20 hyaluronidase from human sperm. *Eur J Biochem* **247**: 810-4.

Baba D, Kashiwabara S, Honda A, Yamagata K, Wu Q, Ikawa M, Okabe M and Baba T (2002). Mouse sperm lacking cell surface hyaluronidase PH-20 can pass through the layer of cumulus cells and fertilize the egg. *J Biol Chem* **277**: 30310-4.

Baker JR, Cifonelli JA and Roden L (1975). The linkage of corneal keratan sulfate to protein. *Connect Tissue Res* **3**: 149-56.

Bame KJ (1993). Release of heparan sulfate glycosaminoglycans from proteoglycans in Chinese hamster ovary cells does not require proteolysis of the core protein. *J Biol Chem* **268**: 19956-64.

Barnes LM, Bentley CM and Dickson AJ (2003). Stability of protein production from recombinant mammalian cells. *Biotechnol Bioeng* **81**: 631-9.

Bendtsen JD, Nielsen H, von Heijne G and Brunak S (2004). Improved prediction of signal peptides: SignalP 3.0. *J Mol Biol* **340**: 783-95.

Bertolami CN and Messadi DV (1994). The role of proteoglycans in hard and soft tissue repair. *Crit Rev Oral Biol* **5**: 311-37.

Bhatia PK and Mukhopadhyay A (1999). Protein glycosylation: implications for in vivo functions and therapeutic applications. *Adv Biochem Eng Biotechnol* **64**: 155-201.

Blumenkrantz N and Asboe-Hansen G (1973). New method for quantitative determination of uronic acids. *Anal Biochem* **54**: 484-9.

Bonner WM and Cantey EY (1966). Colorimetric method for determination of serum hyaluronidase activity. *Clin Chim Acta* **13**: 746-52.

Bianco P, Fisher LW, Young MF, Termine JD and Robey PG (1991). Expression of bone sialoprotein (BSP) in developing human tissues. *Calcif Tissue Int* **49**: 421-26.

Bills CE, Eisenberg H and Pallante SL (1971). Complexes of organic acids with calcium phosphate: the von Kossa stain as a clue to the composition of bone mineral. *Johns Hopkins Med J* **128**: 194-207.

Bonewald LF, Kester MB, Schwartz Z, Swain LD, Khare A, Johnson TL, Leach RJ and Boyan BD (1992). Effects of combining transforming growth factor beta and 1,25-dihydroxyvitamin D3 on differentiation of a human osteosarcoma (MG-63). *J Biol Chem* **267:** 8943-9.

Boskey AL (1996). Matrix proteins and mineralization: an overview. *Connect Tissue Res*. **35**: 357-63.

Boskey AL, Spevak L, Doty SB and Rosenberg L (1997). Effects of bone CS-proteoglycans, DS-decorin, and DS-biglycan on hydroxyapatite formation in a gelatin gel. *Calcif Tissue Int* **61**: 298-305.

Boyan BD, Schwartz Z, Bonewald, LF and Swain LD (1989a). Localization of 1,25-(OH)2D3-responsive alkaline phosphatase in osteoblast-like cells (ROS 17/2.8, MG 63, and MC 3T3) and growth cartilage cells in culture. *J Biol Chem* **264**: 11879-86.

Boyan BD, Schwartz Z, Swain LD, Bonewald LF and Khare A (1989b). Regulation of matrix vesicle metabolism by vitamin D metabolites. *Connect Tissue Res* **22**: 53-61.

Bradford MM (1976). A rapid and sensitive method for the quantitation of microgram quantities of protein utilizing the principle of protein-dye binding. *Anal Biochem* **72**: 248-54.

Brink J and Heldin P (1999). Expression of recombinant hyaluronan synthase (HAS) isoforms in CHO cells reduces cell migration and cell surface CD44. *Exp Cell Res* **252**: 342-51.

Buckwater JA, Glimcher MJ, Cooper RR and Rexker R (1996). Structure, Blood supply cells, matrix and mineralisation. *Bone Biol Instructional Course Lectures* **45**: 371-86.

Byers S, Rozaklis T, Brumfield LK, Ranieri E and Hopwood JJ (1998). Glycosaminoglycan accumulation and excretion in the mucopolysaccharidoses: characterization and basis of a diagnostic test for MPS. *Mol Genet Metab* **65**: 282-90.

Byers S, Lee JL, Fietz M and Thomas B. Characterisation of human hyaluronidase (2005). In: E.A. Balazs and V.C. Hascall (eds), *Hyaluronan: Its Structure, Metabolism,*

Biological Activities and Therapeutic Applications. . Matrix Biology Insitute Press, New Jeresey, USA Vol 1. pp 225-8.

Camenisch TD, Spicer AP, Brehm-Gibson T, Biesterfeldt J, Augustine ML, Calabro A Jr, Kubalak S, Klewer SE and McDonald JA (2000). Disruption of hyaluronan synthase-2 abrogates normal cardiac morphogenesis and hyaluronan-mediated transformation of epithelium to mesenchyme. *J Clin Invest* **106**: 349-60

Caterson B, Flannery CR, Hughes CE and Little CB (2000). Mechanisms involved in cartilage proteoglycan catabolism. *Matrix Biol* **19**: 333-44.

Chen CC and Boskey AL (1985). Mechanisms of proteoglycan inhibition of hydroxyapatite growth. *Calcif Tissue Int.* **37**: 395-400.

Chen CC, Boskey AL and Rosenberg LC (1984). The inhibitory effect of cartilage proteoglycans on hydroxyapatite growth. *Calcif Tissue Int* **36**: 285-90.

Cherr GN, Yudin AI and Overstreet JW (2001). The dual functions of GPI-anchored PH20: hyaluronidase and intracellular signaling. *Matrix Biol* **20**: 515-25.

Christoffersen J and Landis WJ (1991). A contribution with review to the description of mineralization of bone and other calcified tissues in vivo. *Anat Rec* **230**: 435-50.

Collis L, Hall C, Lange L, Ziebell M, Prestwich R and Turley EA (1998). Rapid hyaluronan uptake is associated with enhanced motility: implications for an intracellular mode of action. *FEBS Lett* **440**: 444-9.

Comper WD and Laurent TC (1978). Physiological function of connective tissue polysaccharides. *Physiol Rev* **58**: 255-315.

Comtesse N, Maldener E and Meese E (2001). Identification of a nuclear variant of MGEA5, a cytoplasmic hyaluronidase and a beta-N-acetylglucosaminidase. *Biochem Biophys Res Commun* **283**: 634-40.

Corsi A, Xu T, Chen XD, Boyde A, Liang J, Mankani M, Sommer B, Iozzo RV, Eichstetter I, Robey PG, Bianco P and Young MF (2002). Phenotypic effects of biglycan deficiency are linked to collagen fibril abnormalities, are synergized by decorin deficiency, and mimic Ehlers-Danlos-like changes in bone and other connective tissues. *J Bone Mineral Res* **17**: 1180-9.

Couchman LA and Woods A (1993). Structure and biology of pericellular proteoglycans. In: DD Roberts, RP Mecham (eds), *Cell Surface Proteoglycan and Extracellular Glycoconjugates*. Academic Press, Orlando, Fla, pp 33-82.

Csoka AB, Frost GI and Stern R (2001). The six hyaluronidase-like genes in the human and mouse genomes. *Matrix Biol* **20**: 499-508.

Csoka AB, Scherer SW and Stern R (1999). Expression analysis of six paralogous human hyaluronidase genes clustered on chromosomes 3p21 and 7q31. *Genomics* **60**: 356-61.

Csoka TB, Frost GI, Heng HH, Scherer SW, Mohapatra G and Stern R (1998). The hyaluronidase gene HYAL1 maps to chromosome 3p21.2-p21.3 in human and 9F1-F2 in mouse, a conserved candidate tumor suppressor locus. *Genomic* **48**: 63-70.

Csoka TB, Frost GI, Wong T and Stern R (1997). Purification and microsequencing of hyaluronidase isozymes from human urine. *FEBS Lett* **417**: 307-10.

Cumming DA (1991). Glycosylation of recombinant protein therapeutics: control and function amplications. *Glycobiol* **1**: 115-30.

Daculsi G, Pilet P, Cottrel M and Guicheux G (1999). Role of fibronectin during biological apatite crystal nucleation: ultrastructural characterization. *J Biomed Mater Res* **47**: 228-33.

Davies JA, Fisher CE and Barnett MW (2001). Glycosaminoglycans in the study of mammalian organ development. *Biochem Soc Trans* **29**: 166-71.

DeAngelis, P.L., and A.M. Achyuthan (1996). Yeast-derived DG42 Protein of Xenopus can Synthesize Hyaluronan in vitro. *J Biol Chem* **271**: 23657-23660

Deed R, Rooney P, Kumar P, Norton JD, Smith J, Freemont AJ and Kumar S (1997). Early-response gene signalling is induced by angiogenic oligosaccharides of hyaluronan in endothelial cells. Inhibition by non-angiogenic, high-molecular-weight hyaluronan. *Int J Cancer* **71**: 251-6.

Dickenson JM, Huckerby TN and Nieduszynski IA (1990). Two linkage-region fragments isolated from skeletal keratan sulphate contain a sulphated N-acetylglucosamine residue. *Biochem J* **269**: 55-9.

Dolan M, Horchar T, Rigatti B and Hassell JR (1997). Identification of sites in domain I of perlecan that regulate heparan sulfate synthesis. *J Biol Chem* **272**: 4316-22.

Ducy P, Desbois C, Boyce B, Pinero G, Story B, Dunstan C, Smith E, Bonadio J, Goldstein S, Gundberg C, Bradley A and Karsenty G (1996). Increased bone formation in osteocalcin-deficient mice. *Nature* **382**: 448-52.

Einhorna, TA (1996). The bone organ system. In: R Marucsu, D Feldman and J Kelsey (eds) *Osteoporosis*. Academic Press, San Deigo pp 95-183.

El Hajjaji H, Cole AA and Manicourt DH (2005). Chondrocytes, synoviocytes and dermal fibroblasts all express PH-20, a hyaluronidase active at neutral pH. *Arthritis Res Ther* **7**: 756-68.

Embery G, Rees S, Hall R, Rose K, Waddington R and Shellis P (1998). Calcium- and hydroxyapatite-binding properties of glucuronic acid-rich and iduronic acid-rich glycosaminoglycans and proteoglycans. *Eur J Oral Sci* **106:** 267-73.

Evanko S, and Wight T (1999). Intracellular localization of hyaluronan in proliferating cells. *J Histochem Cytochem* **47**: 1331-42.

Fisher L (1985). *The Nature of Proteoglycan of Bone*. WT Butler, ed. ESBCO Media, Birmingham, pp 188-196S.

Fisher LW, Termine JD, Young MF (1989). Deduced protein sequence of bone small proteoglycan I (biglycan) shows homologywith proteoglycan II (decorin) and several nonconnective tissue proteins in avariety of species.*J Biol Chem* **264**:4571-6.

Fiszer-Szafarz A, Litynska A and Zou L (2000). Human hyaluronidases: electrophoretic multiple forms in somatic tissues and body fluids. Evidence for conserved hyaluronidase potential N-glycosylation sites in different mammalian species. *J Biochem Biophys Methods* **45**: 103-16.

Fiszer-Szafarz B, Czartoryska B and Tylki-Szymanska A. (2005). Serum hyaluronidase aberrations in metabolic and morphogenetic disorders. *Glycoconj J* **22:** 395-400.

Fulop C, Salustri A and Hascall VC (1997). Coding sequence of a hyaluronan synthase homologue expressed during expansion of the mouse cumulus-oocyte complex. *Arch Biochem Biophys* **337**: 261-6.

Flannery C, Little C, Hughes C and Caterson B (1998). Expression and activity of articular cartilage hyaluronidases. *Biochem Biophys Res Commun* **251**: 824-9.

Freeman C and Parish C (1998). Human platelet heparanase: purification, characterization and catalytic activity. *Biochem J* **330**: 1341-50.

Franceschi RT, James WM and Zerlauth G (1985). Alpha, 25-dihydroxyvitamin D3 specific regulation of growth, morphology, and fibronectin in a human osteosarcoma cell line. *J Cell Physiol* **123**: 401-9.

Franceschi R, Romano P and Park K (1988). Regulation of type I collagen synthesis by 1,25-dihydroxyvitamin D3 in human osteosarcoma cells. *J Biol Chem* **263**: 18938-45.

Fritz TA, Gabb MM, Wei G and Esko JD (1994). Two N-acetylglucosaminyltransferases catalyze the biosynthesis of heparan sulfate. *J Biol Chem* **269**: 28809-14.

Frost GI, Csoka, TB, Wong T and Stern, R (1997). Purification, cloning, and expression of human plasma hyaluronidase. *Biochem Biophys Res Commun* **236**: 10-15.

Frost GI and Stern R (1997). A microtiter-based assay for hyaluronidase activity not requiring specialized reagents. *Anal Biochem* **251**: 263-9.

Freeman C and Hopwood J (1992). Lysosomal degradation of heparin and heparan sulphate. *Adv Exp Med Biol* **313**: 121-34.

Fuller M, Chau A, Nowak R, Hopwood J and Meikle P (2006). A defect in exo-degradative pathways provides insight into endo-degradation of heparan and dermatan sulfates. *Glycobiol* **16**: 318-25.

Funderburgh JL (2000). Keratan sulfate: structure, biosynthesis, and function. *Glycobiol* **10**: 951-8.

Gao Y, Wells L, Comer F, Parkere G and Hart G (2001). Dynamic O-glycosylation of nuclear and cytosolic proteins. Cloning and characterization of a neutral, cytosolic β-N-acetylglucosaminidase form human brain. *J Biol Chem* **276**: 9838-45

Gilmour D, Lyon G, Carlton M, Sanes J, Cunningham J, Anderson J, Hogan B, Evans M and Colledge W (1998). Mice deficient for the secreted glycoprotein SPARC/osteonectin/BM40 develope normally but show severe age-onset cataract formation and disruption of the lens. *EMBO J* **17**: 1860-70.

Ginetzimsky A (1958). Role of hyaluronidase in the re-absorption of water in renal tubules: the mechanism of action of the antidiuretic hormone. *Nature* **182**: 1218-9.

Ginsel L and Fransen J (1991). Mannose 6-phosphate receptor independent targeting of lysosomal enzymes. *Cell Biol Int Rep* **15**: 1167-73.

Glimcher M, Hodge J and Schmitt F (1957). Macromolecular aggregation states in relation to mineralization: the collagen-hydroxyapatite system as studied in vitro. *Proc. Natl Acad Sci USA* **43**: 860-6.

Glimcher MJ (1984). Recent sudies of the mineral phase in bone and the possible linkage to the organic matrix of protein-bound phosphate bonds. *Phios Trans Royal Soc London*. **304B**: 479-508.

Glimcher M (1989). Mechanism of calcification: role of collagen fibrils and collagen-phosphoprotein complexes in vitro and in vivo. *Anat Rec* **224**: 139-53.

Glimcher M (1992). The nature of mineral component of bone and the mechanism of bone calcification. In: F Coe F and M Favus (eds) *Disorders of Bone and Mineral Metabolism*. Raven Press, New York , pp 265-86.

Gmache M and Kreil G (1993). Bee venom hyaluronidase is homologous to a membrane protein of mammalian sperm. *Proc Natl Acad Sci USA* **90**: 3569-73.

Gmachl M, Sagan S, Ketter S and Kreil G (1993). The human sperm protein PH-20 has hyaluronidase activity. *FEBS Lett* **336**: 545-8.

Greiling H, Stuhlsatz HW, Eberhard T and Eberhard A (1975). Studies on the mechanism of hyaluronate lyase action. *Connect Tissue Res* **3**: 135-9.

Hasilik A (1992). The early and late processing of lysosomal enzymes: proteolysis and compartmentation. *Experienti* **48**: 130-51.

Hausser H, Ober B, Quentin-Hoffmann E, Schmidt B and Kresse H (1992). Endocytosis of different members of the small chondroitin/dermatan sulfateproteoglycan family. *J Biol Chem* **267**: 11559-64.

Hausser H and Kresse H (1991). Binding of heparin and of the small proteoglycan decorin to the same endocytosis receptor proteins leads to different metabolic consequences. *J Cell Biol* **114**: 45-52.

Haskins ME, Aguirre GD, Jezyk PF and Patterson DF (1980). The pathology of the feline model of mucopolysaccharidosis VI. *Am J Pathol* **101**: 657-74.

Heckel D, Comtesse N, Brass N, Blin N, Zang KD and Meese E (1998). Novel immunogenic antigen homologous to hyaluronidase in meningioma. *Hum Mol Genet* **7**: 1859-72.

Henrissat B and Bairoch A (1993). New families in the classification of glycosyl hydrolases based on amino acid sequence similarities. *Biochem J* **293**: 781-8.

Hildebrand A, Romaris M, Rasmussen LM, Heinegard D, Twardzik DR, Border WA and Ruoslahti E (1994). Interaction of the small interstitial proteoglycans biglycan, decorin and fibromodulin with transforming growth factor beta. *Biochem J* **302**: 527-34.

Hilfer SR (1996). Morphogenesis of the lung: control of embryonic and fetal branching. *Annu Rev Physiol* **58**: 93-113.

Hille-Rehfeld (1995). Mannose 6-phosphate receptors in sorting and transport of lysosomal enzymes .*Biochim Biophys Acta* **1241**: 177-94.

Hiyama K and Okada S (1975). Amino acid composition and physiochemical characterization of chondroitinase from Arthrobacter aurescens. *J Biochem (Tokyo)* **78**: 1183-90.

Hjertquist SO and Vejlens L (1968). The glycosaminoglycans of dog compact bone and epiphyseal cartilage in the normal state and in experimental hyperparathyroidism. *Calcif Tissue Res* **18**: 314-30.

Hocking AM, Shinomura T, McQuillan DJ (1998). Leucine-rich repeat glycoproteins of the extracellular matrix. *Matrix Biol* **17**:1-19.

Hoffman P, Meyer K and Linker A (1956). Transglycosylation during the mixed digestion of hyaluronic acid and chondroitin sulfate by testicular hyaluronidase. *J Biol Chem* **219**: 653-63.

Hopwood JJ and Robinson HC (1974). The alkali-labile linkage between keratan sulphate and protein. *Biochem J* **141**: 57-69

Hovingh P and Linker A (1999). Hyaluronidase activity in leeches (Hirudinea). *Comp Biochem Physiol Mol Biol* **124**: 319-26.

Howard SC, Wittwer AJ and Welply JK (1991). Oligosaccharides at each glycosylation site make structure-dependent contributions to biological properties of human tissue plasminogen activator. *Glycobiol* **1**: 411-8.

Huang L, Cheng YY, Koo PL, Lee KM, Qin L, Cheng JC and Kumta SM (2003). The effect of hyaluronan on osteoblast proliferation and differentiation in rat calvarial-derived cell cultures. *J Biomed Material Res* **15:** 880-4.

Hunnicutt GR, Primakoff P and Myles DG (1996). Sperm surface protein PH-20 is bifunctional: one activity is a hyaluronidase and a second, distinct activity is required in secondary sperm-zona binding. *Biol Reprod* **55**: 80-6.

Hunter GK and Goldberg HA (1993). Nucleation of hydroxyapatite by bone sialoprotein. *Proc Natl Acad Sci USA* **90**: 8562-5.

Hunter GK, Hauschka PV, Poole AR, Rosenberg LC and Goldberg HA (1996). Nucleation and inhibition of hydroxyapatite formation by mineralized tissue proteins. *Biochem J* **317**: 59-64.

Hunziker W and Geuze H (1996). Intracellular trafficking of lysosomal membrane proteins. *Bioessays* **18**: 379-89.

Hyde CE and Old RW (1999). Expression pattern of a novel hyaluronidase during Xenopus embryogenesis. *Mech Dev* **82**: 213-7.

Iozzo RV (1987). Turnover of heparan sulfate proteoglycan in human colon carcinoma cells. A quantitative biochemical and autoradiographic study. *J Biol Chem* **262**: 1888-900.

Iozzo RV (1999). The biology of the small leucine-rich proteoglycans. Functional network of interactive proteins. *J Biol Chem* **74**: 18843-6.

Itano N, and Kimata K (1996). Expression cloning and molecular characterization of HAS protein, a eukaryotic hyaluronan synthase. *J Biol Chem* **271**: 9875-8.

Itano N, Sawai T, Yoshida M, Lenas P, Yamada Y, Imagawa M, Shinomura T, Hamaguchi M, Yoshida Y, Ohnuki Y, Miyauchi S, Spicer AP, McDonald JA and Kimata K (1999). Three isoforms of mammalian hyaluronan synthases have distinct enzymatic properties. *J Biol Chem* **274**: 25085-92.

Ji I and Ji TH (1990). Differential interactions of human choriogonadotropin and its antagonistica glycosylated analog with their receptor. *Proc Natl Acad Sci USA* **87**: 4396-400.

Jones MH, Davey PM, Aplin H and Affara NA (1995). Expression analysis, genomic structure, and mapping to 7q31 of the human sperm adhesion molecule gene SPAM1. *Genomics* **29:** 796-800.

Jorgensen MM, Bross P and Gregersen N (2003). Protein quality control in the endoplasmic reticulum. *APMIS Suppl* **109**: 86-91.

Karsenty G (1998). Transcriptional regulation of osteoblast differentiaition during development. *Front Biosci* **3**: 834-837.

Knudson W, Gundlach MW, Schmid TM and Conrad HE (1984). Selective hydrolysis of chondroitin sulfates by hyaluronidase. *Biochem* **17**: 368-75.

Knudson CB and Knudson W (1993). Hyaluronan-binding proteins in development, tissue homeostasis, and disease. *FASEB J* **15**: 1233-41.

Kreppel LK, Blomberg MA and Hart GW (1997). Dynamic glycosylation of nuclear and cytosolic proteins. Cloning and characterization of a unique O-GlcNAc transferase with multiple tetratricopeptide repeat . *J Biol Chem* **272**: 9308-15.

Kretz KA, Carson GS, Morimoto S, Kishimoto Y, Fluharty AL and O'Brien JS (1990). Characterization of a mutation in a family with saposin B deficiency: aglycosylation site defect. *Proc Natl Acad Sci USA* **87**: 2541-4.

Krishnapillai AM, Taylor KDA, Morris AEJ and Quantick PC (1999). Characterisation of Norway lobster (Nephrops norvegicus) hyaluronidase and comparison with sheep and bovine testicular hyaluronidase. *Food Chem* **65**: 515-21.

Laemmli UK (1970). Cleavage of structural proteins during the assembly of the head of bacteriophage T4. *Nature* **227**: 680-5.

Laurent TC (1970). In: *Chemistry and molecular biology of the intercellular matrix.* EA Balaza (ed), Academic Press, New York, pp 703–32.

Lee JY and Spicer AP (2000). Hyaluronan: a multifunctional, megaDalton, stealth molecule. *Curr Opin Cell Biol* **12**: 581-6.

Lepperdinger G, Mullegger J and Kreil G (2001). Hyal2 - less active, but more versatile? *Matrix Biol* **20**: 509-14.

Lepperdinger G, Strobl B and Kreil G (1998). HYAL2, a human gene expressed in many cells, encodes a lysosomal hyaluronidase with a novel type of specificity. *J Biol Chem* **273**: 22466-70.

Li MW, Cherr GN, Yudin AI and Overstreet JW (1997). Biochemical characterization of the PH-20 protein on the plasma membrane and inner acrosomal membrane of cynomolgus macaque spermatozoa. *Mol Reprod Dev* **48**: 356-66.

Li MW, Yudin AI, Robertson KR, Cherr GN and Overstreet JW (2002). Importance of glycosylation and disulfide bonds in hyaluronidase activity of macaque sperm surface PH-20. *J Androl* **23**: 211-9.

Liaw L, Birk DE, Ballas CB, Whitsitt JS, Davidson JM and Hogan BL (1998). Altered wound healing in mice lacking a functional osteopontin gene. *J Clin Invest* **101**: 1468-78.

Lidholt K, Riesenfeld J, Jacobsson KG, Feingold DS and Lindahl U (1988). Biosynthesis of heparin. Modulation of polysaccharide chain length in a cell-free system. *Biochem J* **254**: 571-8.

Lin Y, Mahan K, Lathrop WF, Myles DG and Primakoff P (1994). A hyaluronidase activity of the sperm plasma membrane protein PH-20 enables sperm to penetrate the cumulus cell layer surrounding the egg. *J Cell Biol.* **125**: 1157-63.

Linker A, Hoffman P and Meyer K (1957). The hyaluronidase of the leech: an endoglucuronidase. *Nature* **180**: 810-1.

Linker A, Meyer K and Hoffman P (1960). The production of hyaluronate oligosaccharides by leech hyaluronidase and alkali. *J Biol Chem* **235**: 924-7.

Lis H and Sharon N (1993). Protein glycosylation. Structural and functional aspects. *Eur J Biochem* **218**: 1-27.

Liu D, Pearlman E, Diaconu E, Guo K, Mori H, Haqqi T, Markowitz S, Willson J and Sy MS (1996). Expression of hyaluronidase by tumor cells induces angiogenesis in vivo. *Proc Natl Acad Sci USA* **93**: 7832-7.

Lohmander LS, De Luca S, Nilsson B, Hascall VC, Caputo CB, Kimura JH and Heinegrad D (1980). Oligosaccharides on proteoglycans from the swarm rat chondrosarcoma. *J Biol Chem* **255**: 6084-91.

Lokeshwar VB, Schroeder GL, Carey RI, Soloway MS and Iida N (2002). Regulation of hyaluronidase activity by alternative mRNA splicing. *J Biol Chem* **277**: 33654-63.

Lu G, Kochoumian L and King TP (1995). Sequence identity and antigenic cross-reactivity of white face hornet venom allergen, also a hyaluronidase, with other proteins. *J Biol Chem* **270**: 4457-65.

Luo G, Ducy P, McKee MD, Pinero GJ, Loyer E, Behringer RR and Karsenty G (1997). Spontaneous calcification of arteries and cartilage in mice lacking matrix GLA protein. *Nature* **386**: 78-81.

Madan AK, Yu K, Dhurandhar N, Cullinane C, Pang Y and Beech DJ (1999). Association of hyaluronidase and breast adenocarcinoma invasiveness. *Oncol Rep* **6:** 607-9.

Maingonnat C, Victor R, Bertrand P, Courel MN, Maunoury R and Delpech B (1999). Activation and inhibition of human cancer cell hyaluronidase by proteins. *Anal Biochem* **268**: 30-4.

Maurer PH and Hudack SS (1952). The isolation of hyaluronic acid from the callus tissue of early healing. *Arch Biochem Biophys* **38**: 49-53.

Markovic-Housley Z, Miglierini G, Soldatova L, Rizkallah P J, Muller U and Schirmer T (2000). Crystal structure of hyaluronidase, a major allergen of bee venom. *Structure Fold Des* **8**: 1025-35.

McDonald JA and Camenisch TD (2003). Hyaluronan: genetic insights into the complex biology of a simple polysaccharide. *Glycoconj J* **19**: 331-9.

McKee CM, Penno MB, Cowman M, Burdick MD, Strieter RM, Bao C and Noble PW (1996). Hyaluronan (HA) fragments induce chemokine gene expression in alveolar macrophages. The role of HA size and CD44. *J Clin Invest* **98**: 2403-13

Meyer MF, Kreil G and Aschauer H (1997). The soluble hyaluronidase from bull testes is a fragment of the membrane-bound PH-20 enzyme. *FEBS Lett* **413**: 385-8.

Meyer MF and Kreil G (1996). Cells expressing the DG42 gene from early Xenopus embryos synthesize hyaluronan. *Proc Natl Acad Sci USA* **93**: 4543-7.

Meyer K (1950). The action of hyaluronidases on hyaluronic acid. *Ann NY Acad Sci.* **52**: 1021-3.

Miller A (1984). Collagen: the organic matrix of bone. *Philo Tran Royal Soc London Biol Sci* **302**: 455-77.

Midura RJ, M^{c}Quillen DJ, Benham KJ, Fisher LW and Hascall VC (1990). A rat osteogenic cell line (UMR 106-01) synthesizes a highly sulfated form of bone sialoprotein. *J Biol Chem* **265**: 5285-91.

Midura RJ, Su X, Morcuende JA, Tammi M and Tammi R (2003). Parathyroid hormone rapidly stimulates hyaluronan synthesis by periosteal osteoblasts in the tibial diaphysis of the growing rat. *J Biol Chem* **278**: 51462-8.

Miura RO, Yamagata S, Miura Y, Harada T and Yamagata T (1995). Analysis of glycosaminoglycan-degrading enzymes by substrate gel electrophoresis (zymography). *Anal Biochem* **225**: 333-40.

Montessuit C, Bonjour JP and Caverzasio J (1995). Expression and regulation of Na-dependent P(i) transport in matrix vesicles produced by osteoblast-like cells. *J Bone Mineral Res* **10**: 625-31.

Morgelin M, Heinegard D, Engel J and Paulsson M (1994). The cartilage proteoglycan aggregate: assembly through combined protein-carbohydrate and protein-protein interactions. *Biophys Chem* **50**: 113-28

Mullegger J and Lepperdinger G (2002). Degradation of hyaluronan by a Hyal2-type hyaluronidase affects pattern formation of vitelline vessels during embryogenesis of Xenopus laevis. *Mech Dev* **111:** 25-35.

Myer K and Rapport MM (1952). Hyaluronidase. *Advances in Enzymology*. **13:** 199.

Myles DG, Hyatt H and Primakoff P (1987). Binding of both acrosome-intact and acrosome-reacted guinea pig sperm to the zona pellucida during in vitro fertilization. *Dev Biol* **121**: 559-67.

Natowicz MR, Short MP, Wang Y, Dickersin GR, Gebhardt MC, Rosenthal DI, Sims KB and Rosenberg AE (1996). Clinical and biochemical manifestations of hyaluronidase deficiency. *N Engl J Med* **335**: 1029-33.

Neufeld EF and Muenzer J (2001). The mucoploysacharidoses. In: Scriver CR, Beaud Sly WS and Valle D (eds), *The Metabolic and Molecular Bases of Inherited Disease.* McGraw Hill, New York, pp 3421-3452.

Nicole S, Davoine CS, Topaloglu H, Cattolico L, Barral D, Beighton P, Hamida CB, Hammouda H, Cruad C, White PS, Samson D, Urtizberea JA, Lehmann-Horn F, Weissenbach J, Hentati F and Fontaine B (2000). Perlecan, the major proteoglycan of basement membranes, is altered in patients with Schwartz-Jampel syndrome (chondrodystrophic myotonia). *Nat Genet* **26**: 480-3.

Nishida Y, Knudson CB, Nietfeld JJ, Margulis A and Knudson W (1999). Antisense inhibition of hyaluronan synthase-2 in human articular chondrocytes inhibits proteoglycan retention and matrix assembly. *J Biol Chem* **274:** 21893-9.

Noonan KJ, Stevens JW, Tammi R, Tammi M, Hernandez JA and Midura RJ (1996). Spatial distribution of CD44 and hyaluronan in the proximal tibia of the growing rat. *J Orthop Res* **14**: 573-81.

Ohya T and Kaneko Y (1970). Novel hyaluronidase from streptomyces. *Biochim Biophys Acta* **198**: 607-9.

Oliferenko S, Kaverina I, Small JV and Huber LA (2000). Hyaluronic acid binding to CD44 activates Rac1 and induces lamellipodia outgrowth. *J Cell Biol* **148**: 1159–64.

Ouskova G, Spellerberg B and Prehm P (2004). Hyaluronan release from Streptococcus pyogenes: export by an ABC transporter. *Glycobiol* **14**: 931-8.

Parodi AJ (2000). Protein glycosylation and its role in protein folding. *Ann Rev Biochem* **69**: 69-93.

Pavasant P, Shizari TM and Underhill CB (1994). Distribution of hyaluronan in the epiphysial growth plate: turnover by CD44-expressing osteoprogenitor cells. *J Cell Sci* **107**: 2669-77.

Posner AS (1985). The mineral of bone. *Clin Orthop Related Res* **200**: 87-99

Pienimaki JP, Rilla K, Fulop C, Sironen RK, Karvinen S, Pasonen S, Lammi MJ, Tammi R, Hascall VC and Tammi MI (2001). Epidermal growth factor activates

hyaluronan synthase 2 in epidermal keratinocytes and increases pericellular and intracellular hyaluronan. *J Biol Chem* **276**: 20428-35.

Pilloni A and Bernard GW (1998). The effect of hyaluronan on mouse intramembranous osteogenesis in vitro. *Cell Tissue Res* **294**: 323-333.

Prehm P (1984). Hyaluronate is synthesized at plasma membranes. *Biochem J* **220**: 597-600.

Primakoff P, Hyatt H and Myles DG (1985). A role for the migrating sperm surface antigen PH-20 in guinea pig sperm binding to the egg zona pellucida. *J Cell Biol* **101**: 2239-44.

Pritchard DG, Lin B, Willingham TR and Baker JR (1994). Characterization of the group B streptococcal hyaluronate lyase. *Arch Biochem Biophys* **315**: 431-7.

Prydz K and Dalen KT (2000). Synthesis and sorting of proteoglycans. *J Cell Sci* **113**: 193-205.

Rai SK, Duh FM, Vigdorovich V, Danilkovitch-Miagkova A, Lerman MI and Miller AD (2001). Candidate tumor suppressor HYAL2 is a glycosylphosphatidylinositol (GPI)-anchored cell-surface receptor for Jaagsiekte sheep retrovirus, the envelope protein of which mediates oncogenic transformation. *Proc Natl Acad Sci USA* **98**: 4443-8.

Ramage P, Hemmig R, Mathis B, Cowan-jacob SW, Rondeau JM, Kallen J, Blommers MJJ, Zurini M and Rüdisser S (2002). Snags with tags: some observations made with (His) 6-tagged proteins. *Life Science News* **11**: 1-4.

Recklies AD, White C, Melching L and Roughley PJ (2001). Differential regulation and expression of hyaluronan synthases in human articular chondrocytes, synovial cells and osteosarcoma cells. *Biochem J* **354:** 17-24.

Reddi AH (1981). Cell biology and biochemistry of endochondral bone development. *Coll Relat Res* **1**: 209-26

Reddi AH, Wientraub S and Muthukumaran N (1987). Biological principles of bone induction. *Orthop Clin North Am* **18**: 207-212.

Rey C, Beshah K, Griffin R and Glimcher MJ (1991). Structural studies of the mineral phase of calcifying cartilage. *J Bone Mineral Res*: **6**: 515-25.

Rey C, Kim HM, Gerstenfeld L and Glimcher MJ (1995). Structural and chemical characteristics and maturation of the calcium-phosphate crystals formed during the calcification of the organic matrix synthesized by chicken osteoblasts in cell culture. *J Bone Mineral Res.* **10**: 1577-88.

Reitinger S, Mullegger J, and Lepperdinger G (2001). Xenopus kidney hyaluronidase-1 (XKH1), a novel type of membrane-bound hyaluronidase solely degrades hyaluronan at neutral pH. *FEBS Lett* **505:** 213-6.

Robey PG (1992).In: Coe FL and Favus MJ (eds), *The Cellular Biology and Molecular Biochemisry of Bone Formation. Disorders of Bone and Mineral Metabolism.*, Raven Press, New York, pp 241-63.

Robey PG and Boskey AL (1996). In: Marucsu R, Feldman D and Kelsey J (eds) *The Biochemistry of Bone. Osteoporosis*. Academic Press, San Deigo, pp 95-183.

Rohrmann K, Niemann R and Buddecke E (1985). Two N-acetylgalactosaminyltransferasess are involved in the biosynthesis of chondroitin sulfate. *Eur J Biochem* **148**: 463-9.

Rouille Y, Rohn W and Hoflack B (2000). Targeting of lysosomal proteins. *Semin Cell Dev Biol* **11**:165-71.

Rohn WM, Rouille Y, Waguri S and Hoflack B (2000). Bi-directional trafficking between the trans-Golgi network and the endosomal/lysosomal system. *J Cell Sci* **113**: 2093-101.

Samiric T, Illic M and Handley C (1996). Large aggregating and small leucine-rich proteoglycan are degraded by different pathways and at different rates in tendon. *Eur J Biochem.* **271**: 3612- 3620.

Schaefer L, Hausser H, Altenburger M, Ugorcakova J, August C, Fisher LW, Schaefer RM and Kresse H (1998). Decorin, Biglycan and their endocytosis receptor in rat renal cortex. *Kidney Int* **54**: 1529-41.

Schwartz NB and Roden L (1975). Biosynthesis of chondroitin sulfate. Solubilization of chondroitin sulfate glycosyltransferases and partial purification of uridine diphosphate-D-galactose:D-xylose galactosyltrans. *J Biol Chem* **250**: 5200-7.

Scott JE (1992). Supramolecular organization of extracellular matrix glycosaminoglycans, in vitro and in the tissues. *FASEB J* **6**: 2639-45.

Selleck SB (2000). Proteoglycans and pattern formation: sugar biochemistry meets developmental genetics. *Trends Genet* **16**: 206-12.

Seligman M, Eilberg RF and Fishman L (1975). Mineralization of elastin extracted from human aortic tissues. *Calcif Tissue Res* **17**: 229-34

Schmitz A and Herzog V (2004). Endoplasmic reticulum-associated degradation: exceptions to the rule. *Eur J Cell Biol* **83**: 501-9.

Schwarz E, Lilie H and Rudolph R (1996). The effect of molecular chaperones on in vivo and in vitro folding processes. *Biol Chem* **377**: 411-6.

Shen B, Shimmon S, Smith MM and Ghosh P (2003). Biosensor analysis of the molecular interactions of pentosan polysulfate and of sulfated glycosaminoglycans with

immobilized elastase, hyaluronidase and lysozyme using surface plasmon resonance (SPR) technology. *J Pharm Biomed Anal* **31**: 83-93.

Slevin M, Krupinski J, Kumar S and Gaffney J (1998). Angiogenic oligosaccharides of hyaluronan induce protein tyrosine kinase activity in endothelial cells and activate a cytoplasmic signal transduction pathway resulting in proliferation. *Lab Invest* **78**: 987-1003.

Spicer AP, Augustine ML and McDonald JA (1996). Molecular cloning and characterization of a putative mouse hyaluronan synthase. *J Biol Chem* **271:** 23400-6.

Spicer AP and McDonald JA (1998). Characterization and molecular evolution of a vertebrate hyaluronan synthase gene family. *J Biol Chem* **273:** 1923-32.

Spicer AP, Olson, JS and McDonald JA (1997). Molecular cloning and characterization of a cDNA encoding the third putative mammalian hyaluronan synthase. *J Biol Chem* **272:** 8957-61.

Spooner BS, Bassett, KE and Spooner BS Jr (1993). Embryonic lung morphogenesis in organ culture: experimental evidence for a proteoglycan function in the extracellular matrix. *Trans Kans Acad Sci* **96:** 46-55.

Stern R (2004). HA catabolism: a new metabolic pathway. *Eur J Cell Biol* **83**: 317–25.

Stern R (2003). Devising a pathway for hyaluronan catabolism: are we there yet?. *Glycobiol* **13**: 105R-115.

Stoolmiller AC, Horwitz AL and Dorfman A (1972). Biosynthesis of the chondroitin sulfate proteoglycan. Purification and properties of xylosyltransferase. *J Biol Chem* **247**: 3525-32.

Sugahara K, Masuda M, Harada T, Yamashina I, De Waard P and Vliegenthart JF (1991). Structural studies on sulfated oligosaccharides derived from the carbohydrate-protein linkage region of chondroitin sulfate proteoglycans of whale cartilage. *Eur J Biochem* **202:** 805-11.

Sugahara K, Ohkita Y, Shibata Y, Yoshida K and Ikegami A (1995a). Structural studies on the hexasaccharide alditols isolated from the carbohydrate-protein linkage region of dermatan sulfate proteoglycans of bovine aorta, demonstration of iduronic acid-containing components. *J Biol Chem* **270:** 7204-12.

Sugahara K, Tsuda H, Yoshida K, Yamada S, de Beer T and Vliegenthart JF (1995b). Structure determination of the octa- and decasaccharide sequences isolated from the carbohydrate-protein linkage region of porcine intestinal heparin. *J Biol Chem* **270:** 22914-23.

Sugahara K, Yamada S, Yoshida K, De Waard P and Vliegenthart JF (1992). A novel sulfated structure in the carbohydrate-protein linkage region isolated from porcine intestinal heparin. *J Biol Chem* **267:** 1528-33.

Sugahara K, Yamashina I, De Waard, P, Van Halbeek H and Vliegenthart JF (1988). Structural studies on sulfated glycopeptides from the carbohydrate-protein linkage region of chondroitin 4-sulfate proteoglycans of swarm rat chondrosarcom a Demonstration of the structure Gal(4-O-sulfate)beta 1-3Gal beta 1-4XYL beta 1-O-Ser. *J Biol Chem* **263:** 10168-74.

Sugars RV, Milan AM, Brown JO, Waddington RJ, Hall RC and Embery G (2003). Molecular interaction of recombinant decorin and biglycan with type I collagen influences crystal growth. *Connect Tissue Res* **44:** 189-95.

Takagaki K, Munakata H, Majima M, Kakizaki I and Endo M (2000). Chimeric glycosaminoglycan oligosaccharides synthesized by enzymatic reconstruction and their use in substrate specificity determination of Streptococcus hyaluronidase. *J Biochem (Tokyo)* **127:** 695-702.

Takagaki K, Nakamura T, Izumi J, Saitoh H, Endo M, Kojima K, Kato I and Majima M (1994). Characterization of hydrolysis and transglycosylation by testicular hyaluronidase using ion-spray mass spectrometry. *Biochem* **33:** 6503-7.

Tam YC and Chan EC (1985). Purification and characterization of hyaluronidase from oral Peptostreptococcus species. *Infect Immun* **47:** 508-13.

Tenenbaum HC and Hunter GK (1987). Chondroitin sulphate inhibits calcification of bone formed *in vitro*. *Bone Miner Res* **2**: 43-51.

Termine JD, Kleinman HK, Whitson SW, Conn KM, McGarvey ML and Martin R (1981). Osteonectin, a bone-specific protein linking mineral to collagen. *Cell* **26**: 99-105.

Thaler CD and Cardullo RA (1995). Biochemical characterization of a glycosylphosphatidylinositol-linked hyaluronidase on mouse sperm. *Biochem* **34**: 7788-95.

Thomas L, Byers HR, Vink J and Stamenkovic I (1992). CD44H regulates tumor cell migration on hyaluronate-coated substrate. *J Cell Biol* **118**: 971-7.

Thomas L, Etoh T, Stamenkovic I, Mihm MC Jr and Byers HR (1993). Migration of human melanoma cells on hyaluronate is related to CD44 expression. *J Invest Dermatol* **100**:115-20.

Toma L, Pinhal MA, Dietrich CP, Nader HB and Hirschber CB (1996). Transport of UDP-galactose into the Golgi lumen regulates the biosynthesis of proteoglycans. *J Biol Chem* **271:** 3897-901.

Toole BP and Gross J (1971). The extracellular matrix of the regenerating newt limb; synthesis and removal of hyaluronate prior to differentiation. *Devel Biol* **25:** 57-72.

Toole BP (1997). Hyaluronan in morphogenesis. *J Intern Med* **242:** 35-40.

Triffit JT (1980). In: Yrist MR, Lippincoft JB (eds), *The organic matrix of bone tissue.* Fundamental and clinical bone physiology, pp: 45-82.

Triggs-Raine B, Salo TJ, Zhang H, Wicklow BA and Natowicz MR (1999). Mutations in HYAL1, a member of a tandemly distributed multigene family encoding disparate hyaluronidase activities, cause a newly described lysosomal disorder, mucopolysaccharidosis IX. *Proc Natl Acad Sci USA* **96:** 6296-300.

Turnbull JE and Gallagher JT (1988). Oligosaccharide mapping of heparan sulphate by polyacrylamide-gradient-gel electrophoresis and electrotransfer to nylon membrane. *Biochem J* **251**: 597-608.

Varki A (1993). Biological roles of oligosaccharides: all of the theories are correct. *Glycobiol* **3**: 97-130.

Waddington RJ, Roberts HC, Sugars RV and Schönherr E (2003). Differential roles for small leucine-rich proteoglycans in bone formation. *Euro Cell Material* **6**: 12-21.

Watanabe K and Yamaguchi Y (1996). Molecular identification of a putative human hyaluronan synthase. *J Biol Chem* **271**: 22945-8.

Weigel P, Hascall V and Tammi M (1997). Hyaluronan synthases *J Biol. Chem.* **272**: 13997-14000.

Weigel PH (2005). In: Balazs EA and Hascall VC (eds) Current Progress and Limitations in Understanding the Molecular and Cellular Functions of Hyaluronan Synthases. *Hyaluronan: Its Structure, Metabolism, Biological Activities and Therapeutic Applications,* . Matrix Biology Insitute Press, New Jeresey, USA pp 173-179.

West DC, Hampson IN, Arnold F and Kumar S (1985). Angiogenesis induced by degradation products of hyaluronic acid. *Science* **228**: 1324-6.

Wiebkin OW and Muir H (1977). Synthesis of proteoglycans by suspension and monolayer cultures of adult chondrocytes and de novo cartilage nodules-the effect of hyaluronic acid. *J Cell Sci* **27:** 199-211.

Wilkinson BM, Regnacq M and Stirling CJ (1997). Protein translocation across the membrane of the endoplasmic reticulum. *J Membrane Biol* **155**: 189-97

Withers SG and Aebersold R (1995). Approaches to labeling and identification of active site residues in glycosidases. *Protein Sci* **4**: 361-72.

Wurm F (1997). In: Hauser H and Wagner R (eds), Aspect of gene transfer and gene amplification in recombinant mammalian cells. *Mammalian cell biotechnology in protein production.* Waltar de Gruyter, Berlin, pp 87-120.

Wurm F (2004) Production of recombinant protein therapeutics in cultivated mammalian cells. *Nature Biotech.* **22**: 1393-98.

Xu T, Bianco P, Fisher LW, Longenecker G, Smith E, Goldstein S, Bonadio J, Boskey A, Heegaard AM, Sommer B, Satomura K, Dominguez P, Zhao C, Kulkarni AB, Robey PG and Young MF (1998). Targeted disruption of the biglycan gene leads to an osteoporosis-like phenotype in mice. *Nat Genet* **20**: 78-82.

Yamada M, Hasegawa E and Kanamori M (1977). Purification of hyaluronidase from human placenta. *J Biochem (Tokyo)* **81**: 485-94.

Yanagimachi R (1994). Fertility of mammalian spermatozoa: its development and relativity. *Zygote* **2**: 371-2.

Yanagishita M and Hascall VC (1984). Metabolism of proteoglycans in rat ovarian granulosa cell culture. Multiple intracellular degradative pathways and the effect of chloroquine. *J Biol Chem* **259**: 10270-83.

Yanagishita M and Hascall VC (1992). Cell surface heparan sulfate proteoglycans. *J Biol Chem* **267**: 9451-4.

Yamaguchi Y, Mann DM and Rouslahti E (1990). Negative regulation of transforming growth factor-β by the proteoglycan decorin. *Nature* **346**: 281-4.

Yoshida M, Itano N, Yamada Y and Kimata K (2000). *In vitro* synthesis of hyaluronan by a single protein derived from the mouse HAS1 gene and characterization of amino acid residues essential for the activity. *J Biol Chem* **275**: 497-506.

Yudin AI, Li MW, Robertson KR, Cherr GN and Overstreet JW (2001). Characterization of the active site of monkey sperm hyaluronidase. *Reproduction* **121**: 735-43.

Zhang L, David G and Esko JD (1995). Repetitive Ser-Gly sequences enhance heparan sulfate assembly in proteoglycans. *J Biol Chem* **270**: 27127-35.

Zhang L and Esko JD (1994). Amino acid determinants that drive heparan sulfate assembly in a proteoglycan. *J Biol Chem* **269**: 19295-9.

Zhang H and Martin-DeLeon PA (2003). Mouse Spam1 (PH-20) is a multifunctional protein: evidence for its expression in the female reproductive tract. *Biol Reprod* **69**: 446-54.

Zhang R, Tsai-Morris CH, Kitamura M, Buczko E and Dufau ML (1991). Changes in binding activity of luteinizing hormone receptors by site directed mutagenesis of potential glycosylation sites. *Biochem Biophys Res Commun* **181**: 804-8.

Appendix I:

Materials

Apppendix I.i Tissue Culture materials

Ascorbate-2-phosphate	Wako Pure Chemical Industry, Osaka, Japan
BODIPy-C5 sphingolipid	Molecular Probes, Eugene, OR, USA
CHO-K1 cell line	AATC Manassasa, VA, USA
Dexamethasone	SIMGA St. Louis, MO, USA
DMEM	Gibco BRL, Rockville, MD, USA
DPX mounting solution	BDH Laboratory Supplies, Poole, UK
FBS	CSL Ltd, Australia Parkville, Vic, Austraila
H^3-glucosamine	Amersham Pharmacia, Piscataway, NJ, USA
Ham's F12	Gibco BRL, Rockville, MD, USA
Lysotracker	Molecular Probes, Eugene, OR, USA
Mitotracker red	Molecular Probes, Eugene, OR, USA
MG63 cell line	AATC, Manassas, VA, USA
G418 sulphate (Neomycin) Geneticin	Gibco-BRL, Rockville, MD, USA
PBS	CSL Ltd, Australia Parkville, Vic, Austraila
^{35}S sulphate	PerkinElmer Life and Analytical Sciences, Boston, MA, USA
Tracker Blue-White DPX	Molecular probes, Eugene, OR, USA
Trypsin	CSL Ltd , Park Ville, Vic, Austraila

Addendix I.ii Molecular biology materials

Ampicillin	Sigma, St. Louis, MO, USA
AmpliTaq gold	Applied Biosystems, Foster City, CA ,USA
Big Dye terminator V2 reagent	PerkinElmer Life and Analytical Sciences, Boston,

	MA, USA
Calf intestinal phosphatase	Roche, Basel, Switzerland
DH5α *E. coli*	TaKaRa Bio Inc, Shiga, Japan
DNA MidiPrep kit	Qiagen, Hilden, Germany
Gel purification kit	Qiagen, Hilden, Germany
Ethidium bromide	Amresco, Solon, OH, USA
Fugene6	Roche, Basel, Switzerland
pGFP-N1	Clontech, Mountain View, CA, USA
Platinum Taq DNA pcDNA 3.1 TOPO v5 HIS	Invitrogen , Carlsbad, CA, USA
Polymerase Pfx High Fidelity buffer	Invitrogen, Carlsbad, CA, USA
Restriction enzymes	New England Biolabs, Ipswich, MA, USA
Restriction enzymes	Roche, Basel, Switzerland
RNA'se-free DNAse I	Roche, Basel, Switzerland
RNEasy mini kit	Qiagen, Hilden, Germany
Site-directed mutagenesis kit	Stratagene, La Jolla, CA, USA
Syber Green	Molecular Probes, Eugene, OR, USA
T4 DNA ligase	New England Biolabs, Ipswich, MA, USA
Taq polymerase	Roche, Basel, Switzerland
Trizol	Gibco BRL, Rockville, MD, USA

Appendix I.iii Protein Biochemistry materials

4%-20% Gradient PAGE	Gradipore, French's Forest, NSW, Australia
Acrylamide (30%)	BioRad, Hercules, CA, USA
Amicon YM10 membrane	Millipore, Billerica, MA, USA
Bradford dye	BioRad, Hercules, CA, USA
Mouse anti-His_6 antibody	Roche, Basel, Switzerland.
PVDF membrane	NEN, Boston, MA, USA
Prestained low range marker	Gibco BRL, Rockville, MD, USA
^{35}S-methionine	Amersham Pharmacia, Piscataway, NJ, USA
Sheep anti-rabbit horseradish peroxidase (SAR HRP)	Silenus, Hawthorn, Vic, Australia
Sheep anti-mouse FITC conjugated	Silenus, Hawthorn, Vic, Australia
Streptavidin-conjugated HRP	Silneus, Hawthorn, Vic, Australia
Talon resin	Clontech, Mountain View, CA, USA
TNT T7 Quick Couple *in vitro* transcription and translation	Promega, Madison, WI, USA

Appendix I.iv Carbohydrate biochemistry materials

Chondroitin sulphate A bovine trachea (C6S)	Sigma, St. Louis, MO, USA
Chondrotin sulphate B porcine intestinal (DS)	Sigma, St. Louis, MO, USA
Chondroitin sulphate C shark cartilage (C4S)	Sigma, St. Louis, MO, USA
Chondroitinase ABC	ICN, Irvine, CA, USA
Desuphated chondroitin	Seikagaku Corporation, Chuo-ku, Tokyo, Japan
Dialysis tubing (15 kDa)	Selby Scientific Ltd, Clayton, Vic, Australia

Hyaluronan (umbilical cord)	ICN, Irvine, CA, USA
Hyaluronidase streptomyces	ICN, Irvine, CA, USA
Hyaluronidase testicular	ICN, Irvine, CA, USA
Optiphase High Safe liquid scintillation fluid	Wallac, Turku, Finland
Q-Sepharose	Sigma, St. Louis, MO, USA

Appendix II:

GeneBank sequences

Abbreviation	Gene Name	GeneBank Reference
Bee HYAL	bee venom hyaluronidase	L10710
Hs HAS-1	human hyaluronan synthase-1	BC035837
Hs HAS-2	human hyaluronan synthase- 2	HSU54804
Hs HAS-3	human hyaluronan synthase-3	AF232772
Hs HYAL-1	human hyaluronidase-1	U96078
Hs HYAL-P1	human hyaluronidase-pseudo gene	AF051769
Hs HYAL-2	human hyaluronidase-2 (lysosomal HYAL)	HSU0957
Hs HYAL-3	human hyaluronidase-3	AF036035
Hs HYAL-4	human hyaluronidase-4 (chondroitinase)	AF009010
Hs PH20	human testicular hyaluronidase	S67798
Mm *hyal*-1	mouse hyaluronidase-1	AF422176
Mm *hyal-p1*	mouse hyaluronidase-pseudo gene	AK01657
Mm *hyal*-2	mouse hyaluronidase-2 (lysosomal HYAL)	AF302843
Mm *hyal*-3	mouse hyaluronidase-3	AF074489
Mm *hyal*-4	mouse hyaluronidase-4 (chondroitinase)	AK014599
Mm *ph*20	mouse testicular hyaluronidase	U33958
XL HYAL	frog hyaluronidase	AF3949612
XL HYAL-2	frog hyaluronidase-2 (lysosomal)	AF314207
XL HYALK	frog kidney hyaluronidase	AF134981

Addendum

Page 22, line 10	"impling" should be replaced with "implying.
Page 24, line 16	"osteopotin" should be replaced with "osteopontin".
Page 27, line 20	"lacunare-canalicular' should be replaced with "lacunar-canalicular.
Page 44, line33	"alcian" should be replaced with "Alcian".
Page 50, line 17	This line should read "Total radiolabelled gags were extracted by rotating the cell layer for 24-h at 4°C".
Page 55, line 7	This paragraph should be referenced with "(Livak and Schmittgen, 2001)".
	Livak K and Schmittgen T (2001). Analysis of relative gene expression data using real-time quantitative PCR and the $2^{-\Delta\Delta Ct}$ method. *Methods* **25**: 402-408.
Page 61, line 8	"glycoylastion" should be replaced with "glycosylation".
Page 71, line 15	"amnio" should be replaced with "amino".
Page 81, line 81	"labelle" should be replaced with "labelled".
Page 87, line 6	"(section 4.6)" should be replaced with "(section 2.2.6)".
Page 91, line 11 and line 13	"(Figure 4.7; panels E, F and G, lanes 3-7)" should be replaced with "(Figure 4.7; panels D, E and F, lanes 3-7)".
Page 100, line 6	This line should read "were digested at pH 3.5 (A to E) and pH 7 (F to J)".
Page 108, line 5	"investergated" should be replaced with "investigation" and "encorparation" should be replaced with "incorporation".
Page 112, line 19	"(desulphayed CS)" should be replaced with "(desulphated CS)".
Page 114, line 17	"tranfer" should be replaced with 'transfer".
Page 118, line 4	"implys" should be replaced with "implies".
Page 127, line 3	"celllayer" should be replaced with "cell layer".